

The Podocyte in Proteinuric Renal Diseases

Ihmoda Ahmad Ihmoda

**A thesis submitted to the University of Edinburgh
for the degree of MD**

2006

Dedication

In the memory of my father

To my mother

To my wife, son, and daughter

To my brothers and sisters

Declaration

I hereby declare that, apart from the acknowledged assistance, this thesis is all my own work and no part of it has been submitted for any degree.

1

Ihmoda Ahmad Ihmoda

Acknowledgment

First and foremost, I offer my sincerest gratitude to my supervisor professor AN Turner, professor of nephrology at the University of Edinburgh for his knowledge and time. His enthusiasm for my project consistently energized me, driving me to push myself, to read more, to write and rewrite. He was very patient and approachable at any time and he was supervising me in a concerned way.

I am grateful to Dr Richard Phelps, senior lecturer in nephrology at the University of Edinburgh. My work has benefited a lot from his comments and suggestions resulting in substantial improvements in this thesis

Many thanks to Pat Swan, senior technician at the University of Edinburgh. She was extremely kind and supportive and helped in approaching the molecular biology techniques.

My special thanks to my current and past colleagues at the Renal and Autoimmunity Group:

Lucy Eggins

Dr Juan Zou

Dr Lorna Henderson

Dr Fathi Lajili

Vicky Thomson

Dr Julia Marley

Lorraine Rose

Dr Christina Summers

Dawn Hibbert

Dr Walaa Saweirs

Dr Nick Sargeant

Davina Wojtacha

Karen Anderson

I would like to acknowledge the help of the nursing staff at the outpatient department of Edinburgh Royal Infirmary for their help with samples collection.

People in the other groups of the Centre for Inflammation were very helpful and supportive, thanks a lot to them.

Finally, I wish to express my love and gratitude to thank my dearest ones, my wife Huda and kids; Ahmad and Najma who have given me strength and love throughout the years of this project.

This research was possible due to the support of the Libyan General Secretariat of Higher Education.

Abstract

Introduction

Podocytes are highly specialized epithelial cells with complex morphology which cover the outer surface of the glomerular basement membrane and form the final barrier to protein loss during glomerular filtration. Podocyte injury is characterised by the presence of proteinuria, even without any detectable morphological changes, and there is compelling evidence that further damage to podocytes is central to the development of focal and complete glomerulosclerosis and development of chronic renal failure. It is an attractive idea that podocyuria could be a prognostic marker enabling high-risk patients to be targeted for specific therapy. Detection of urinary podocytes by immunofluorescence has indeed been reported to reflect glomerulonephritis activity in both animals and man, but most publications concerning patients are from a single group.

Aims

1. To test the hypothesis that it would be prognostically useful to be able to identify podocytes in urine of patients with proteinuric renal disease, and that a reverse transcriptase polymerase chain reaction (RT-PCR) method would be an efficient and clinically applicable way to do this.
2. To create an animal model in which a graded podocyte injury could be induced, and examined alone or in combination with other pathology. This would be useful to test the hypothesis that treatment that protects the podocyte would ameliorate the disease.

Materials and Methods

1. Total RNA was extracted from urine samples (20 ml each) of 70 proteinuric (urine protein \geq +++) renal patients at the renal outpatient department of Edinburgh Royal Infirmary. This was followed by RT-PCR for nephrin, podocalyxin (podocyte specific mRNAs) and β -actin (positive control)

cDNAs. Immunofluorescence was conducted on urine samples of 100 patients with similar criteria using an anti-synaptopodin antibody (podocyte antibody).

2. Induction of specific podocyte injury with diphtheria toxin (DT) in a transgenic mice expressing human diphtheria toxin receptor (hDTR) on podocytes. Mice DTR is normally resistant to the effects of DT. These transgenic mice were generated by male pronuclear microinjection of murine fertilized ova with the plasmid (pIN); a construct contains murine nephrin promoter (podocyte promoter) and hDTR gene which is human Heparin Binding-Epidermal Growth Factor cDNA (hHB-EGF cDNA).

Results

1. All of the 70 urine samples were negative for podocyte protein mRNAs by RT-PCR, although many samples gave positive β -actin results, and control human kidney cDNA gave consistently positive results. Of 100 urine samples examined by immunofluorescence, only one (1%) gave a positive result. The technique was tested with human cultured podocytes and found to detect 10-20% of the actual number of podocytes in urine, and a similar proportion of control cells.
2. Two trials of male pronuclear microinjection of fertilized murine ova with podocyte construct were undertaken. The first microinjection trial was unsuccessful but four hDTR transgenic founders (tg21.1, tg47.1, tg57.1, tg65.1) were established with the second round of microinjections. They gave identical results in two genotyping PCRs. These founders have shown the capability of passing the transgene to their phase 1 offspring.

Discussion

1. The results of urine examination for podocytes contrast with those reported by Hara and colleagues (1995 and 1998). This could be partly because they examined selected high risk patients, but it may also be relevant that

podocalyxin can be found on platelets and elsewhere. I looked at a clinically relevant population using clinically applicable tests. I did not find evidence that urinary podocyte excretion commonly occurs at detectable levels in these patients.

2. The tg21.1 and tg57.1 founders produced relatively adequate offspring at phase 1. So, the plan was to stop parents from breeding and preserve them, test some of their phase 1 offspring kidneys with anti-hEGF antibody to look for the expression of hDTR on podocytes and set the rest of their offspring to breed. The parents of tg47.1 and tg65.1 did not produce adequate offspring for anti-hEGF staining, so they are and their phase 1 offspring continue to active breed.

Conclusions

1. Looking for urinary podocytes is not a clinically useful technique in patients with proteinuria.
2. Podocyte construct (pIN) has proved its validity by generating four transgenic founders by male pronuclear microinjection and furthermore, all of them have passed the transgene to their offspring.

Contents

Title	1
Dedication	2
Declaration	3
Acknowledgment	4
Abstract	6
Contents	9
List of figures	15
List of tables	17
Abbreviations	18
 Chapter 1: Introduction	 19
Diseases causing proteinuria are associated with podocytes	20
Minimal change disease and focal segmental glomerulosclerosis	22
Membranous nephropathy	22
Genetic disorders of podocytes	23
Origin and development of podocytes	23
Replication of podocytes	27
Structure of podocytes	29
Filtration slits	33
Function of podocytes	34
Pathology of podocytes	38
Models and mechanisms of podocyte injury	38
Podocyte injury and nephron loss	41
Podocyte injury and loss in urine	44
Aims of the project	51
 Chapter 2: Materials and Methods	 52
Materials	53
Oligonucleotide primers	53

cDNA oligonucleotide primers	53
DNA oligonucleotide primers	54
General materials	57
Patients	57
Ethical permission and approval	57
Methods	58
Nucleic acids methods	58
Total RNA extraction by TRIzol	58
DNaseI treatment and cDNA synthesis	58
cDNA Polymerase chain reaction	60
DNA extraction from cultured human B cells	60
Total RNA extraction by Agilent total RNA isolation mini kit (phenol-free method)	61
Agarose gel electrophoresis	63
cDNA oligonucleotide primers	63
Making and transformation of competent E.coli (DH5) with plasmid DNA	64
Transformation of competent E.coli with plasmid DNA	64
Making of agar plates	65
Minipreparation of plasmid DNA	65
Midipreparation of plasmid DNA	66
Maxipreparation of plasmid DNA	67
Restriction enzyme analysis of plasmid DNA preparation	68
Sequencing of plasmid DNA midipreparation	68
DNA oligonucleotide primers	68
Taq DNA polymerase PCR of murine nephrin gene fragment (podocyte promoter)	69
Proofreading DNA polymerase PCR of murine nephrin gene fragment (podocyte promoter)	69
Purification of PCR product	70

Subcloning of the nephrin gene fragment into pCR [®] 4Blunt-Topo and production of pCR4BN	70
Gel purification of DNA	70
Subcloning of the nephrin gene fragment from pCR4BN into pMS7 and production of pIN (podocyte construct)	71
Microinjection of murine fertilized ova with the plasmid pIN (podocyte construct)	71
DNA extraction from the potentially transgenic mice ear punches	72
Southern blotting hybridization of the potentially transgenic mice DNA	72
Immunofluorescence methods	73
Indirect surface staining of cultured human B cells	73
Cytospin of cultured human B cells and staining with Haematoxylin and Eosin	74
Cytospin and direct surface staining of cultured human B cells with anti-DR, DP, DQ antibody	74
Cytospin and indirect surface staining of cultured human B cells with L243 antibody	75
Staining of HeLa cells with anti-cytokeratin 8 antibody	75
Staining of human kidney sections with anti-synaptopodin antibody	76
Staining of urinary sediments with anti-synaptopodin, anti-WT1 and anti-cytokeratin 8 antibodies	76

Chapter 3: Detection of podocyte-specific proteins mRNA in the urine of proteinuric renal patients	78
Introduction	79
Results	80
Optimization of nephrin and podocalyxin cDNA PCR conditions	80
RNA purification methods do not appear to be equal	81
Glycogen and tRNA are equal in total RNA precipitation	82

β-actin and podocalyxin cDNA primers work on human genomic DNA but nephrin primers do not	83
DNaseI destroys all DNA in the presence of AMV-RT buffer	84
Heat kills DNaseI before cDNA synthesis	85
MMLV-RT appears better than AMV-RT	86
Failure of DNaseI activity explains apparent superiority of MMLV-RT	87
Sensitivity of β-actin, podocalyxin and nephrin cDNA PCR	88
Patients results	89
Discussion	90
 Chapter 4: Detection of podocytes and/or their fragments in the urinary sediment of proteinuric renal patients	94
Introduction	95
Results	96
Indirect surface staining of cultured human B cells	96
Cytospin of cultured human B cells and staining with Haematoxylin and Eosin	97
Cytospin and direct surface staining of cultured human B cells with fluorescence anti-DR, DP, DQ antibody (single layer)	98
Cytospin and indirect surface staining of cultured human B cells with L243 antibody (double layer)	99
Staining of HeLa cells with anti-cytokeratin 8 antibody	100
Staining of human kidney sections with anti-synaptopodin and anti-CD2AP antibodies	101
Staining of urinary sediments with anti-cytokeratin 8 antibody	102
Staining of urinary sediments with anti-synaptopodin antibody	103
Patients results	104
Discussion	105
 Chapter 5: Control experiments on podocytes	108
Introduction	109

Results	110
Staining of podocytes on coverslips with anti-synaptopodin antibody	110
Spiking of urine with podocytes and staining with anti-synaptopodin antibody	111
Spiking of PBS with HeLa cells and staining with anti-cytokeratin 8 antibody	112
Spiking of urine with podocytes and RNA extraction: urinary podocyte mRNA method appears to be working	113
Why all samples were positive for nephrin, podocalyxin and β -actin cDNAs PCR? perhaps be due to contamination	114
Discussion	115

Chapter 6: Production and microinjection of podocyte

Construct	118
Introduction	119
Results	121
Verification of the plasmid pMS7	121
Production of murine nephrin gene fragment (podocyte promoter) with polymerase chain reaction	123
Subcloning of the nephrin gene fragment into pCR [®] 4Blunt-Topo and production of pCR4BN	124
Subcloning of the nephrin gene fragment from pCR4BN into pMS7 and production of pIN (podocyte construct)	125
Mice genotyping primers work on pIN DNA but not wild type mouse DNA	127
Genotyping PCRs for the potentially transgenic mice DNA	128
Genotyping PCRs for the potentially transgenic mice DNA with different annealing temperature	129
Genotyping PCRs for the potentially transgenic mice DNA with low magnesium concentration	130

Genotyping PCRs for the potentially transgenic mice DNA with 40 cycles	131
Control PCR for the potentially transgenic mice DNA genotyping PCR	132
Spiking of the potentially transgenic mice DNA with pIN DNA	133
Measurement of genomic copies of the potentially transgenic mice DNA and pIN copies used in PCR	134
Sensitivity of genotyping PCRs	135
Southern blotting hybridization of the potentially transgenic mice DNA	136
Second microinjection trial proved the effectiveness of the technique: four transgenic founders were established	137
Genotyping PCRs of phase 1 of tg21.1 offspring	138
Genotyping PCRs of phase 1 of tg47.1 offspring	139
Genotyping PCRs of phase 1 of tg57.1 offspring	140
Genotyping PCRs of phase 1 of tg65.1 offspring	141
Discussion	142
 Chapter 7: General discussion	146
General discussion	147
Conclusions	153
Further work	153
 References	154
 Appendix	174

List of figures

- Figure 1.1** The Structure of normal glomerulus.
- Figure 1.2** Scheme of differentiation of individual nephric units.
- Figure 1.3** Peripheral glomerular area.
- Figure 1.4** Podocyte cell architecture.
- Figure 1.5** The composition of the filtration barrier.
- Figure 1.6** Podocyte degenerative changes.
- Figure 2.1** Map of pIN sequencing primers.
- Figure 2.2** Map of mice genotyping primers.
- Figure 2.3** Extracted human genomic DNA.
- Figure 3.1** Optimization of nephrin and podocalyxin cDNA PCR conditions.
- Figure 3.2** TRIzol is better than Agilent kit in RNA purification.
- Figure 3.3** Glycogen and tRNA are equal in total RNA precipitation.
- Figure 3.4** β -actin and podocalyxin cDNA primers work on human DNA.
- Figure 3.5** DNaseI destroys all DNA in RNA prep.
- Figure 3.6** Heat kills DNaseI before cDNA synthesis.
- Figure 3.7** MMLV-RT appears better than AMV-RT.
- Figure 3.8** DNaseI works inefficiently in MMLV-RT buffer.
- Figure 3.9** PCR of urinary β -actin cDNA of proteinuric patients.
- Figure 4.1** Indirect surface staining of cultured human B cells.
- Figure 4.2** Cytospin of cultured human B cells and staining with Haematoxylin and Eosin.
- Figure 4.3** Cytospin and direct surface staining of cultured human B cells with anti-DR, DP, DQ antibody.
- Figure 4.4** Cytospin and indirect surface staining of cultured human B cells with L243 antibody.
- Figure 4.5** Staining of HeLa cells with anti-cytokeratin 8 antibody.
- Figure 4.6** Staining of human kidney sections with anti-synaptopodin antibody.
- Figure 4.7** Staining of urinary sediments with anti-cytokeratin 8 antibody.
- Figure 4.8** Staining of urinary sediments with anti-synaptopodin antibody.
- Figure 5.1** Staining of podocytes with anti-synaptopodin antibody on coverslips.

- Figure 5.2** Staining of spiked urinary podocytes with anti-synaptopodin antibody.
- Figure 5.3** Staining of spiked HeLa cells in PBS with anti-cytokeratin 8 antibody.
- Figure 5.4** PCR of spiked urinary podocytes cDNAs.
- Figure 5.5** Podocalyxin cDNA PCR.
- Figure 6.1** Enzyme restriction analysis of pMS7 DNA midipreparation.
- Figure 6.2** restriction enzyme analysis and sequencing map of pMS7.
- Figure 6.3** Nephtrin gene fragment PCR.
- Figure 6.4** Enzyme restriction analysis of pCR4BN DNA minipreparation and midipreparation.
- Figure 6.5** Enzyme restriction analysis of pIN DNA minipreparation, midipreparation and maxipreparation.
- Figure 6.6** pIN map.
- Figure 6.7** Optimization of genotyping PCRs.
- Figure 6.8** The potentially transgenic mice genotyping (16 samples).
- Figure 6.9** Genotyping PCRs with different annealing temperature.
- Figure 6.10** Genotyping PCRs with low magnesium concentration.
- Figure 6.11** Genotyping PCRs with 40 cycles.
- Figure 6.12** Control PCR for the potentially transgenic mice DNA genotyping PCR.
- Figure 6.13** Spiking of the potentially transgenic mice DNA with pIN DNA.
- Figure 6.14** Sensitivity of genotyping PCRs.
- Figure 6.15** Southern blotting hybridization of the potentially transgenic mice DNA.
- Figure 6.16** Genotyping PCRs of the transgenic founders.
- Figure 6.17** Genotyping PCRs of phase 1 of tg21.1 offspring.
- Figure 6.18** Genotyping PCRs of phase 1 of tg47.1 offspring.
- Figure 6.19** Genotyping PCRs of phase 1 of tg57.1 offspring.
- Figure 6.20** Genotyping PCRs of phase 1 of tg65.1 offspring.

List of tables

Table 1.1	Urinary podocalyxin excretion in different renal diseases.
Table 1.2	Urinary podocytes in different renal diseases.
Table 1.3	Effect of treatment on urinary podocytes.

Abbreviations

ACE	Angiotensin converting enzyme.
AHN	Active Heymann nephritis.
AMV-RT	Avian myeloblastosis virus reverse transcriptase.
Ang II	Angiotensin II.
CD2AP	CD2-associated protein.
DT	Diphtheria toxin.
FGF-2	Fibroblast growth factor-2.
FSGS	Focal and segmental glomerulosclerosis.
GBM	Glomerular basement membrane.
GLEPP1	Glomerular epithelial protein 1.
hDTR	Human diphtheria toxin receptor.
hHB-EGF cDNA	Human Heparin Binding-Epidermal Growth Factor cDNA.
MAP 3	Membrane associated protein 3.
MAP 4	Membrane associated protein 4.
MCD	Minimal change disease.
MMLV-RT	Moloney murine leukaemia virus reverse transcriptase.
MN	Membranous nephropathy.
PAN	Puromycin aminonucleoside nephrosis.
PCR	Polymerase chain reaction.
PHN	Passive Heymann nephritis.
RT-PCR	Reverse transcriptase-polymerase chain reaction.
TGF-β	Transforming growth factor- β .
WT1	Wilm's tumour suppressor gene.
ZO-1	Zonula occludens 1.

Chapter 1

Introduction

This thesis concerns the podocyte in proteinuric renal diseases. In the Introduction, first there is a brief description of the human diseases in which podocyte injury seem to be central in their pathogenesis. Second, podocytes origin and development are discussed because the importance of the limited proliferation capacity of these cells after their injury in glomerular diseases. Third, podocytes structure and function are covered because they form the final barrier of protein loss during glomerular filtration. Fourth, animal models and mechanisms of podocytes injury are reviewed with their relation to clinical practice, as well as the evidence behind urinary podocyte in glomerular diseases. Finally, at the end of this chapter the aims of this project are presented.

The podocyte is one of four cell types that are found in the glomerulus; endothelial cells, mesangial cells, parietal epithelial cells and visceral epithelial cells (podocytes). The endothelial cells cover the inner aspects of the capillary loops; mesangial cells and mesangial matrix occupy the axial region of the capillary convolute and parietal epithelial cells cover the inner aspect of Bowman's capsule (figure 1.1).

Podocytes are highly specialized and terminally differentiated epithelial cells with complex morphology which cover the outer surface of the glomerular basement membrane (GBM) and form the final barrier to protein loss during glomerular filtration process (figure 1.1).

Diseases causing proteinuria are associated with podocytes

The evidence for a central role of podocyte injury in the development of glomerular disease is substantial. The early events of podocyte injury are characterised by the presence of proteinuria even without any detectable morphological changes, and further damage to podocytes is central to the development of focal and complete glomerulosclerosis and the development of chronic renal failure.

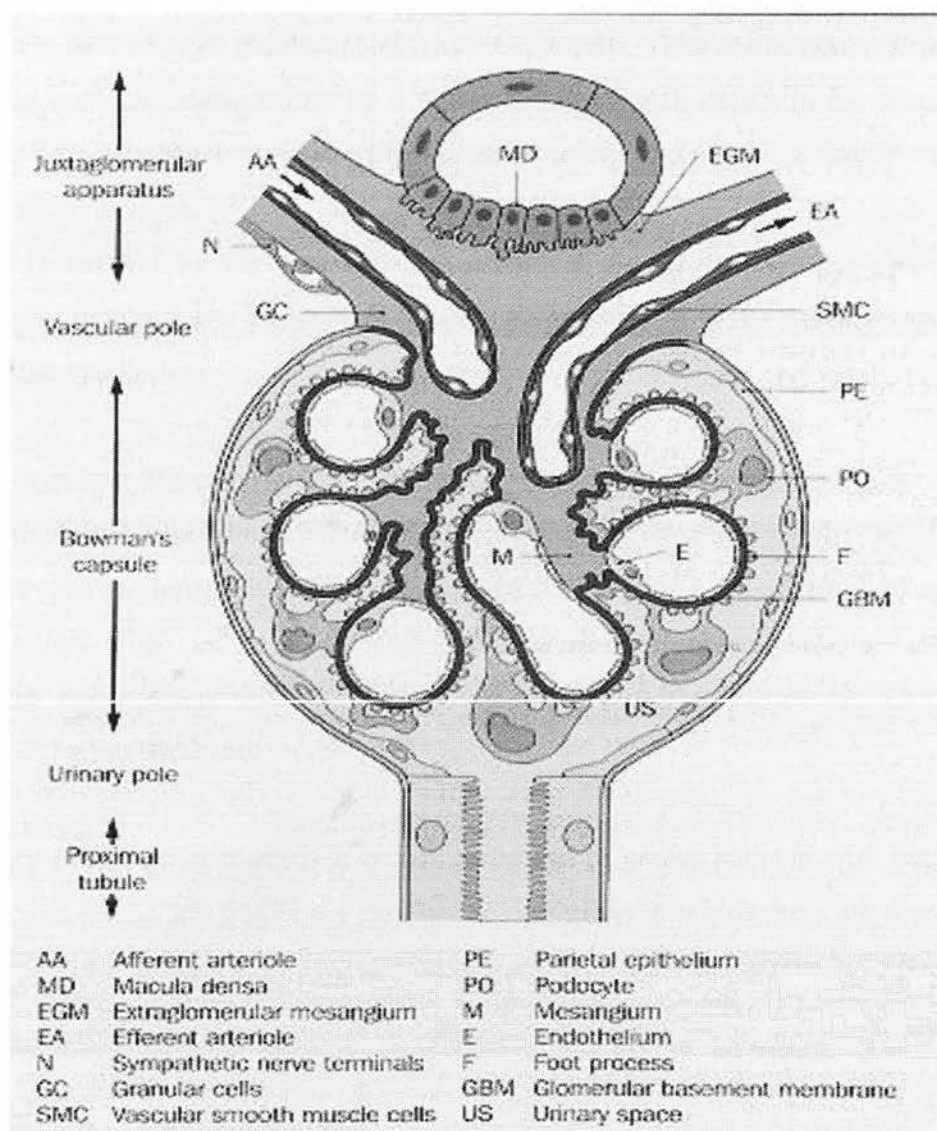


Figure 1.1. The Structure of normal glomerulus
(Feehally and Johnson, 2000)

Minimal change disease and focal segmental glomerulosclerosis

Minimal change disease (MCD) and focal segmental glomerulosclerosis (FSGS) are the cause of nephrotic syndrome in about 90% of children aged less than 10 years, about 50-70% of older children, and 20-35% of adults. They are considered together because both are characterised by a diffuse capillary wall defect in the absence of immune deposits, have common clinical features, and are treated in a similar way.

MCD is defined by the absence of histological glomerular changes apart from podocyte foot process effacement in patients presenting with steroid responsive nephrotic syndrome.

FSGS was first described in 1957 and is now a common glomerular lesion in patients with nephrotic and non-nephrotic range proteinuria. It accounts for 10-30% of chronic glomerulonephritis. FSGS is defined histologically by segmental capillary obliteration with increased mesangial matrix deposition, intracapillary hyaline deposits, podocytes proliferation (in some variants) and focal adhesions of capillary tuft to Bowman's capsule.

Primary FSGS (idiopathic) is a common disease in young patients with nephrotic syndrome. Secondary FSGS is a mixture of conditions in which there are segmental scars, and as discussed later progression of these diseases may be related to podocyte injury.

Membranous nephropathy

Membranous nephropathy (MN) is the main cause of nephrotic syndrome in adults. It is a glomerular disease characterised by the thickening of the glomerular capillary wall without any increase in the mesangial cellularity or expansion, and immune deposits (IgG and complements components) development on the subepithelial surface of the glomerular capillary wall. The deposition of these immune complexes leads to the increase of glomerular permeability to proteins and development of nephrotic syndrome. MN is associated commonly with systemic lupus

erythematusus, diabetes mellitus, hepatitis B infection, drugs (gold, penicillamine and non-steroidal anti-inflammatory agents) and malignancy.

Experimental evidence (below, pathology of podocytes) also points to a central role of podocytes in the pathogenesis of MCD, FSGS and MN.

Genetic disorders of podocytes

Mutations of podocyte proteins genes cause inherited proteinuric diseases. Nephrin gene (NPHS1) mutation leads to the development of Finnish type nephrotic syndrome (Kestila et al., 1998). CD2 associated protein (CD2AP) gene mutation leads to congenital nephrotic syndrome (Shih et al., 1999). Podocin gene (NPHS2) mutation leads to the development of autosomal recessive FSGS (Boute et al., 2000). α -Actinin-4 gene (ACTN-4) mutation leads to the development of autosomal dominant FSGS (Kaplan et al., 2000). Wilm's tumour suppressor gene (WT1) mutation leads to primary steroid-resistant FSGS (Denamur et al., 2000).

Origin and development of podocytes

The epithelial cells of most organs of the body form by an extension of a pre-existing epithelial sheet during embryogenesis by a process known as branching morphogenesis. The epithelial cells of the ureter and collecting ducts form by such a process (Grobstein, 1953; Saxen, 1987). The epithelial cells of tubules and within the glomeruli are formed by direct conversion of mesenchyme to epithelium (Saxen, 1987).

Human metanephric development begins during the fifth week of gestation (figure 1.2). It is characterised by aggregation of nephrogenic mesenchyme opposite to branches of the ureteral bud (vesicle stage), formation of the primitive S body consisting of presumptive glomerular and tubular epithelium, followed sequentially by capillary ingrowth, GBM formation, and differentiation of glomerular parietal, visceral and tubular epithelium. Development proceeds in a centrifugal fashion as newly forming glomeruli are layered in opposition to more mature glomeruli (Platt et al., 1983).

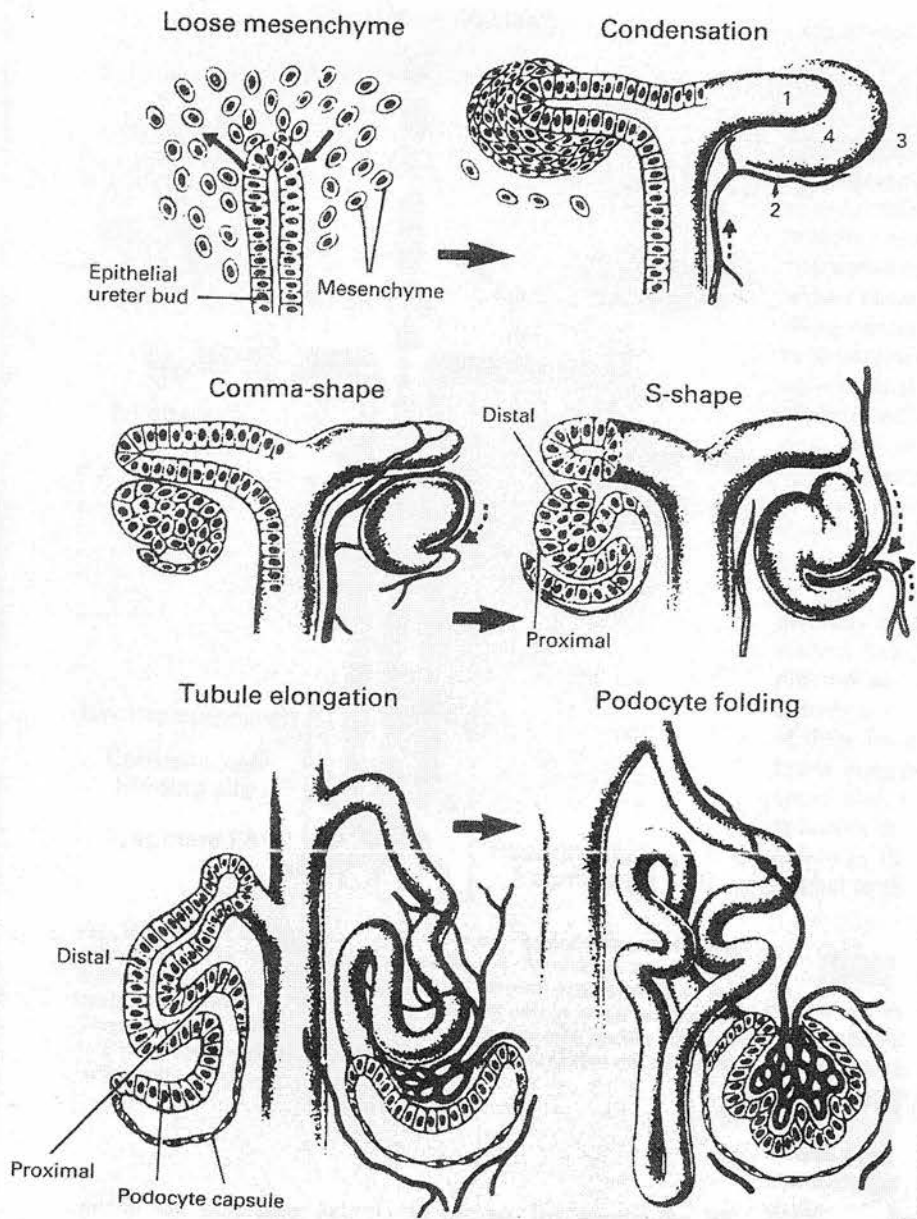


Figure 1.2. Scheme of differentiation of individual nephric units.

The epithelial ureter bud will branch into the mesenchyme as a result of an interaction between the ureter and mesenchyme (indicated by arrows). The stage at the top right shows the different cell lineages that begin to emerge once the ureter epithelium has branched once into the mesenchyme; (1) ureter epithelium, (2) blood vessels, (3) uncondensed mesenchyme that will differentiate into stroma, (4) condensed mesenchyme that will convert into epithelium. The condensed mesenchyme soon develops into a comma-shaped and S-shaped epithelium, and proximal and distal tubules can be distinguished. The glomerulus has begun to form at S-shaped stage. Blood vessels can be seen within the developing glomerulus at the comma shaped stage (Sorokin and Ekblom, 1992).

In mouse at eleven days of gestation the ureter begins to grow into the metanephric mesenchyme, initiating epithelial tube formation. In turn mesenchyme stimulates further ingrowth and branching of the ureter (figure. 1.2). It is at the branching tips of the ureter that mesenchyme is induced to form epithelium (Sorokin and Ekblom, 1992).

Epithelial cell development can be stimulated *in vivo* by the epithelium of the ureter (Sorokin and Ekblom, 1992) and *in vitro* by a spinal cord (Saxen et al., 1983). Nephron segmentation *in vitro* into Bowman's capsule, glomerular podocytes, and distal and proximal tubules is similar to that occurs *in vivo* (Ekblom et al., 1981).

Saxen (1987) reported that glomerular (and podocyte) development can be divided into four stages (renal vesicle, S-shaped body stage, capillary loop stage and maturing glomeruli). The early stages of podocyte development are renal vesicle stage and S-shaped body stage; the later stages represent the more advanced stages of podocyte maturation (Mundel and Kriz, 1995).

Immature cells (vesicle and S-shaped body stages) have high rate of multiplication; this is related to the expression of the proliferating cell nuclear antigen (PCNA) in these cells. This is not expressed by capillary loop stage cells (Nagata et al., 1993). Mitotic figures are frequently seen in the nephrogenic vesicle and S-shaped bodies (Nagata et al., 1993). Developing podocytes lose their mitotic activity once they reach capillary loop stage of their development (Nagata et al., 1993; Mundel and Kriz, 1995).

During S-shaped body stage the occluding junctions appear at the apical surface of the developing podocytes. These occluding junctions migrate from the apex to the base. Initially broad epithelial processes cover the whole outer aspect of the developing basement membrane. After junctional migration interdigitation of epithelial processes is seen, and the processes are joined by focal occluding junctions. With more elaborate interdigitation, fewer intercellular spaces are closed by occluding junctions. The junctions become less and less extensive, and normal slit

architecture with foot processes bridged by slit membranes start to form (Reeves et al., 1978; Reeves et al., 1980). When developing podocytes enter the capillary loop stage their complex architecture starts to establish. This includes the appearance of foot processes and formation of slit diaphragms (Mundel and Kriz, 1995).

A number of proteins that are podocyte-specific in adult kidney start to appear about S-shaped stage of glomerulogenesis:

- Schnabel and associates (1989) examined the appearance and distribution of podocalyxin on the podocytes during glomerulogenesis. They found that podocalyxin appeared first on the apical surface of the developing podocytes of the S-shaped body above the level of occluding junctions. Podocalyxin becomes detectable during S-shaped body stage of glomerular development on the apical and lateral surfaces of podocytes, shortly after the migration of occluding junctions (Reeves et al., 1978).
- The foot processes of podocytes are attached together by slit diaphragm. One of the components of this structure is zonula occludens1 (ZO-1), a protein that is specific for tight junctions. It appears during S-shaped body stage of glomerular development. It was present when the apical junctional complexes between presumptive podocytes are composed of typical tight and adhering junctions, they migrate together along the lateral cell surface, disappeared and replaced by slit diaphragms (Schnabel et al., 1990).
- Mundlos and colleagues (1993) demonstrated that the expression of Wilm's tumour suppressor gene (WT1) protein occurs during S-shaped body stage of glomerulogenesis and reaches its highest level in this stage also.

During the maturing glomeruli stage, the glomeruli resemble those in adult kidneys but their diameter is smaller in rats (Abrahamson, 1991). Double basement membranes (subepithelial and subendothelial), which appear during earlier stages of development, disappear at this stage (Senior et al., 1988; Laurie et al., 1989).

Basement membrane laminin synthesis is now mostly performed by mature podocytes (Abrahamson and Perry, 1986). At capillary loops expansion areas where podocytes foot processes formation and interdigitation becomes more active, loops of GBM localize at subepithelial areas (Abrahamson, 1986; Abrahamson, 1987).

Replication of podocytes

It is often suggested that podocytes are post-mitotic cells, and that once injured they can not replicate to compensate the dead cells, but as pointed by Nagata and collaborators (1993) no studies have demonstrated that unequivocally. Podocytes have a differentiated cell shape and are found in unique position. Their cell bodies are floating within the filtrate in Bowman's capsule and attached to glomerular capillaries by the foot processes. This arrangement seems to be incompatible with cell replication (Nagata and Kriz, 1992).

Several studies have shown that podocytes do not replicate during postnatal normal life, under the effect of different experimental injuries and during hypertrophic renal growth (Pabst and Sterzel, 1983; Rasch and Norgaard, 1983; Fries et al., 1989; Nagata and Kriz, 1992).

Nagata and Kriz (1992) analyzed podocytes lesion in young rats after uninephrectomy. They reported that with overall glomerular growth after uninephrectomy, a pronounced hypertrophy of podocytes was observed but the mean number of podocytes per glomerulus did not change. They assumed that podocytes can not sustain the same degree of growth as the glomerular tuft as a whole, and podocyte hypertrophy is soon followed by maladaptive changes which end with cell destruction.

It has been suggested that the occasional appearance of mitotic figures (Pabst and Sterzel, 1983; Rasch and Norgaard, 1983; Schwartz and Lewis, 1985) may be explained by incomplete mitosis leading to binucleated or multinucleated cells. A study by Shankland and co-workers (1997) showed that the low proliferative capacity of podocytes in response to an injury may be due to an increase in the

expression of a specific cyclin kinase inhibitors p21 and p27 which block the important regulatory role of cyclins in cell proliferation.

Other studies have shown that although podocytes can undergo mitosis but not complete cell division during postnatal life or under experimental and pathological conditions, collapsing glomerulopathies including HIV-associated nephropathy and idiopathic collapsing glomerulopathy were exceptions to this rule (Barisoni et al., 1999; Barisoni et al., 2000). They demonstrated that podocytes de-differentiate, as reflected by loss of maturity markers such as synaptopodin. Podocyte proliferation leads to pseudocrescent formation and compression of glomerular tuft (Barisoni et al., 2000).

Kriz and associates (1994c) demonstrated that podocytes under certain stimuli can re-enter the cell cycle and undergo mitosis but can not complete cell division. They examined the effects of the fibroblast growth factor 2 (FGF-2) on the podocytes and observed the appearance of binucleated or multinucleated cells and mitotic figures. These cells exhibited degeneration changes including cell body attenuation, extensive pseudocysts formation, foot processes fusion and local detachment from the GBM. They concluded that podocytes can enter mitosis but can not complete cell division.

Podocytes failure to complete cell division appears to be of a critical importance for chronic renal failure development. Their inadequate proliferative response following an injury may contribute to the development of progressive glomerulosclerosis in different glomerular diseases (Kriz et al., 1994a; Shankland et al., 1997).

On the other hand urinary podocytes from rats with experimental membranous nephropathy (Petermann et al., 2003) and experimental diabetic nephropathy (Petermann et al., 2004) can be grown, replicate and increase in number in tissue culture.

It can be seen that differentiated podocytes can undergo mitosis but not complete cell division and in contrast to that, de-differentiated podocytes can proliferate.

Structure of podocytes

The GBM provides the primary structural support for the glomerular tuft. The basic unit of glomerular tuft is a single capillary. Endothelial and mesangial cells are located inside the GBM and podocytes are attached to its outer aspect. (Mundel and Kriz, 1995). Podocytes are highly differentiated cells. They can be divided into three structurally and functionally different parts: cell body, major processes and foot processes. Cell bodies and major processes are not attached directly to the GBM, but float freely in the filtrate in Bowman's space, leaving a sub-cell body space between the cell body and the foot processes (figure 1.3). From the cell body major processes arise directly or after additional branching, split into foot processes. The foot processes will form a characteristic interdigitating pattern with foot processes of neighbouring cells (figure 1.4), leaving in between the filtration slits (Mundel and Kriz, 1995; Kriz et al., 1998a).

Podocytes have a large nucleus and prominent nucleolus (figure 1.3). Their cell body contains a well-developed Golgi system, abundant rough and smooth endoplasmic reticulum, prominent lysosomes, and many mitochondria. The well-developed endoplasmic reticulum and Golgi apparatus reflect a high capacity for protein synthesis. They also contain endocytotic vesicles and multivesicular bodies which suggest strong endocytotic activity (Mundel and Kriz, 1995; Kriz et al., 1998a).

Podocytes have a complex shape; this is primarily related to their well-developed cytoskeleton which maintains also podocytes processes (Kriz et al., 1998a). Drenckhahn and Franke (1988) found that microtubules and intermediate filaments, such as vimentin and desmin, dominate in the cell body and primary processes as well the foot processes. This system is composed of actin, myosin II, α -actin, talin, and vinculin.

Microtubule-associated protein 3 (MAP 3), is a heat stable protein. It is distributed in many tissues and MAP 3 containing cells appeared to have in common a symmetric morphology with long processes that need structural support. In kidney MAP 3 is limited to podocytes and associated with microtubules and intermediate filaments but not with microfilaments (Huber and Matus, 1990). Abundant amounts of microfilaments are located in the foot processes. It has been reported that a complete microfilament-based contractile apparatus is present in microtubule-associated protein 4 (MAP 4), and found to be associated with the prominent bundles of microtubules in the large processes (Parysek et al., 1984).

The microfilaments loop-shaped bundles, with their limbs run in the longitudinal axis of the foot processes. The bends of these loops are located centrally at the transition to the primary processes, and are probably connected to the microtubules by another microtubule associated protein, namely τ (tau), which is located at those sites (Sanden et al., 1995).

Kriz and colleagues (1994d) demonstrated that, peripherally, the actin bundles appear to anchor in the dense cytoplasm associated with the basal cell membrane of podocytes, the sole plates of foot processes. Adler (1992), Cybulsky and collaborators (1992) reported that sole plates of podocyte foot processes anchoring to the GBM by $\alpha 3\beta 1$ -integrin. Integrins interact with the actin cytoskeleton via talin and vinculin within the dense cytoplasm of the sole plates (Kriz et al., 1998a).

Podocytes are polarized epithelial cells with luminal and abluminal membrane domains. The border between the abluminal and luminal membranes is delineated by the slit diaphragm (Mundel and Kriz, 1995; Kriz et al., 1998a). The abluminal domain is completely embedded into the GBM

The luminal membrane of podocytes contains several specialized membrane proteins; which some of them have been used as a podocyte identification markers as described below; including the complement receptor C3b (shin et al., 1977), the gp330/megalin (Kerjaschki and Farquhar, 1983), the human equivalent of

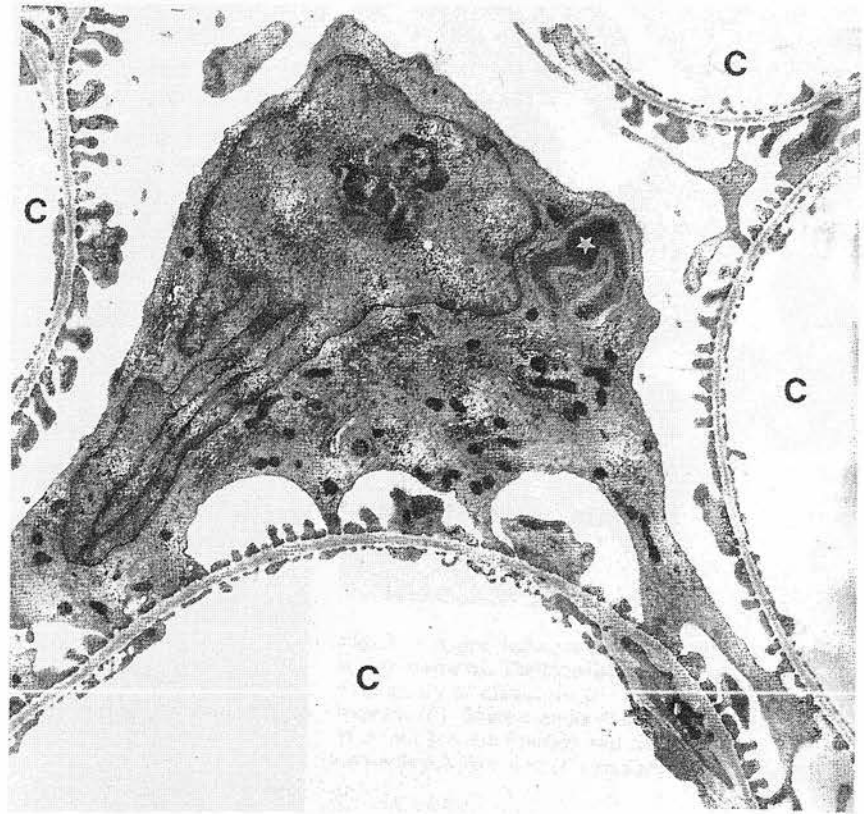


Figure 1.3. Peripheral glomerular area.

Four capillary loops (c) are seen with a podocyte in the centre. Podocyte cell bodies are connected to the capillary wall by their cell processes, which establish the interdigitating foot process pattern on the outer surface of the GBM. Near the nucleus with a prominent nucleolus, a characteristic membrane bound inclusion body (asterix) is seen (Mundel and Kriz, 1995).

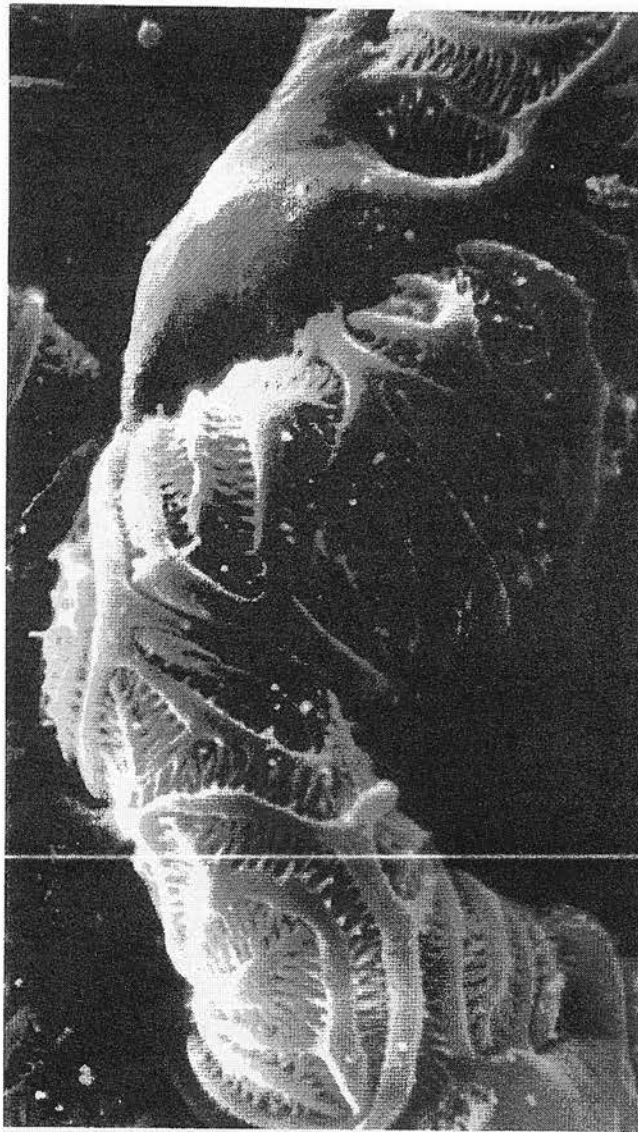


Figure 1.4. Podocyte cell architecture.

Large cell bodies are seen that are fixed to the capillaries by their major processes. Foot processes arise from the major processes and form the characteristic interdigitating pattern with the foot processes of a neighbouring cell, leaving in between the filtration slits (Mundel and Kriz, 1995).

podocalyxin (Kerjaschki et al., 1986), dipeptidyl peptidase IV (Natori et al., 1987), the endothelial and podocyte 1 antigen (EnPo 1 antigen) (Kloth et al., 1992), The glomerular epithelial protein 1 (GLEPP1) (Thomas et al., 1994), the Alzheimer amyloid precursor protein (Beer et al., 1995), and a 43 KD transmembrane protein (Breiteneder et al., 1995).

On the luminal surface of podocytes is a well-developed glycocalyx which is composed of sialoglycoproteins. Kerjaschki and associates (1984), Huang and Langlois (1985) reported that podocalyxin and podoendin respectively are part of these sialoglycoproteins. Mendrick and Rennke (1988) showed that sialoglycoprotein 115/107 KD (SGP 115/107) is part of the sialoglycoproteins on the luminal surface of podocytes.

Cholesterol is present in the luminal podocytes membrane. Orci and co-workers (1982) believed that cholesterol has an important role in the stability of podocytes shape, and its complexes link the cytoskeletal components to the cell membrane.

Filtration slits

The filtration slits are the sites of fluid flow between the podocytes. The slit diaphragm which is the principal filtration barrier to plasma proteins has a continuous junctional band, 300-500 Å wide, present in all filtration slits, and formed in podocytes foot processes. It was proposed that, the slit diaphragm has a zipper-like structure with alternating periodic cross bridges extending from the podocyte plasma membrane to a central filament which run parallel to and equidistant from the cell membranes. The dimension and spacing of the cross bridges defined a uniform population of a rectangular slits approximately 40 by 140 Å in cross section and 70 Å in length. The total area of the slits is 2-3% of the total surface area of the glomerular capillaries (Rodewald and Karnovsky, 1974; Furukawa et al., 1991).

Wartiovaara and colleagues (2004) reported using electron tomography that, the slit diaphragm is a uniformly wide organised network of winding strands. The complex network contains a class of 35 nm long cross strands which border lateral pores

smaller than albumin and stains for nephrin. They also reported that, patients with Finnish type nephrotic syndrome and nephrin knockout mice have narrow filtration slits lacking the slit diaphragm and the 35 nm strands. These results suggested an important role of nephrin in the structure of slit diaphragm and its pores.

Nephrin was the first protein to be localized to the slit diaphragm area (Holthofer et al., 1999; Holzman et al., 1999). It is a transmembrane protein with structural and signalling functions. It associates intracellularly with podocin (Roselli et al., 2002) and CD2AP (Shin et al., 2001). Other proteins localized at the slit diaphragm area include the tight junction protein ZO-1 (Schnabel et al., 1990), α , β , and γ catenin (Reiser et al., 2000), FAT which is a member of the cadherin superfamily (Inoue et al., 2001), and P-cadherin (Reiser et al., 2000).

Function of podocytes

Podocytes have many functions including GBM turnover, maintenance of the filtration barrier, capillary tuft support, and regulation of glomerular filtration.

The GBM is located between the endothelial cells and the podocytes. It usually thought that the GBM primarily is derived from the epithelium. Podocytes have long been known to synthesize type IV collagen (Walker, 1973). However, endothelial cells express (Foidart and Reddi, 1980; Foidart et al., 1980) and can under culture conditions, synthesized basement membrane (Jaffe et al., 1976). Sariola and colleagues (1984) demonstrated that podocytes and glomerular endothelial cells contribute to the formation of GBM. Lee and collaborators (1993) found that the mesangium has a role in the synthesis of GBM. However from an in vitro model lacking endothelial and mesangial cells, podocytes alone are able to synthesize a complete basement membrane (Bernstein et al., 1981; Bonadio et al., 1984).

The protein components of the GBM synthesized by the podocytes include type IV collagen (Courtoy et al., 1982), heparan sulphate proteoglycan (Stow et al., 1989), laminin (Abrahamson, 1985; St John and Abrahamson, 2001), fibronectin (Courtoy et al., 1982), entactin (Bender et al., 1981), and syndecan (Vainio et al., 1989).

The filtration slits are very permeable to water but prevent passage of most serum albumin and larger plasma proteins. The filtration barrier consists of the fenestrated endothelium, the GBM, and the podocytes foot processes with the interposed slit membrane (figure 1.5). The filtration route is extracellular and the filtrate passes through the endothelial fenestrate, across the GBM, and through the slit diaphragms of the filtration slits. Charge, size, and shape determine the specific permeability of a macromolecule. It has been suggested that intrinsic negative charges which prevent protein loss are present in the GBM (Rennke et al., 1975), but Daniels (1994) found that the restriction in albumin permeability due to glomerular charge requires the presence of glomerular cells. Other studies suggest that the component responsible for size selectivity is the slit membrane, and it is responsible for a half of the hydraulic resistance while the GBM is responsible for the other half (Daniels et al., 1992; Drumond and Deen, 1994; Edwards et al., 1997a; Edwards et al., 1997b).

Podocytes and mesangium have an important role in the structural support of the glomerular capillaries. They stabilize the folding pattern of the glomerular tuft and then the architecture of the capillaries. Kriz and co-workers (1994b) demonstrated that podocytes can provide the stabilizing function alone without the mesangium. Podocytes also counterbalance the expanding force on the capillary wall exerted by the transmural pressure gradient.

Kriz and collaborators (1998a) explained the cytoskeletal organization of the podocytes processes and their relevance to the support function. Firstly, podocytes interconnect neighbouring capillaries, thereby maintaining the folding pattern of the glomerular tuft (Mundel and Kriz, 1995). Podocytes frequently fill the narrow angles between neighbouring capillaries by large cell processes, thereby fixing opposite parts of the GBM onto one another. The podocytes processes filling these angles contain microfilaments, and are sites of the synaptopodin accumulation (Mundel et al., 1991). The relevance in maintaining these angles is seen after total mesangial dissolution (Bagchus et al., 1986). Even after total mesangiolysis, those angles are

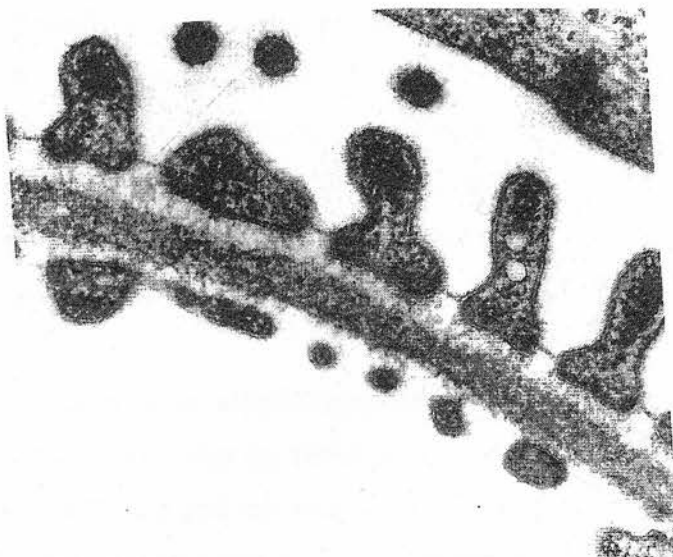


Figure 1.5. The composition of the filtration barrier.

The glomerular filter consists of three components: fenestrated endothelium, GBM, and podocyte foot processes with the interposed slit membrane (Mundel and Kriz, 1995).

maintained and stabilizing the folding pattern of the GBM (Kriz et al., 1995a). Secondly, podocytes are attached by foot processes to the external surface of GBM and act as numerous, small stabilizing patches on the GBM, counteracting locally the elastic distension of the GBM.

Glomerular filtration is determined by the transmural pressure gradient and the ultrafiltration coefficient (glomerular filtration rate = transmural pressure gradient X ultrafiltration coefficient). The ultrafiltration coefficient is the product of the hydraulic permeability and filtration area. Dworkin and Brenner (1992) believe that the regulation of ultrafiltration coefficient occurs through changes in filtration area due to an action of the mesangium, but several other studies do not support this assumption (Sakai and Kriz, 1987; Anderson et al., 1989; Denton et al., 1992).

The role of podocytes in ultrafiltration coefficient regulation is not fully clear. Andrews (1988) reported that the filtration slit area is responsible for the changes of ultrafiltration coefficient and this was supported by the correlation of ultrafiltration coefficient reduction with decrease in total filtration slit length in membranous and minimal change nephropathies (Drumond et al., 1994).

Podocytes may regulate ultrafiltration coefficient by a dynamic function and this is supported by the presence of many vasoactive substances receptors on the podocytes and they include: atrial natriuretic peptide (Yamamoto et al., 1994; Zhao et al., 1994), bradykinin (Pavenstadt et al., 1992; Ardaillou et al., 1996), nitric oxide (Mundel et al., 1995), angiotensin II (Yamada et al., 1990; Shake et al., 1992; Sharma et al., 1992; Gloy et al., 1997; Henger et al., 1997), parathyroid hormone and parathyroid hormone-related peptide (Lee et al., 1996; Massfelder et al., 1996), and acetylcholine (Lebrun et al., 1992).

Pathology of podocytes

Models and mechanisms of podocyte injury

There are a number of experimental models of podocyte injury with observed anatomical and functional changes which strongly suggest that podocyte injury is important.

Puromycin aminonucleoside nephrosis (PAN) is a model of minimal change nephropathy and FSGS. The injection of PAN leads to podocyte foot processes effacement and development of proteinuria (Inokuchi et al., 1996) which progresses to focal glomerulosclerosis (Diamond and Karnovsky., 1986). Expression of α -actinin which precedes foot processes effacement increased in podocytes in PAN (Smoyer et al., 1997). An increase in the expression of heparanase which mediates loss of glomerular charge selectivity has been reported in PAN (Levidiotis et al., 2001). Upregulation of heparin-binding epidermal growth factor-like growth factor has been found in PAN (Paizis et al., 1999), and the injection of a monoclonal antibody to it was reported to be followed by an increase in the PAN-induced proteinuria and decrease in podocyte adhesion to laminin and fibronectin, suggesting the epidermal growth factor-like growth factor has a role in podocytes adhesion (Khong et al., 2000). PAN-induced proteinuria is associated with downregulation of nephrin mRNA and protein expression (Khong et al., 2000), decreased expression of podoplanin (Breiteneder et al., 1997) and disruption of podocalyxin-erizn complexes (Takeda et al., 2001).

Protamine sulphate (PS) injection causes podocyte changes similar to those occur in PAN nephropathy (Andrews, 1975). PS nephropathy is associated with an increase in the expression of podocytes phosphotyrosine and the newly phosphorylated proteins are concentrated along newly formed tight junctions and basal membrane of the foot processes. ZO-1 was found to be a target of tyrosine phosphorylation (Kurihara et al., 1992). The effect of PS on podocytes can be controlled by tyrosine phosphatases (Reiser et al., 2000). PS nephropathy is also associated with processes retraction, cell

rounding and loss of actin filament bundles (Reiser et al., 2000). PS causes an increase in $[Ca^{2+}]_i$ in podocytes which is not completely reversible leading to the suggestion that PS induces an impairment of $[Ca^{2+}]_i$ regulation (Rudiger et al., 1999). This was supported by the finding that perfusion of kidneys with PS nephropathy with a low extracellular Ca^{2+} solution lead to 50% reduction in podocytes damage (Kerjaschki., 1978).

Complement activation is a crucial step in the induction of complement-mediated podocyte injury and development of proteinuria. Depletion of complement completely inhibits proteinuria (Cybulsky et al., 1986; Savin et al., 1994). Active Heymann nephritis (AHN) is a model of human membranous nephropathy which was developed in rats by immunising them with fraction 1A (a crude renal tubular preparation). This immunisation induced the production of IgG autoantibodies after the formation of large subepithelial immune deposits which include IgG, C3, and membrane attack components (C5b-9) of complement (Heymann et al., 1967; Kerjaschki and Neale, 1996). Most of the animals developed proteinuria within 8 weeks of immunization. The target autoantigen of AHN is a transmembrane renal glycoprotein named megalin. Passive Heymann nephritis (PHN) can be induced by injecting a heterologous antibody against rat megalin or fraction 1A into rat, so unlike AHN this is not an autoimmune disease. Progressive staining of heterologous IgG in the subepithelial immune deposits is associated with podocyte foot process effacement. C3 and C5b-9 membrane attack complex are also present in distribution similar to heterologous IgG, which suggest that IgG in the immune complexes may activate complement (Kerjaschki and Neale, 1996).

Fibroblast growth factor-2 (FGF-2) has a role in the regulation of basic functions of podocytes. Podocytes from FGF-2 knock-out mice grow tightly one to another, they have actin disorganization, decreased expression of synaptopodin and WT1, inhibition of their mesenchymal differentiation and abnormal ZO-1 expression (Davidson et al., 2001). Long term treatment of rats with FGF-2 lead to the development of albuminuria, podocyte injury, FSGS and chronic renal failure. Mitotic figures have been observed in podocytes of these rats without real cell

division and because of that it has been suggested that FGF-2 stimulate podocytes to undergo mitosis (Kriz et al., 1995b).

The reactive oxygen product hydrogen peroxide (H_2O_2) is a cellular injury mediator and acts directly or indirectly as a source of hypochloride, which is formed in the presence of chloride and myeloperoxidase, an enzyme secreted by polymorphonuclear white blood cells (Johnson et al., 1994). In vivo investigation of H_2O_2 glomerular toxicity has shown that its intra-arterial injection leads to derangement in glomerular permselectivity. H_2O_2 induced proteinuria was inhibited by pre-treatment with catalase, and by desferrioxamine which suggested that its toxicity is iron dependent (Yoshioka et al., 1991). Many glomerular diseases have been associated with high level of reactive oxygen species including puromycin nephrosis (Ricardo et al., 1975), Heyman nephritis (Shah, 1988) and the Mpv 17 (-/-) mouse, a model of steroid-resistant FSGS (Binder et al., 1999). Pre-treatment of these animals with the scavengers of reactive oxygen species has been shown to prevent foot processes effacement and proteinuria (Ricardo et al., 1975; Shah., 1988; Grone et al., 1997; Binder et al., 1999).

It has been reported that mechanical stress induces a change in cultured mouse podocyte morphology and actin skeleton reorganization, like thinning and elongation of foot processes and reduction in cell body size (Endlich et al., 2001). Mechanical stress decreases podocytes growth (Petermann et al., 2002).

The understanding of podocyte role in the development of experimental glomerular disease and proteinuria made them a potential target of treatment of proteinuria in clinical practice. This was described in Angiotensin converting enzyme (ACE) inhibitors (Ruggeneti et al., 2000) and angiotensin II (Ang II) receptors blockers (Nakamura et al., 1999) which have beneficial effects on proteinuria and progression of chronic renal disease.

It has been suggested that podocytes counteract the pressure dependent elastic distension of glomerular capillaries. Failure to do so in the presence of high glomerular pressure leads to capillary dilatation, a condition which was reported to precede the development of segmental glomerulosclerosis (Kriz et al., 1998b). Based on that ACE inhibitors and Ang II receptors blockers protect podocytes indirectly by controlling high glomerular pressure and in turn prevent the development of glomerulosclerosis.

Podocyte injury and nephron loss

There is strong evidence to support the hypothesis that, if podocyte can not be readily replaced in glomerular disease, as suggested above this may lead eventually to nephron loss, reduction in renal function and development of chronic renal diseases. Podocyte injury can lead to glomerular degenerative and inflammatory changes and development of FSGS and glomerular crescent respectively (Pavenstadt et al., 2003).

The hypothesis of degenerative changes of podocytes has been principally described by Kriz's group in different animal models of glomerular diseases including; glomerular hypertension (Nagata et al., 1992), after long treatment with FGF-2 (Kriz et al., 1995b) and in Milan normotensive rats (Floege et al., 1997).

The degenerative changes of podocytes in glomerular diseases (figure 1.6) consists of cell hypertrophy, foot process effacement, cell body attenuation, pseudocyst formation, cytoplasmic overload with reabsorption droplets, and finally detachment from GBM. Foot process effacement is the result of adaptive changes in cell shape and hypertrophy of the contractile apparatus which reinforces the supportive role of podocytes (Shirato et al., 1996), cell body attenuation and pseudocysts are the result of mechanical overexpansion (Nagata et al., 1992), cell hypertrophy is due to hyperfiltration (Nagata et al., 1992), accumulation of absorption droplets is because of increased lysosomal uptake and degradation of filtered proteins (Davies et al., 1978) and finally podocyte detachment from GBM is due to impaired connection with it (Cho et al., 1993).

Kriz and colleagues (2001) reported that podocyte loss could lead to nephron degeneration via three steps. The first step is podocyte loss, and because the remaining podocytes are unable to replicate they compensate for their loss by hypertrophy to take over the increased load of work. The second step is tuft adhesion formation, and that when the remaining podocytes fail to cover the places of lost podocytes the naked GBM will result allowing access to GBM by parietal epithelial cells of Bowman's capsule. A gap in the parietal epithelium will develop and the injured glomerular tuft portion will be in direct contact with the interstitium through it. Such a circumscribed tuft adhesion is the initial lesion in the development of segmental glomerulosclerosis. The third step is misdirected filtration when the capillaries in the tuft adhesion deliver their filtrate into the space between the parietal epithelium and its basement membrane instead of into Bowman's capsule. Interstitial fibroblast will response to that by making a dense cover of sheetlike processes to enclose the focus of misdirected filtration, preventing the filtrate from spread to the surrounding interstitium. This leads to the formation of crescent-shaped paraglomerular space which by the effect of continuing filtration tends to enlarge by separating the parietal epithelium from its basement membrane in all directions. As a result to that the parietal epithelium gap will increase and the adherent sclerotic tuft will become progressively herniated in the enlarging paraglomerular space.

Hir and co-worker (2001) postulated that the glomerular inflammation starts inside the GBM and podocytes become involved through the spread of inflammatory mediators and stimulate a hyperactive response of podocytes. Podocytes develop large number of retracted fingerlike processes at their apical cell surface. These processes extend in all direction and may touch the parietal epithelium, pierce through it between the parietal epithelial cells and fix to the parietal basement membrane. This leads to the stimulation and proliferation of the parietal epithelial cells and formation of a cellular crescent.



Figure 1.6. Podocyte degenerative changes.
Injured podocyte with foot process effacement (Pavenstadt et al., 2003)

Podocyte injury and loss in urine

A non-invasive technique for the diagnosis of podocyte shedding was described by Hara and colleagues (1995), who examined the urinary sediment of 59 patients with different renal diseases and 12 healthy control aged 3-23 years (table 1.1) by indirect immunofluorescence using a monoclonal antibody to podocalyxin (a glycoprotein prominently expressed on podocytes). They reported three different structures (casts, cells and granules) which stained positive for podocalyxin in the urinary sediments. The number of casts and cells were counted in each partitioned area on a slide (cytospun urine sediments on the slides were partitioned into 6 areas of approximately 1 X 1 cm² each by PAP pen) and scored as, 0 = none/area, 1 = 1-10/area, 2 = 11-30/area and 3 = >31/area. The amount of granules was scored as, 0 = none/area, 1 = a few/area, 2 = moderate/area and 3 = numerous/area. Their results (table 1.1) showed that casts were found in the urinary sediment of 33% of patients with Lupus nephritis, 50% of patients with minimal change and IgA nephropathies, 75% of patients with mesangiocapillary glomerulonephritis and 100% of patients with Alport syndrome; post-streptococcal acute glomerulonephritis and Henoch-Schoenlein purpura nephritis. Cells positive for podocalyxin were found in a few patients with lupus nephritis, IgA nephropathy and Alport syndrome as well as all patients with post-streptococcal acute glomerulonephritis and Henoch-Schoenlein purpura nephritis. Granules were found in all patients with membranous nephropathy, Alport syndrome, post-streptococcal acute glomerulonephritis and Henoch-Schoenlein purpura nephritis as well as some patients with mesangiocapillary glomerulonephritis, minimal change, lupus nephritis and IgA nephropathies. The urinary sediment from control subjects, patients with urological diseases, patients with non-glomerular haematuria, post-transplantation and renal failure were negative for podocalyxin. This group concluded that podocytes and their related structures which are positive for podocalyxin are excreted in the urine in different types of glomerulonephritis, particularly those with acute onset, and their amount reflect the degree of podocyte injury in glomerular diseases.

Cases & Number	Casts				Cells				Granules			
	0	1	2	3	0	1	2	3	0	1	2	3
Normal control (12)	12				12				12			
Urological diseases (5)	5				5				5			
Non-glomerular haematuria (5)	5				5				5			
Post-renal transplantation & renal failure (6)	6				6				6			
Membranous nephropathy (2)	2				2						1	1
Mesangiocapillary glomerulonephritis (4)	1	2	1		4				3	1		
Minimal change nephropathy (6)	3			3	6				3	2	1	
Lupus nephritis (6)	4			2	5	1			4	1	1	
IgA nephropathy (12)	6	2	1	3	10	2			3	7	2	
Alport syndrome (4)		1	1	2	3	1				2	1	1
Post-streptococcal glomerulonephritis (5)			2	3		2	2	1		2	2	1
Henoch-Schoenlein purpura nephritis (4)			1	3		1	2	1		1	2	1

Table 1.1: Urinary podocalyxin excretion in different renal diseases (Hara et al., 1995)

Based on their results from the above study, that urinary podocytes were absent in normal control, non-glomerular diseases (urological diseases and non-glomerular haematuria) and glomerular non-inflammatory diseases (minimal change and membranous nephropathies) and their presence in the urine of glomerular inflammatory diseases (lupus nephritis, IgA nephropathy, Alport syndrome, post-streptococcal acute glomerulonephritis and Henoch-Schoenlein purpura nephritis), the same group was (1998) examined the urine from a group of patients and control subjects focusing only on the whole urinary podocytes in these different diseases and not other structures since their number may reflect their injury occurring in the glomeruli. Also they looked at the difference between acute (within 6 months after disease onset) and chronic (more than 6 months after disease onset) diseases. They used a modified scoring system from the above study (0 = none/area, 1 = 1-3/area, 2 = 4-10/area, 3 = 11-30/area, 4 = >31/area), and reported that normal control, patients with non-glomerular diseases and patients with glomerular non-inflammatory diseases showed no podocytes in their urine. Podocytes were detected in the urine from patients with glomerular inflammatory diseases. Also, significantly higher scores of urinary podocytes were found in the acute than chronic disease (table 1.2).

The role of podocyte injury in the acute phase of glomerular disease became more obvious when the same group could not detect any urinary podocytes using anti-podocalyxin antibody from patients with chronic renal failure but could from healthy controls as well as positive control subjects who were patients with active IgA nephropathy and normal renal function. They concluded that urinary podocytes may be used as a marker of disease severity during the acute but not the chronic stage of renal disease (Ebihara et al., 2000).

Monoclonal anti-podocalyxin antibody was used to stain the urine samples of patients with diabetic nephropathy in different stages to study the role of podocytes in this disease as well as the effect of angiotensin converting enzyme inhibitor trandolapril on podocytes injury (Nakamura et al., 2000b). Urinary podocytes were absent in healthy controls, diabetic patients with normoalbuminuria and diabetic

Cases & Number		Urinary podocytes				
		0	1	2	3	4
Normal	Normal control (12)	12				
Non-glomerular diseases	Urinary tract infection (3)	3				
	Non-glomerular haematuria (3)	3				
Glomerular non-inflammatory diseases	Minimal change nephropathy (10)	10				
	Membranous nephropathy (3)	3				
Glomerular inflammatory diseases	Haemolytic uraemic syndrome (2)	1				1o
	Alport syndrome (3)		1*	1*	1*	
	Post-streptococcal glomerulonephritis (5)			1o	3o	1o
	Mesangiocapillary glomerulonephritis (5)	2	1*	1*	1o	
	Henoch-Schoenlein purpura nephritis (7)	2			1o	4o
	Lupus nephritis (7)	3	1*	3*		
	IgA nephropathy (27)	6	3* 4o	4* 6o	1o	3o

Table 1.2: Urinary podocytes in different renal diseases (Hara et al., 1998).

Acute (o) = within 6 months after disease onset.

Chronic (*) = more than 6 months after disease onset.

patients with chronic renal failure. Podocytes were detected in diabetic patients with macroalbuminuria and microalbuminuria. Podocytes were significantly higher in diabetic patients with macroalbuminuria than microalbuminuria which reduced after 2 months treatment with trandolapril in the both groups.

FSGS can be missed on renal biopsy of patients with nephrotic syndrome. Nakamura and associates (2000c) stained urine samples from patients with nephrotic syndrome due to minimal change glomerulonephritis and idiopathic FSGS with podocalyxin antibody to see any difference between them in terms of urinary podocytes. Also they studied the effect of immunosuppressive therapy on urinary podocytes level. After 6 months of treatment with prednisolone of minimal change nephropathy patients, all of them achieved remission and after 12 months of treatment with prednisolone and cyclophosphamide or mizoribine of idiopathic FSGS patients, half of them achieved remission. Urinary podocytes were not detected in the healthy controls and in patients with minimal change glomerulonephritis. Podocytes were detected in the urine of all patients with idiopathic FSGS before treatment (mean, 4.2 cells/ml) then decreased in the patients who achieved remission (mean, 1.2 cells/ml). The urinary podocytes did not change in the other patients who did not achieve remission even after the treatment. They concluded that urinary podocytes can be used as a diagnostic tool to differentiate between minimal change nephropathy and FSGS. Podocytes can also mark disease progression in FSGS.

Another study was conducted by Hara and co-workers (2001) to look at podocyte injury in FSGS. Urine samples of patients with minimal change nephropathy, membranous nephropathy and FSGS were stained with monoclonal podocalyxin antibody as above. They reported higher podocyte excretion in focal and segmental glomerulosclerosis (median, 1.3 cells/ml) in comparison to minimal change nephropathy (median, 0 cells/ml) and membranous nephropathy (median, 0 cells/ml). These results supported an important role of podocyte injury in the pathogenesis of FSGS.

Urine samples from patients with systemic lupus erythematosus were examined with the same technique (see above) to look at the role of podocytes (Nakamura et al., 2000d) in this disease. Two groups of patients were studied, one group with active disease and another group with stable disease. Podocytes were detectable in the first group but not in the clinically stable patients. Patients with podocytes in urine were examined monthly for podocytes and after treatment with methylprednisolone followed by prednisolone they were absent. They concluded from this study that urinary podocytes may be used for the assessment of disease severity in lupus nephritis.

The same group reported later that urinary podocytes can be reduced in renal patients with proper treatment and argued that could be a reflection of the alteration of podocytes injury process (table 1.3).

The viability of urinary podocytes has been investigated in experimental renal diseases. Petermann and colleagues (2003) studied the urinary podocytes from rats with experimental membranous nephropathy. Urine was collected from these rats, centrifuged, resuspended in tissue culture media and then seeded on collagen coated tissue culture plates. The cell number was measured, the cell type was identified by staining with podocytes specific antibodies and the cell morphology was assessed by light and electron microscopy. The cells stained positive for podocytes specific proteins (synaptopodin, nephrin, podocin, WT1 and GLEPP1) when they obtained from the urine and express podocytes specific proteins at the level of mRNA and proteins when they grew in tissue culture. Podocyte foot processes were shown with electron microscopy. Podocytes number increased during the first 5 days in tissue culture but apoptosis increased dramatically to reduce the number of podocytes. A similar study was conducted by the same group in rats with experimental diabetic nephropathy and they were able to grow viable podocytes in tissue culture (Petermann et al., 2004).

Disease	Treatment and duration	Urinary podocytes before treatment	Urinary podocytes after treatment	Reference
Diabetic nephropathy (type2 with microalbuminuria)	dilazep dihydrchloride for 6 months	mean, 1.3 cells/ml	mean, 0.4 cells/ml	Nakamura et al., 2000a
IgA nephropathy	trandolpril for 3 months	mean, 2.6 cells/ml	mean, 1.2 cells/ml	Nakamura et al., 2000e
IgA nephropathy	candesartan cilexetil for 3 months	mean, 2.7 cells/ml	mean, 1.3 cells/ml	Nakamura et al., 2000e
IgA nephropathy	verapamil for 3 months	mean, 2.4 cells/ml	mean, 1.6 cells/ml	Nakamura et al., 2000e
Lupus nephritis (diffuse proliferative)	azathioprine and cyclophosphamide for 12 months	mean, 3.8 cells/ml	Reduced with cyclophosphamide more than azathioprine	Nakamura et al., 2001b
Diabetic nephropathy (type2 with microalbuminuria)	pioglitazone for 6 months	mean, 0.9 cells/ml	mean, 0.1 cells/ml	Nakamura et al., 2001a
Chronic glomerulonephritis	cerivastatin for 6 months	mean, 1.6 cells/ml	mean, 0.9 cells/ml	Nakamura et al., 2002
Diabetic nephropathy (nephrotic syndrome)	Low density lipoprotein apheresis for 9 weeks	mean, 4.8 cells/ml	mean, 0.9 cells/ml	Nakamura et al., 2005

Table 1.3: Effect of treatment on urinary podocytes.

Aims of the project

The general aim of this project was to study the role of the podocyte in proteinuric renal disease. Podocytes are highly specialized and terminally differentiated epithelial cells located on the outer surface of the GBM. Their foot processes interdigitate around the GBM and form the filtration slits which are the principle structures for glomerular filtration.

Proteinuria is a manifestation of early podocyte injury even without any changes in the glomerular structure, and further damage to podocytes is central to the development of glomerulosclerosis and chronic renal failure.

Mutations of the podocyte proteins genes cause inherited proteinuric diseases including; Finnish type nephrotic syndrome, congenital nephrotic syndrome, autosomal recessive FSGS, autosomal dominant FSGS and primary steroid-resistant FSGS.

Detection of urinary podocytes and/or their fragments with immunofluorescence (using podocyte protein antibody) in the urine of patients with proteinuric renal diseases has been reported mostly by one group to reflect disease activity.

The specific aims of this project were:

1. To test the hypothesis that it would be prognostically useful to be able to identify podocytes in urine of patients with proteinuric renal disease, and that a reverse transcriptase polymerase chain reaction method would be an efficient and clinically applicable way to do this (chapter 3 and chapter 4).
2. To create an animal model in which a graded podocyte injury could be induced, and examined alone or in combination with other pathology. This would be useful to test the hypothesis that treatment that protects the podocyte would ameliorate the disease (chapter 6).

Chapter 2

Materials and Methods

Materials

Oligonucleotide primers

Oligonucleotide primers were obtained from TANG Ltd except random hexamer pd(N)6 from Promega and M13For and M13Rev primers from haematology department of Edinburgh Royal Infirmary

cDNA oligonucleotide primers

- Nephtrin cDNA primers

1. HuNeph1For 5`-GAG AGG ACC ACC TCA GGC AG-3`
HuNeph1Rev 5`-GCT CTC GGT TCA CTG TCT CC-3`
Band size is 310bp
2. HuNeph2For 5`-GAA TTG CTG AAG GAT GGG AA-3`
HuNeph2Rev 5`-GGT GCT TCC CAC TTT GTT GT-3`
Band size is 377bp

- Podocalyxin cDNA Primers

1. HuPodo1For 5`-GAC AGC AAA TAG GCC TCT GC-3`
HuPodo1Rev 5`-ATA GGT GTC CTG GTG GCA AG-3`
Band size is 290bp
2. HuPodo2For 5`-TGG GAG TGA TTC CCT GAG AC-3`
HuPodo2Rev 5`-GTC TGA GCT TTT GGC CTT TG-3`
Band size is 217bp

- β -actin cDNA Primers

- B-actinFor 5`-CCA CCA ACT GGG ACG ACA TG-3`
B-actinRev 5`-GTC TCA AAC ATG ATC TGG GTC ATC-3`
Band size is 150bp

DNA oligonucleotide primers

- pMS7 sequencing primers

M13For and M13Rev

- Murine nephrin gene fragment PCR primers

MONPHSF1 5`-GCC GCC GGG AGG TGA GAG GTT TGT AG-3`

MONPHSNotF2 5`-TCC TGG AGA AGC GGC CGC CGG GAG-3`

MONPHSBamREV 5`-CTG TGG GAT CCT TAG CTC CCA TCA C-3`

MonephBamRev2 5`-AGC TCG GAT CCA CCA GCA GCT-3

Band size is 1315bp

- pCR4BN sequencing primers

M13For and M13Rev

- pIN sequencing primers (figure 2.1)

M13Rev and M13 Rev

monephrinMidFor 5`-ATG GCC CAG GGA TTC AGG TGC-3`

monephrinMidRev 5`-GCT TGG ACC CAG TGT GAA CTC-3`

monephrin3pFor 5`-GCT GGT GAT GGG AGC TAA GGA-3`

B-intronRev 5`-ATC ATG AGG GTC CAT GGT GAT-3`

EGF-For 5`-GGT TAT TGT GCT GCT TCA TCA-3`

EGF-Rev 5`-GAT AGG CAG CCT GCA CCT GAG-3`

EGF-For2 5`-TCC AAA CCG GGC CCC TCT GCT-3`

b-globin5pRev 5`-GGA ATG GAC AGC AGG GGG CTG-3`

- Mice genotyping primers (figure 2.2)

1. pINPCR-For1 5`-GGA AGA GAG AAG GGC GAG TT-3`

pINPCR-Rev1 5`-GGG TCC ATG GTG ATA CAA GG-3`

Band size is 243bp (nephrin gene/intron genotyping)

2. pINPCR-For2 5`-GGT GGT GCT GAA GCT CTT TC-3`

pINPCR-Rev2 5`-GCT TGT GGC TTG GAG GAT AA-3`

Band size is 228bp (hDTR gene genotyping)

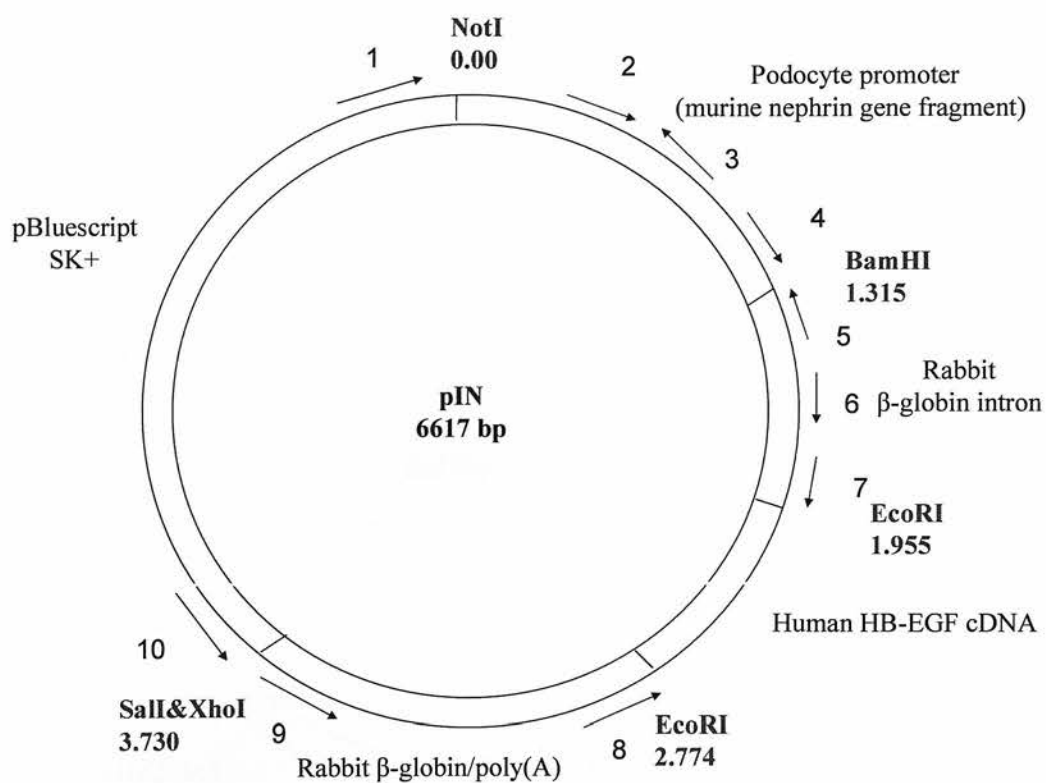


Figure 2.1: Map of pIN sequencing primers

- | | |
|---------------------|---------------------|
| 1 = M13Rev | 2 = MonephrinMidFor |
| 3 = monephrinMidRev | 4 = monephrin3pFor |
| 5 = B-intronRev | 6 = EGF-For2 |
| 7 = EGF-For | 8 = EGF-Rev |
| 9 = b-globin5pRev | 10 = M13For |

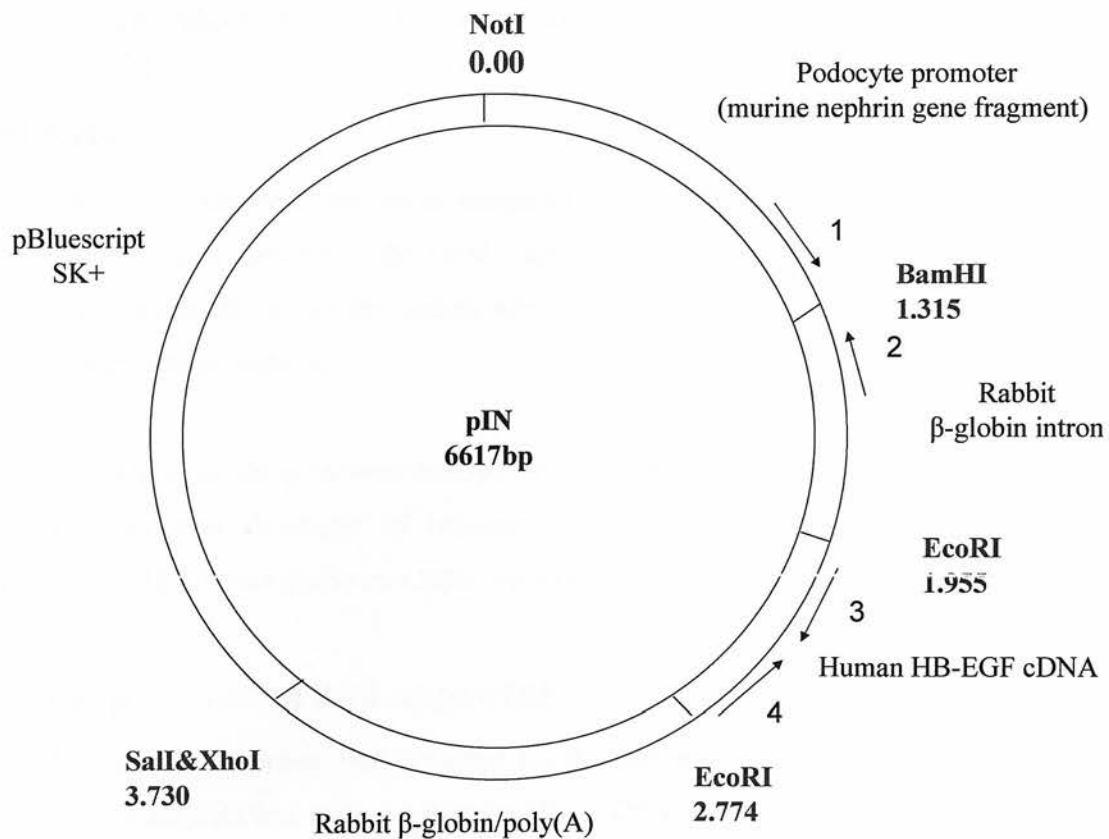


Figure 2.2: Map of mice genotyping primers

- 1 = pINPCR-For1
- 2 = pINPCR-Rev1
- 3 = pINPCR-For2
- 4 = pINPCR-Rev2

General materials

Molecular biology enzymes were obtained from Promega, total RNA isolation mini kit was obtained from Agilent and DNA was prepared by QIAGEN kit. The plasmid pMS7 was a gift from Dr Saito.

The other materials are described in the methods.

Patients

Total RNA was extracted from urine samples (20 ml each) of 70 proteinuric (urine protein \geq +++) renal patients at the renal outpatient department of Edinburgh Royal Infirmary. Immunofluorescence studies were conducted on urine samples of 100 patients with similar criteria.

Although individual samples were anonymised, they were known to include samples from patients with diagnosis of minimal change disease, FSGS, membranous nephropathy, IgA nephropathy and lupus nephritis (multiple examples in each case)

Ethical permission and approval

Ethical Committee approval was obtained for the human studies in this project and work involve animals was carried out under Home Office project licence (60/3088).

Methods

Nucleic acids methods

Total RNA extraction by TRIzol

Urine samples were collected and kept at room temperature until processed (within 3-4 hours). The samples were centrifuged at 2500 rpm for 5 minutes at 4°C and the pellets were resuspended in 500 ul of urine, divided into two Eppendorff tubes and homogenised in 800 ul of TRIzol (phenol and guanidine thiocyanate) from Invitrogen (Chomczynski and Sacchi, 1987). After addition of 100 ul of chloroform, samples were vortexed, incubated on ice for 5 minutes and centrifuged at 14,000 rpm for 5 minutes. The aqueous and organic layers were separated. RNA was precipitated from the aqueous layer by adding an equal volume (300 ul) of isopropanol, followed by incubation at room temperature for 10 minutes, adding at this stage 10 ul of glycogen (Invitrogen), followed by centrifugation at 14,000 rpm for 5 minutes. The pellets were washed with 500 ul of ethanol 75% and dissolved finally in 15 ul of nuclease-free water.

DNaseI treatment and cDNA synthesis

DNaseI treatment of the extracted total RNA and cDNA synthesis for use in the polymerase chain reaction were carried out using two methods.

In the first method (Konnai et al., 2003) this was done in two steps. Firstly, 1 ul DNaseI (1 u/ul) was added to the total RNA (50 ul) and incubated at room temperature for 15 minutes. 1 ul of 25mM EDTA was added then they were incubated at 65°C for 10 minutes to inactivate the DNaseI, which could otherwise destroy the cDNA later. This was followed by ethanol precipitation to remove the EDTA (which may inactivate the reverse transcriptase during cDNA synthesis), by adding 1/10 volume of 5M NaCl (5 ul) and 3 volumes of ethanol 100% (150 ul). This reaction was incubated at -20°C for 2 hours, and then was spun at 14,000 rpm for 5

minutes. The pellet was washed with 250 ul of ethanol 75%, and finally dissolved in 30 ul of nuclease-free water.

Secondly, cDNA synthesis was done in three different reactions as below:

Reagent	DNaseI+/RT+	DNaseI-/RT+	DNaseI-/RT-
AMV RT buffer (5X) 5 ul (see below for composition)		5 ul	5 ul
NTPs (1:10)	1 ul	1 ul	1 ul
Rnase inhibitor	0.5 ul	0.5 ul	0.5 ul
AMV RT (5 units)	0.5 ul	0.5 ul	-
Nuclease-free water	10 ul	10 ul	10.5 ul
	17 ul	17 ul	17 ul

3 ul of random hexamer [pd(N)6] and 5 ul of total RNA were heated at 70°C for 10 minutes, then cooled at room temperature for 10 minutes before the 17 ul reaction mixture was added (25 ul reaction). These then were incubated at 42°C for one hour.

The second method (Huang et al., 1996), allows DNaseI to work in the AMV RT buffer (5X - 250mM Tris-HCl, 250mM KCl, 50mM MgCl₂, 2.5mM spermidine and 50mM DTT). DNaseI was inactivated by heat alone to minimise RNA loss during its ethanol precipitation and other manoeuvres. This method all takes place in a single tube.

The method as below:

Reagent	DNaseI+/RT+	DNaseI-/RT+	DNaseI-/RT-
RNA	5 ul	5 ul	5 ul
RT buffer (5X)	5 ul	5 ul	5 ul
NTPs	1 ul	1 ul	1 ul
Rnase inhibitor	0.5 ul	0.5 ul	0.5 ul
Nuclease-free water	9 ul	10 ul	10.5 ul
Rnase-free DNaseI	1 ul	-	-
	21.5 ul	21.5 ul	21.5 ul

The reagents were incubated at 37°C for 30 minutes, then at 75°C for 10 minutes. 3 ul of pd(N)6 was added and continued at 75°C for further 5 minutes. The reagents were left to cool at room temperature for 10 minutes before 0.5 ul of AMV-RT (5 units) was added to the (DNaseI+/RT+) and (DNaseI-/RT+) reactions. All were incubated at 42°C for one hour.

cDNA Polymerase chain reaction

This was performed by using Ready to Go PCR beads (Amersham Pharmacia Biotech Inc). These premixed 0.2 ml thin-walled tubes contain buffers, dNTPs, Taq DNA polymerase enzyme (2.5 units), stabilizers and Bovine Serum Albumin (BSA). When dissolved in a final volume of 25 ul PCR reaction (20.5 ul of nuclease-free water, 1 ul of 25mM MgCl₂, 0.75 ul of forward primer, 0.75 ul of reverse primer and 2 ul of cDNA which was added after the hot start as explained below) the beads at this stage contains 200uM in 10mM Tris-HCl (pH 9 at room temperature) of each dNTPs, 50mM KCl and 2.75mM of MgCl₂ (1 ul of 25mM MgCl₂ was added to beads content of 1.5mM of MgCl₂). This reaction was subjected to hot start in the PCR machine at 75°C for 10 minutes followed by addition of 2 ul of the cDNA. The program was; 95°C for 1 minute (denaturation); 65°C for 1 minute (annealing); 72°C for 1½ minute (elongation) and run for 30 cycles. The final elongation temperature was 72°C for 10 minutes.

DNA extraction from cultured human B cells

10 ml of cultured human B cells (DR2Lum) were provided kindly by Dr Juan Zou. The concentration of them was one million cell/ml. They were divided in two tubes (5ml each) and centrifuged at 12,000 rpm for 5 minutes at 4°C. The supernatants were discarded and the pellets were resuspended in 200 ul of phosphate buffered saline (PBS). The mixtures were incubated at 70°C for 10 minutes after addition of 20 ul of proteinase K. 200 ul of ethanol (100%) was added and mixed thoroughly before were transferred into DNeasy spin columns (Qiagen) and placed in 2 ml collection tubes (provided with the buffers), then centrifuged at 8000 rpm for one minute at room temperature (the principle of this method is that buffering conditions are adjusted to provide optimal DNA-binding conditions when the lysate loaded on

the DNeasy spin columns and during a brief centrifugation DNA will bind selectively to the DNeasy membrane and the contaminants pass through. DNA eluted after two washing steps). The flow-through and collection tubes were discarded and the DNeasy spin columns were placed in new collection tubes. 500 ul of buffer AW1 was added and centrifuged at 8000 rpm for one minute at room temperature. The flow-through and collection tubes were discarded and the DNeasy spin columns were placed in new collection tubes. 500 ul of buffer AW2 was added and centrifuged at 14,000 rpm for 3 minutes at room temperature to dry the DNeasy membranes. The flow-through and collection tubes were discarded and The DNeasy spin columns were placed in eppendorff tubes. 200 ul of buffer AE was added (to elute DNA), incubated at room temperature and spun at 8000 rpm. The extracted DNA was checked by loading 2 ul of each sample on agarose gel 1% and visualized under ultraviolet transilluminator by ethidium bromide (figure 2.3). The concentration of the DNA was measured after combination of both samples (400 ul) and found to be 100 ng/ul which is diluted and because of that ethanol precipitation was done. Ethanol precipitation was by adding 1/10 of 3M Na acetate (40 ul) and 2 volumes of 100% ethanol (800 ul), and then incubated at -20°C for 30 minutes. This mixture was spun at 14,000 rpm at room temperature for 10 minutes and the supernatant was discarded. The pellet was washed by 1 ml of ethanol 70% and spun for one minute at room temperature. The supernatant was discarded; the pellet was air dried and dissolved in 40 ul of 10mM Tris Cl (pH 8.5). DNA concentration was 500 ng/ul.

Total RNA extraction by Agilent total RNA isolation mini kit (phenol-free method)

Urine samples were collected as described above and centrifuged at 2500 rpm for 5 minutes at 4°C and the pellets were resuspended in 500 ul of lysis solution (contains guanidine isothiocyanate)/β-mercaptoethanol mixture; then transferred into mini prefiltration column and centrifuged at 14,000 for 3 minutes at room temperature (most of DNA and other contaminants are removed at this stage). 600 ul of ethanol (70%) was added to the filtrate and mixed till it become homogenous. 700 ul of ethanol/lysis mixture was transferred into mini isolation column and centrifuged at 14,000 rpm for 30 seconds at room temperature (RNA loaded from the mixture on the

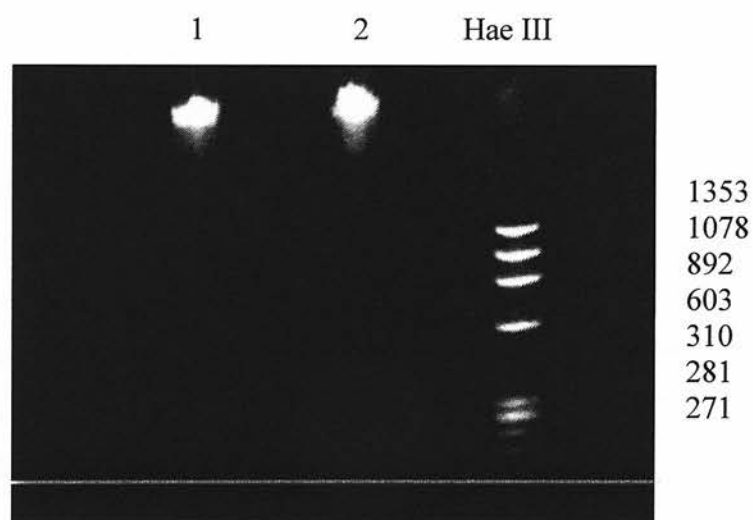


Figure 2.3. Extracted human genomic DNA

No.1 and 2 is human genomic DNA which was extracted from cultured human B cells.

column at this step);the flow-through was discarded and RNA loaded column was transferred into collection tube. 500 ul of wash solution was added and centrifuged at 14,000 for 30 seconds at room temperature; flow-through was discarded and the column replaced in another collection tube (the washing step was done twice). The mini isolation column was spun dry at 14,000 rpm for 2 minutes at room temperature and RNA was eluted by adding 20 ul of nuclease-free water; incubated at room temperature for 1 minute and spun at 14,000 for 1 minute at room temperature.

Agarose gel electrophoresis

Agarose (CLP) was weighed in a small flask and 50 ml of buffer TBE (1x) was added. The agarose was melted by heat in a microwave at 60°C for 60 seconds. Once the agarose melted 5 ul of ethidium bromide (attach to cDNA to be visualised by ultraviolet transilluminator) was added; and then poured in gel electrophoresis apparatus. The agarose was left to polymerize by cooling at room temperature for 30 minutes. Loading buffer was used to load cDNA/DNA and Hae III (DNA marker) after removing gel tank edges and tooth barrier as well as covering the gel with 50 ml of buffer TBE (1x). The electrophoresis machine was sat at 100v; 25w; 75mA and run for 45 minutes. The gel was visualised by ultraviolet transilluminator to look for the appropriate band size and finally photographed.

cDNA oligonucleotide primers

The national centre for Biotechnology Information (NCBI) Entrez Gene database was used to search for human nephrin and podocalyxin cDNA sequences. The primer3 program (<http://frodo.wi.mit.edu/cig-bin/primer3-www.cgi>) was used to design two pairs of primers for nephrin and podocalyxin cDNA (band size range 200-400 bp). β -actin primers (common for mouse and human) were provided kindly by Dr Julia Marley. When the primers were received aliquots of 1 ug/ul in water were made. 1/10 dilution from these aliquots was used as the working dilution for PCR. The conditions of these PCRs were optimized using a human kidney cDNA (control cDNA) which was provided kindly by Professor Neil Turner, and then these primers were used to do cDNA PCR for nephrin and podocalyxin.

Making and transformation of competent E.coli (DH5) with plasmid DNA

The E.coli was grown on agar plate (without added antibiotic) by overnight incubation at 37°C. In the following day 50 ml of SOB medium with added magnesium sulphate in sterilized (with boiling water) grooved flask was inoculated with 5-10 colonies from E.coli plate. The flask with its contents was incubated in a shaker at 225 rpm for 3-5 hours at 37°C till the optical density of E.coli was 0.3-0.4 at 550 nm. After that the contents was transferred to chilled 50 ml falcon tube, centrifuged at 2000-4000 rpm at 4°C for 10 minutes, then the supernatant was discarded and the bacterial pellet was resuspended in 10-15 ml of chilled transforming buffer. The mixture was incubated on ice for 10-15 minutes then centrifuged as above and the bacterial pellet was resuspended in 2-5 ml of chilled transforming buffer. 140 µl of DD solution was added into the centre of the mixture then the whole tube contents were swirled immediately. The mixture was incubated on ice for further 10 minutes and then 140 µl of DD solution was added and incubated for 20 minutes on ice. 50 µl of E.coli in transforming buffer and DD solution mixture and few microlitres of plasmid DNA (amount and dilution depend on DNA concentration of each plasmid) was mixed together in a microcentrifuge tube and incubated on ice for 30 minutes. E.coli in the mixture was subjected to heat shock by incubation in a water bath at 42°C for 90 seconds followed by incubation on ice for 2 minutes. 200 µl of SOC medium (pre-warmed at room temperature) was added and incubated in a shaker at 225 rpm for 60 minutes at 37°C. The contents then were spread on agar plate with added ampicillin, inverted and incubated overnight at 37°C and the following day stored at 4°C for further experiments.

Transformation of competent E.coli with plasmid DNA

The plasmid DNA was added to a vial of competent E.coli (One Shot, Invitrogen) and incubated on ice for 5 minutes. E.coli was subjected to heat shock by incubation in a water bath at 42°C for 30 second followed by incubation on ice for 2 minutes. During ice incubation 250 µl of SOC medium (pre-warmed at room temperature) was added. The mixture was incubated horizontally in a shaker at 225 rpm for 60 minutes at 37°C. The contents then were spread on agar plate with added ampicillin, inverted

and incubated overnight at 37°C and the following day stored at 4°C for further experiments.

Making of agar plates

Bacto-agar was added to SOB medium to make 1.5% (1.5 g/100ml) agar plates and autoclaved. Once the temperature of the mixture reached approximately 50-55°C ampicillin was added (1 ul of 50 mg/100ml of ampicillin per 1 ml of the mixture). 30 ml was poured per each 90 mm Petri dish and stored at 4°C till used.

Minipreparation of plasmid DNA

The minipreparation technique was used for the production of small quantities of plasmid DNA from transformed E.coli for restriction enzyme analysis. 15 ml tubes with 2 ml of LB medium and 2 ul of 50 mg/ml ampicillin was inoculated with a single colony of transformed E.coli (to avoid contamination) and incubated in a shaker at 225 rpm overnight at 37°C. The following day 1.5 ml was processed for DNA extraction and 0.5 ml was saved at 4°C for plasmid DNA midipreparation. The 1.5 ml volume was transferred to a microcentrifuge tube and centrifuged at 14,000 rpm for 3 minutes at room temperature and the supernatant was aspirated and discarded. The bacterial pellet was resuspended in 100 ul of GTE by vigorous vortexing, then 200 ul of 0.2 M NaOH/0.1% SDS solution was added and mixed by inversion 4-6 times. To this mixture 150 ul of chilled 5M/3M potassium acetate was added, mixed by gentle vortex and incubated on ice for 15 minutes. The contents were centrifuged at 14,000 rpm for 5 minutes at room temperature and the supernatant was transferred to a new microcentrifuge tube and 200 ul of phenol was added. This was followed by vortex and centrifugation at 14,000 rpm for 2 minutes at room temperature. The top layer (approximately 300 ul) of the supernatant was transferred to third microcentrifuge tube. DNA was precipitated by 100 ul of 100% isopropanol, then mixed together by vortex and centrifuged at 14,000 rpm for 5 minutes at room temperature. The supernatant was discarded and DNA pellet was washed with 1 ml of 70% ethanol. The supernatant was discarded and DNA pellet was left to air dry for 10-15 minutes at room temperature and finally it was dissolved in 30-40 ul of TE buffer, 5-10 ul of which were used for restriction enzyme analysis.

Midipreparation of plasmid DNA

The midipreparation technique was used for the production of medium quantities and clean qualities of plasmid DNA from transformed *E.coli* for plasmid DNA sequencing because RNA is destroyed by RNase in this technique. This was done using plasmid DNA midiprep kit from Qiagen. A grooved sterile (with boiling water) flask with 50 ml of LB medium and 50 ul of 50 mg/ml ampicillin was inoculated with 100 ul of the saved plasmid DNA minipreparation after its restriction enzyme analysis and incubated in a shaker at 225 rpm overnight at 37°C. The following day the bacterial suspension was transferred to an Oakridge tube and centrifuged at 6000 rpm for 15 minutes at 4°C. The supernatant was discarded and the bacterial pellet was resuspended in 4 ml buffer P1 with added RNase and mixed by vortex. 4 ml of buffer P2 was added and mixed by gentle inversion for 4-6 times, then incubated at room temperature for 5 minutes. 5 ml of chilled buffer P3 was added, mixed gently immediately by inversion for 4-6 times and then incubated on ice for 15 minutes. The mixture was centrifuged at 13,000 rpm for 30 minutes at 4°C and the supernatant was transferred to another Oakridge tube. The supernatant was recentrifuged at 13,000 rpm for 15 minutes at 4°C and during this stage a Qiagen-tip 100 was equilibrated by 4 ml of buffer QBT and the column was allowed to empty by gravity. The supernatant was applied to Qiagen-tip 100 and it was allowed to enter the resin by gravity flow. This tip was washed twice by 10 ml of buffer QC which was allowed to flow by gravity. Plasmid DNA was eluted from the tip with 5 ml of buffer QF in a third Oakridge tube and precipitated by 3.5 ml of room temperature isopropanol. The mixture was mixed and centrifuged at 11,500 rpm for 30 minutes at 4°C and the supernatant was discarded. 2 ml of 70% ethanol was added, then divided into two microcentrifuge tubes, centrifuged at 14,000 rpm at room temperature for 10 minutes and the supernatant was discarded. Plasmid DNA pellets were air dried at room temperature and finally dissolved in 10-20 ul of TE buffer and the two samples were combined. The optical density of DNA was measured by ultraviolet spectrophotometer. This plasmid DNA was tested with restriction enzyme analysis and used for plasmid DNA sequencing.

Maxipreparation of plasmid DNA

The maxipreparation technique was used for the production of large quantities and clean qualities of pIN plasmid DNA (podocyte construct) from transformed E.coli to use for mice microinjection. This was done using plasmid DNA maxiprep kit from Qiagen. A grooved sterile (with boiling water) flask with 50 ml of LB medium and 50 ul of 50 mg/ml ampicillin was inoculated with 100 ul of the saved plasmid DNA minipreparation after its restriction enzyme analysis and sequencing of its midipreparation DNA incubated in a shaker at 225 rpm overnight at 37°C. This was used to inoculate 500 ml of LB with 500 ul of 50 mg/ml ampicillin and incubated as above. The following day the bacterial suspension was transferred to a 500 ml centrifugation bottle and centrifuged at 5100 rpm for 25 minutes at 4°C. The supernatant was discarded and the bacterial pellet was resuspended in 10 ml of buffer P1 with added RNase and mixed by vortex and transferred to Oakridge tube. 10 ml of buffer P2 was added and mixed by gentle inversion for 4-6 times, then incubated at room temperature for 5 minutes. 10 ml of chilled buffer P3 was added, mixed gently immediately by inversion for 4-6 times and then incubated on ice for 20 minutes. The mixture was centrifuged at 13,000 rpm for 30 minutes at 4°C and the supernatant was transferred to another Oakridge tube. The supernatant was recentrifuged at 13,000 rpm for 15 minutes at 4°C and during this stage a Qiagen-tip 500 was equilibrated by 10 ml of buffer QBT and the column was allowed to empty by gravity. The supernatant was applied to Qiagen-tip 500 and it was allowed to enter the resin by gravity flow. This tip was washed twice by 30 ml of buffer QC which was allowed to flow by gravity. Plasmid DNA was eluted from the tip with 15 ml of buffer QF in a third Oakridge tube and precipitated by 10.5 ml of room temperature isopropanol. The mixture was mixed and centrifuged at 11,500 rpm for 30 minutes at 4°C and the supernatant was discarded. 5 ml of 70% ethanol was added, then divided into 4 microcentrifuge tubes, centrifuged at 14,000 rpm at room temperature for 10 minutes and the supernatants were discarded. Plasmid DNA pellets were air dried at room temperature and finally dissolved in 20-25 ul of TE buffer and the 4 samples were combined. The optical density of DNA was measured by ultraviolet spectrophotometer. This plasmid DNA was tested with restriction enzyme analysis and used for plasmid pIN DNA microinjection.

Restriction enzyme analysis of plasmid DNA preparation

This was done for the midipreparation of the plasmid pMS7, minipreparation and midipreparation of the plasmid pCR4BN as well as minipreparation, midipreparation and maxipreparation of the plasmid pIN DNA, restriction enzyme and its buffer, BSA and nuclease free water were incubated at 37°C for one hour.

Sequencing of plasmid DNA midipreparation

This was done for the midipreparation DNA of the plasmids pMS7, pCR4BN and pIN at haematology department of Edinburgh Royal Infirmary to prove the right sequences. 500 ng of DNA and sequencing primers (100 pmol/ul) were sent and the results were received as an electronic version. DNA strider 1.2 was used to read the results which were checked by Entrez Gene database of the National Centre for Biotechnology Information (NCBI).

DNA oligonucleotide primers

Murine nephrin gene fragment (podocyte promoter) PCR primers were similar to the primers used by Moeller and colleagues (2002) with added NotI and BamHI restriction sites. They reported that 1.25 kb nephrin gene fragment has lead to specific podocyte expression of betagalactosidase gene and not in any of the other tested tissue. NotI and BamHI restriction sites are the subcloning sites of this fragment into pMS7 to produce pIN podocyte construct. The primer3 program (<http://frodo.wi.mit.edu/cig-bin/primer3-www.cgi>) was used to design two pairs of primers for mice genotyping PCRs. When the primers were received aliquots of 1ug/ul in water were made and 1/10 dilution from these aliquots was used as the working dilution for PCR. Sequencing primers of around 21 bp were designed and their working dilution was 100 pmol/ul.

Taq DNA polymerase PCR of murine nephrin gene fragment (podocyte promoter)

This was done first to optimize the conditions of the nephrin gene fragment PCR and it consists of two Taq polymerase PCRs. In the first PCR MONPHSF1 primer, MONPHSBamREV primer and wild type mouse DNA were used. In the second PCR MONPHSNotF2 primer, MONPHSBamREV primer and first PCR product as a template to introduce NotI restriction site were used. This was performed by using Ready to Go PCR beads (Amersham Pharmacia Biotech Inc). These are premixed 0.2 ml thin-walled tubes containing buffers, dNTPs, Taq DNA polymerase enzyme (2.5 units), stabilizers and Bovine Serum Albumin (BSA). When dissolved in a final volume of 25ul PCR reaction (20.5ul of nuclease-free water, 1ul of 25mM MgCl₂, 0.75ul of forward primer, 0.75ul of reverse primer and 2ul of DNA which was added after the hot start as explained below) the beads at this stage contains 200uM in 10mM Tris-HCl (pH 9 at room temperature) of each dNTPs, 50mM KCl and 2.75mM of MgCl₂ (1ul of 25mM MgCl₂ was added to beads content of 1.5mM of MgCl₂). This reaction was subjected to hot start in the PCR machine at 75°C for 10 minutes followed by addition of 2ul of the DNA. The program was; 95°C for 1 minute (denaturation); 60°C for 1 minute (annealing); 72°C for 1½ minute (elongation) and run for 30 cycles. The final elongation temperature was 72°C for 10 minutes.

Proofreading DNA polymerase PCR of murine nephrin gene fragment (podocyte promoter)

This PCR was performed using Vent DNA polymerase (New England BioLabs) because of its lower error rate and to produce blunt ended PCR product. 50 ul reaction was consisted of 2 ul of MONPHSNotF2 primer, 2 ul of MONPHSBamREV primer, 1 ul of 100 mM MgSO₄, 4.5 of thermopol buffer (10X), 3 ul of dNTPs, 30.5 ul of nuclease-free water and 2 ul (1:4 dilution) of first Taq DNA polymerase PCR product. This reaction was subjected to hot start in the PCR machine at 75°C for 10 minutes followed by addition of 5ul of Vent DNA polymerase dilution (1.1 ul of thermopol buffer, 7.4 ul of nuclease-free water and 1.5 ul; 3 units of Vent DNA polymerase). The program was; 95°C for 1 minute (denaturation); 60°C for 1 minute

(annealing); 72°C for 1½ minute (elongation) and run for 30 cycles. The final elongation temperature was 72°C for 10 minutes. This PCR was repeated as described above using MONPHSNotF2 primer, MonephBamRev2 and the product of Vent polymerase PCR as a template (see discussion for details).

Purification of PCR product

This was performed using Qiagen kit (desalting and concentrating DNA from solutions protocol). The product was transferred from the PCR tube to a microcentrifuge tube and 3 volumes of buffer QX1 were added to one volume of PCR product. Qiaex II was resuspended by vortex for 30 seconds and 15-20 ul of it was added and the mixture then incubated at room temperature for 10 minutes (vortexed every 2 minutes). The mixture then was centrifuged at 14,000 rpm for 30 seconds at room temperature and the supernatant was removed. The pellet was washed twice with 500 ul of buffer PE, and then air-dried for 15 minutes until its colour was changed to white colour. DNA was eluted with 20 ul of 10mM Tris. Cl (pH 8.5), centrifuged at 14,000 rpm for 30 seconds at room temperature and the supernatant was transferred to a new microcentrifuge tube because it contains the pure DNA. 1 ul of the pure DNA was loaded on agarose gel to prove its presence after the purification.

Subcloning of the nephrin gene fragment into pCR[®]4Blunt-Topo and production of pCR4BN

1 ul of nephrin gene fragment (PCR product), 1 ul of pCR4 Blunt-Topo (Invitrogen) and 1 ul of its salt solution were added to 3 ul of nuclease-free water and incubated at room temperature for 10 minutes

Gel purification of DNA

DNA was visualised by ethidium bromide staining on an ultraviolet transilluminator and the wanted band was excised from agarose gel. DNA was purified from agarose gel using Qiagen kit (DNA extraction from agarose gels protocol). 1 ml of buffer QX 1 and 10 ul of Qiaex II (resuspended by vortex) were added to the excised gel fragment which contains the DNA and incubated at 50°C for 10 minutes (vortexed

every 2 minutes during this incubation). The mixture was centrifuged for 14,000 rpm for 30 seconds at room temperature and the supernatant was discarded. The pellet was resuspended in 500 ul of buffer QX 1, centrifuged as above and the supernatant was discarded. The last step was repeated twice with buffer PE to wash the DNA pellet which was left at room temperature for 5-10 minutes to air dry. 20 ul of 10mM Tris. Cl (pH 8.5) was added, vortexed, incubated at room temperature for further 5 minutes and then centrifuged at 14,000 rpm for 30 seconds at room temperature. The supernatant was transferred to a new microcentrifuge tube because it contains the pure DNA. 1 ul of the pure DNA was loaded on agarose gel to prove its presence after the purification.

Subcloning of the nephrin gene fragment from pCR4BN into pMS7 and production of pIN (podocyte construct)

The plasmids pMS7 (vector) and pCR4BN (contains the insert which is the nephrin gene fragment) were digested with NotI and BamHI restriction enzyme. The plasmid pMS7 was then dephosphorylated by calf intestinal alkaline phosphatase (promega) to prevent it from relegation. This enzyme was inactivated by incubation at 70°C for 15 minutes. The restriction digest reactions were loaded on 1% TBE agarose gel and the appropriate vector and insert band were excised and purified as described above. The purified vector and insert were ligated with T4 DNA ligase and produced pIN (podocyte construct). E.coli was transformed with the plasmid pIN and miniprep, midiprep and maxiprep of its DNA was performed.

Microinjection of murine fertilized ova with the plasmid pIN (podocyte construct)

In the first trial of murine fertilized ova microinjection, the conditions of NotI and XhoI enzyme restriction analysis and its photograph, pIN sequencing, pIN map and 50 ul (1 ug/ul) of pIN maxiprep DNA were sent to the Human Genetic Unit at Western General Hospital in Edinburgh. In the second trial of microinjection, 3 ug of pIN maxiprep DNA was digested with NotI and XhoI restriction enzymes, gel purified, ethanol precipitated and sent to Rederivation Unit at Edinburgh Royal

Infirmary with a photograph of the restriction enzyme analysis and a photograph of the purified liner pIN construct as well as pIN map.

DNA extraction from the potentially transgenic mice ear punches

Sixty nine ear punches of 3 weeks age of mice were sent to us for DNA extraction and PCR genotyping. DNA was extracted using DNeasy purification kit from Qiagen. 180 ul of buffer ATL and 20 ul of proteinase K were added to the ear punches in microcentrifuge tubes, vortexed and incubated at 55°C overnight. The next day 400 ul of buffer AL (with added ethanol) was added and then vortexed. The mixtures were transferred to DNeasy mini spin columns placed in 2 ml new collection tubes and centrifuged at 8000 rpm for 1 minute at room temperature and the flow through were discarded with their collection tubes. DNeasy mini spin columns were placed in another 2 ml new collection tubes, 500 ul of buffer AW1 was added and centrifuged at 8000 rpm for 1 minute at room temperature and the flow through were discarded with their collection tubes. DNeasy mini spin columns were placed in another 2 ml new collection tubes, 500 ul of buffer AW2 was added and centrifuged at 14,000 rpm for 3 minute at room temperature to dry the DNeasy membranes and the flow through were discarded with their collection tubes. DNeasy mini spin columns were placed in microcentrifuge tubes, 100 ul of buffer AE was added and incubated at room temperature for 1 minute and centrifuged at 8000 rpm for 1 minute at room temperature and the eluted DNA was used for genotyping PCRs.

Southern blotting hybridization of the potentially transgenic mice DNA

Both genotyping PCRs were done on the potentially transgenic mice DNA and were run on 2% TBE agarose gel. These gels were visualised by ethidium bromide on ultraviolet transilluminator and photographed were taken with ruler. The DNA was denatured into ssDNA by soaking the gels into denaturation buffer (1.5M NaCl and 0.5M NaOH) for 30 minutes at room temperature (ssDNA will work as a complementary strand for the radiolabelled probe) after cutting one edge of the gels as a marker. The gels then were placed upside down into appropriate amount of denaturation buffer (works as a transfer buffer) and covered with multiple layers in

the order; nylon membrane (MEN), two layers of filtering papers (Hybond blotting paper from Amersham Pharmacia Biotech), two layers of roller tissue and appropriate weight to press the layers (to transfer the ssDNA from gels to nylon membrane). This was incubated for 12-24 hours. The nylon membranes then were peeled off the gels, placed on its back side, marked with blue ballpoint pen for the cut edges, name, date and wells. These membranes were washed by appropriate amount of washing buffer; 2X SSC (1/10 of 20X SSC: 0.3M Na acetate and 3M NaCl) and rotated for 15 minutes. The membranes then were air-dried at room temperature for 30 minutes. The ssDNA was fixed on the nylon membranes by sandwiching them between two filtering papers and incubated at 80°C for 30 minutes. The blotted nylon membranes were hybridized at Human Genetic Unit at Western General Hospital with radiolabelled probes. These probes were the purified products from PCR amplification of pIN with genotyping primers, which were radiolabelled with 32p. These PCRs were used as a positive control of the potentially transgenic mice DNA southern blotting hybridization.

Immunofluorescence methods

Indirect surface staining of cultured human B cells

Two volumes of cultured human B cells (1×10^6 cells in 200 μ l of media) were provided kindly by Dr Lorna Henderson. These two volumes were placed in two wells of 96 wells plate and one sample was used for immunofluorescence staining and the other sample was used as a negative control (no primary antibody was used). 5 μ l of the primary antibody (HLA DR7 IgM-Biotinylated Monoclonal Antibody from One Lambda Inc) was added to the positive sample and both samples were incubated on ice for 30 minutes. Then they were centrifuged at 1000 rpm for 4 minutes at 4°C and the supernatant was discarded. The cellular pellets were washed by addition of 200 μ l of FACS buffer (0.2% NaN₃ and 1% FBS in PBS) with BSA; which blocks the non-specific binding sites of the secondary antibody, centrifuged as above and the supernatant was discarded. This washing step was repeated and the pellets were resuspended in 200 μ l of FACS buffer. 5 μ l of the secondary antibody (Streptavidin, R-phycoerythrin conjugate from sigma) was added and incubated on

ice for 30 minutes. Then they were centrifuged at 1000 rpm for 4 minutes at 4°C and the supernatant was discarded. To wash the cellular pellets 200 ul of FACS buffer was added centrifuged as above and the supernatant was discarded. The washing step was done twice. Finally the pellets were resuspended in FACS buffer, wrapped in foil, examined with light and immunofluorescence microscopy (a drop of the suspension was placed on a glass slide and covered with coverslip) with different magnification and photographed with a digital camera.

Cytospin of cultured human B cells and staining with Haematoxylin and Eosin

Cultured human B cells were provided by Dr Juan Zou. They were spun at 1000 rpm for 4 minutes at 4°C and resuspended in 1 ml of PBS (contains 1×10^5 cells which is the optimal number for good cytopspin results in 20 ul of PBS). The cytopspin machine (Cytospin4-Thermo Shandon) was set at 300 rpm for 3 minutes. Poly-L-lysine coated glass slides (sigma-aldrich) were marked and dated by pencil then placed in the metallic device of cytopspin machine. The slides were covered with filter papers which have a hole on each side. Samples containers were placed on the filter papers. These containers have two opening; the upper opening where the samples loaded and the side opening placed on the filter paper hole and finally 20 ul of B cell aliquot was loaded. The cytopspin technique is that after the samples were loaded the cells passed from the containers through the filter papers holes which suck any fluid to attach on the slides. After 3 minutes of cytopspin the sample left to air dry at room temperature for one hour. The sample then fixed in methanol for one minute, stained with eosin for 2 minutes, stained with haematoxylin for one minute, washed with distilled water and kept at room temperature overnight to dry. The following day the sample was examined under the light microscope with different magnification and photographed with a digital camera.

Cytospin and direct surface staining of cultured human B cells with anti-DR, DP, DQ antibody

Cultured human B cells were spun at 1000 rpm for 4 minutes at 4°C and resuspended in 2 ml of PBS. Two volumes of 134 ul of B cells (1×10^5 cells each) were cytopspun on Poly-L-lysine coated cells. They left at room temperature for 30 minutes to air

dry, then fixed with acetone for 5 minutes at 4°C. They were washed with PBS several times and one sample was incubated for 30 minutes with 100 ul (1:50 dilution in PBS) of mouse anti-human HLA class II DP, DQ, DR (Serotec). This antibody is labelled with FITC green. The other sample was incubated for 30 minutes with 100 ul (1:50 dilution in PBS) of mouse IgG2a negative control:FITC. This antibody has FITC stain but does not react with human class II molecules. The slides then were washed with PBS several times and mounted with 50% glycerol in PBS. They were examined with light and immunofluorescence microscopy with different magnification and photographed with a digital camera (same setting for both slides).

Cytospin and indirect surface staining of cultured human B cells with L243 antibody

Cultured human B cells were spun at 1000 rpm for 4 minutes at 4°C and resuspended in 2 ml of PBS. Two volumes of 100 ul of B cells (1×10^5 cells each) were cytospun on Poly-L-lysine coated cells. They left at room temperature for 30 minutes to air dry, then fixed with acetone for 5 minutes at 4°C. They were washed with PBS several times and one sample was incubated for 60 minutes with 100 ul of mouse anti-human HLA class II L243 antibody (antibody supernatant in PRMI 1640 medium - GIBCO). The blockage of non specific binding sites was done at the same time of the antibody incubation with 100 ul of 2% BSA in PBS. The other sample was incubated for 60 minutes with 100 ul of 2% BSA in PBS. The slides then were washed with PBS several times and incubated for 30 minutes with 100 ul (1:50 dilution in PBS) of goat anti-mouse IgG-FITC conjugate (sigma). Then washed with PBS several times and mounted with 50% glycerol in PBS. They were examined with light and immunofluorescence microscopy with different magnification and photographed with a digital camera.

Staining of HeLa cells with anti-cytokeratin 8 antibody

HeLa cells were grown overnight on coverslips in RPMI 1640 medium (GIBCO) and provided kindly by Brian McHugh. HeLa cells are immortalized cell line and they are human epithelial cells from a fatal cervical carcinoma transformed by human papillomavirus 18 (HPV18). Once received the next day two coverslips were

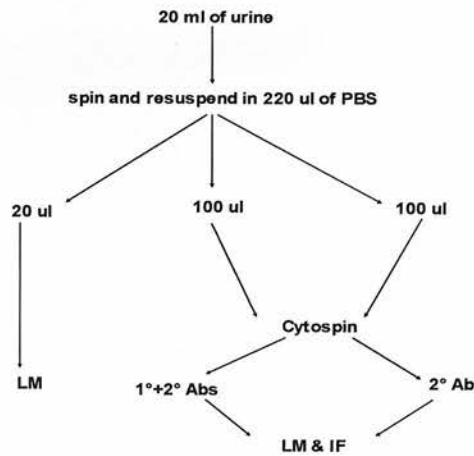
checked under the light microscope. Then they were washed with PBS several times, air dried for 30 minutes at room temperature and fixed with acetone for 5 minutes at 4°C. Washed several times with PBS and permeabilized with 100 ul of 0.3% Triton X-100 in PBS for 5 minutes at room temperature, then washed with PBS. One coverslip was incubated for 60 minutes with 100 ul (1:100 dilution in 2% of BSA in PBS) of mouse anti-cytokeratin 8 antibody (sigma) at room temperature and the other coverslip was incubated for the same period with 100 ul of 2% BSA in PBS. After several washing with PBS the coverslips were incubated for 30 minutes with 100 ul (1:50 dilution in PBS) of goat anti-mouse IgG:FITC conjugated (sigma) at room temperature. The slides were washed with PBS several times and mounted with 50% glycerol in PBS. They were inverted up side down on a glass slides and examined with light and immunofluorescence microscopy with different magnification and photographed with a digital camera.

Staining of human kidney sections with anti-synaptopodin antibody

1 ml of mouse monoclonal anti-synaptopodin antibody was sent to Dr Chris Bellamy at Edinburgh Royal Infirmary. A dilution of 1:100 of the antibody was made and it was tested on human kidney sections with immunoperoxidase staining.

Staining of urinary sediments with anti-synaptopodin, anti-WT1 and anti-cytokeratin 8 antibodies

The urine samples (20 ml) were processed within 3-4 hours. They were spun at 2500 rpm for 5 minutes at 4°C and the urinary sediment of each sample was resuspended in 220 ul of PBS and divided as explained below.



20 ul was examined under light microscopy before staining to check for the presence of cells in this sediment and photographed by digital camera. The rest of the suspension was divided into two samples of 100 ul each. They were then cytospun onto Poly-L-lysine coated glass slides. They were left at room temperature for 30 minutes to air dry, then fixed with acetone for 5 minutes at 4°C. They were washed with PBS several times and permeabilized with 100 ul of 0.3% of Triton X-100 in PBS. Then washed with PBS several times and one sample was incubated for 60 minutes with 100 ul (1:100 dilution in 2% BSA in PBS) of mouse monoclonal anti-synaptopodin antibody (Progen) or rabbit polyclonal anti-WT1 antibody (Santa Cruz biotechnology) or mouse monoclonal anti-cytokeratin 8 antibody. The other sample was incubated for 60 minutes with 100 ul of 2% BSA in PBS. The slides then were washed with PBS several times and incubated for 30 minutes with 100 ul (1:50 dilution in PBS) of goat anti-mouse IgG-FITC conjugate (Sigma) or donkey anti-rabbit IgG:PE conjugate (Santa Cruz biotechnology). Then washed with PBS several times and mounted with 50% glycerol in PBS. They were examined with light and immunofluorescence microscopy with different magnification (each slide was examined in 10 minutes) and photographed with a digital camera.

Please note that the magnification provided in the figures depicting microscopy findings needs to be multiplied by a factor of 10 in order to give the correct magnification.

Chapter 3

Detection of podocyte-specific proteins mRNA in the urine of proteinuric renal patients.

Introduction

Podocytes or visceral epithelial cells are highly differentiated cells located on the outer surface of the glomerular capillaries. Podocytes are terminally differentiated cells and have limited capacity for regeneration.

Li and colleagues (2001) reported development of non-invasive method for acute rejection by the detection of mRNA of cytotoxic proteins (perforin and granzyme B) in the urine with reverse transcriptase polymerase chain reaction (RT-PCR). Szeto and associates (2005) have found that urinary mRNA of Transforming Growth Factor β (TGF- β) is correlated with renal function, the degree of histological damage as well as intra-renal level in patients with chronic renal diseases; and this can be used as a non-invasive investigation for the assessment of the severity of these diseases.

Nephrin and podocalyxin mRNAs were chosen as markers for podocyte injury in urine of proteinuric patients because they are podocyte-specific mRNAs and β -actin mRNA was used as a positive control for total RNA extraction because it is present in abundant amount in cells.

Because the aim was to develop a clinically useful test the samples were processed within 3-4 hours (to be adaptable for clinical practice) without trying to preserve mRNA by any way. Optimization has been done for every single step in the method thereafter. This was for cDNA PCR conditions, total RNA extraction from patients urine, DNaseI treatment, and cDNA synthesis. Finally cDNA PCR sensitivity was calculated.

Results

Optimization of nephrin and podocalyxin cDNA PCR conditions

PCR conditions for nephrin and podocalyxin cDNA were optimized using the control cDNA. Three different annealing temperatures were compared for two pairs of nephrin cDNA primers and two pairs of podocalyxin cDNA primers. The optimal annealing temperature for HuNeph1For & HuNeph1Rev and HuPodo1For & HuPodo1Rev was 70°C and for HuNeph2For & HuNeph2Rev and HuPodo2For & HuPodo2Rev was 65°C (figure 3.1).

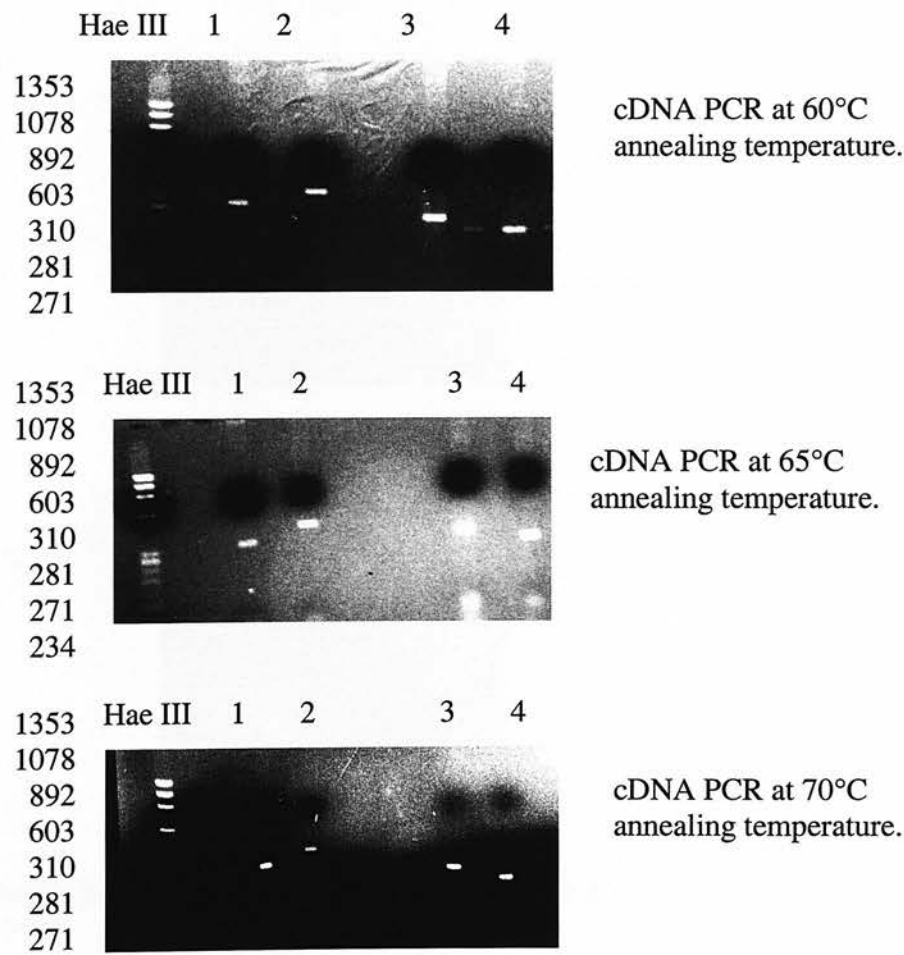


Figure 3.1. Optimization of nephrin and podocalyxin cDNA PCR conditions

- 1 = HuNeph1For and HuNeph1Rev (310 bp)
- 2 = HuNeph2For and HuNeph2Rev (377 bp)
- 3 = HuPodo1For and HuPodo1Rev (290 bp)
- 4 = HuPodo2For and HuPodo2Rev (217 bp)

RNA purification methods do not appear to be equal

Two different methods were used to extract total RNA from the urine of proteinuric renal patients. The extraction was by TRIzol and Agilent total RNA isolation mini kit. Two sets of 7 tubes of urine samples (10 ml each) with added human B cells in the order 1 million; 500,000; 100,000; 10,000; 1000; 100; 10 went through total RNA extraction by the two methods, treated similarly with DNaseI (second method), cDNA was synthesized with AMV-RT and finally β -actin cDNA PCR was done. The results showed that TRIzol method is 10-fold better than Agilent total RNA isolation mini kit (figure 3.2).

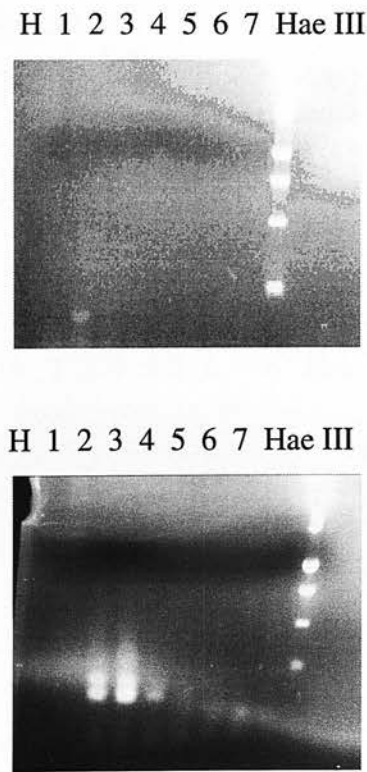


Figure 3.2. TRIzol is better than Agilent kit in RNA purification (β -actin cDNA PCR)

- | | |
|-------------------|---------------------|
| H = water control | 1 = 1 million cells |
| 2 = 500,000 cells | 3 = 100,000 cells |
| 4 = 10,000 cells | 5 = 1000 cells |
| 6 = 100 cells | 7 = 10 cells |

Glycogen and tRNA are equal in total RNA precipitation

This was a trial to increase the amount of extracted total RNA by adding two different RNA precipitants. Total RNA was extracted from two sets of 8 tubes of urine samples with added B cells in the order 1 million; 500,000; 100,000; 10,000; 1000; 100; 10; 1. RNA was extracted by TRIZol method and in one set of dilution was precipitated by adding glycogen and in the other by tRNA to the top layer (aqueous phase) from chloroform stage just before isopropanol precipitation. Then it treated with DNaseI (second method) and cDNA was synthesized with AMV-RT. β -actin cDNA PCR showed that glycogen and tRNA are equal in terms of total RNA precipitation, but either was 10,000-fold better in comparison to the result when neither of them was used (figure 3.3).

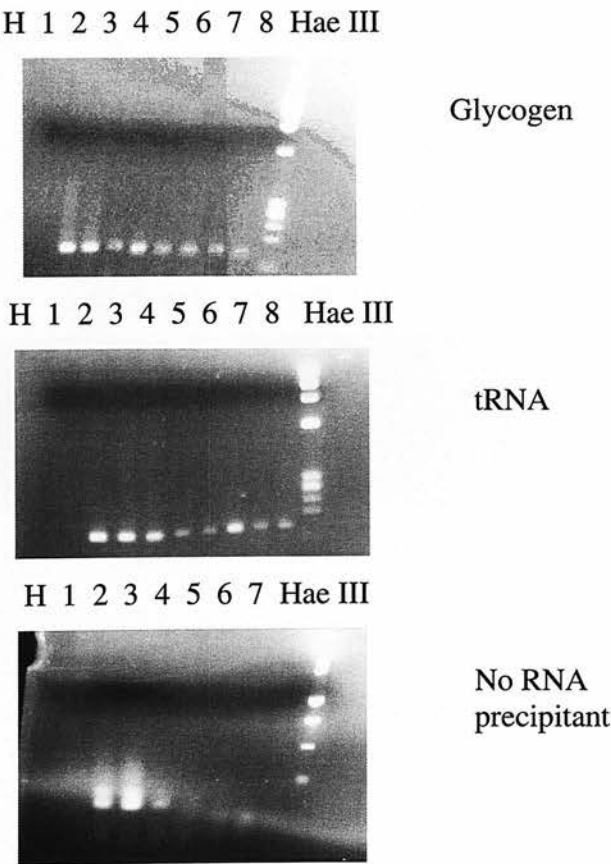


Figure 3.3. Glycogen and tRNA are equal in total RNA precipitation (β -actin cDNA PCR)

H = water control
3 = 100,000 cells
6 = 100 cells

1 = 1 million cells
4 = 10,000 cells
7 = 10 cells

2 = 500,000 cells
5 = 1000 cells
8 = 1 cell

β-actin and podocalyxin cDNA primers work on human genomic DNA but nephrin primers do not

A dilution series of 1 ug; 0.1 ug; 0.01 ug; 0.001 ug; 0.0001 ug in 25 ul of nuclease-free water was made from human B cells genomic DNA. 2 ul from each of them was used for β-actin, podocalyxin and nephrin PCR. The rationale behind this was to know whether, if the extracted RNA was contaminated with DNA, would that interfere with the cDNA PCR results for β-actin, podocalyxin and nephrin. The results showed positive bands in 1 ug; 0.1 ug; 0.01 ug and 0.001 ug lanes of β-actin and 1 ug; 0.1 ug; 0.01 ug lanes of podocalyxin but no positive bands for nephrin. In other words β-actin and podocalyxin cDNA primers work on human genomic DNA but nephrin do not (figure 3.4).

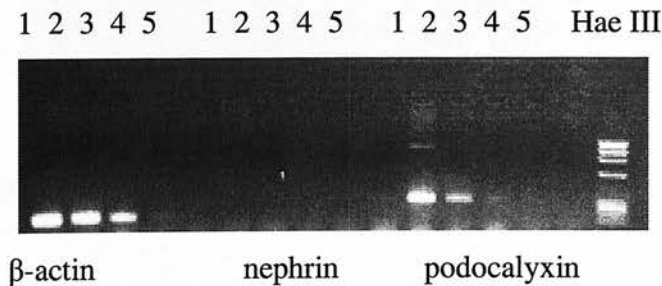


Figure 3.4. β-actin and podocalyxin cDNA primers work on human genomic DNA but nephrin do not

- 1 = 1 ug/25ul
- 2 = 0.1 ug/25ul
- 3 = 0.01 ug/25ul
- 4 = 0.001 ug/25ul
- 5 = 0.000 1ug/25ul

DNaseI destroys all DNA in the presence of AMV-RT buffer

During RNA extraction DNA may come through as well, and that is why RNA extraction was followed by DNaseI treatment before cDNA synthesis. To test the efficiency of DNaseI, a dilution series of 1 ug; 0.1 ug; 0.01 ug; 0.001 ug; 0.0001 ug in 5 ul nuclease-free water was made from human B cells genomic DNA and the whole 5 ul was used instead of total RNA (second method of DNaseI treatment and cDNA synthesis). 2 ul of this reaction was used to do β -actin, podocalyxin and nephrin PCR. The result showed that DNaseI destroyed all DNA (figure 3.5).

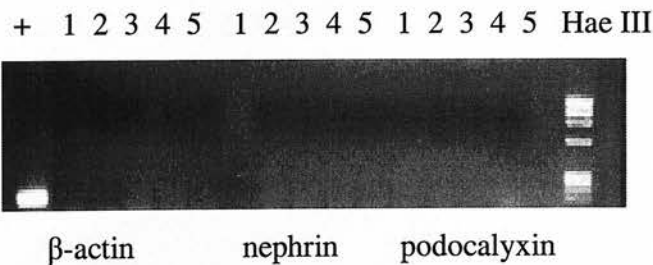


Figure 3.5. DNaseI destroys all DNA in RNA prep

- + = positive control
- 1 = 1 ug/25ul
- 2 = 0.1 ug/25ul
- 3 = 0.01 ug/25ul
- 4 = 0.001 ug/25ul
- 5 = 0.0001 ug/25ul

Heat kills DNaseI before cDNA synthesis

In the second method of DNaseI treatment of total RNA and cDNA synthesis both occur in the same microcentrifuge tube. DNaseI could destroy the synthesized cDNA later if its enzymatic activity persisted. DNaseI was inactivated by heat (75°C for 10 minutes). To test whether heat inactivation alone was efficient, a dilution series of 1 ug; 0.1 ug; 0.01 ug; 0.001 ug; 0.0001 ug in 5 ul nuclease-free water was made from human B cells genomic DNA and the whole 5 ul was added instead of reverse transcriptase (as you can see from the second method of DNaseI treatment this enzyme has been added and inactivated by heat). 2 ul of this reaction was used to do β -actin, podocalyxin and nephrin PCR. The result showed positive bands in β -actin and podocalyxin indicating that DNaseI was completely destroyed by heat. The added DNA gave positive PCR results (upper result) identical to the PCR results (lower result) without DNaseI treatment (figure 3.6).

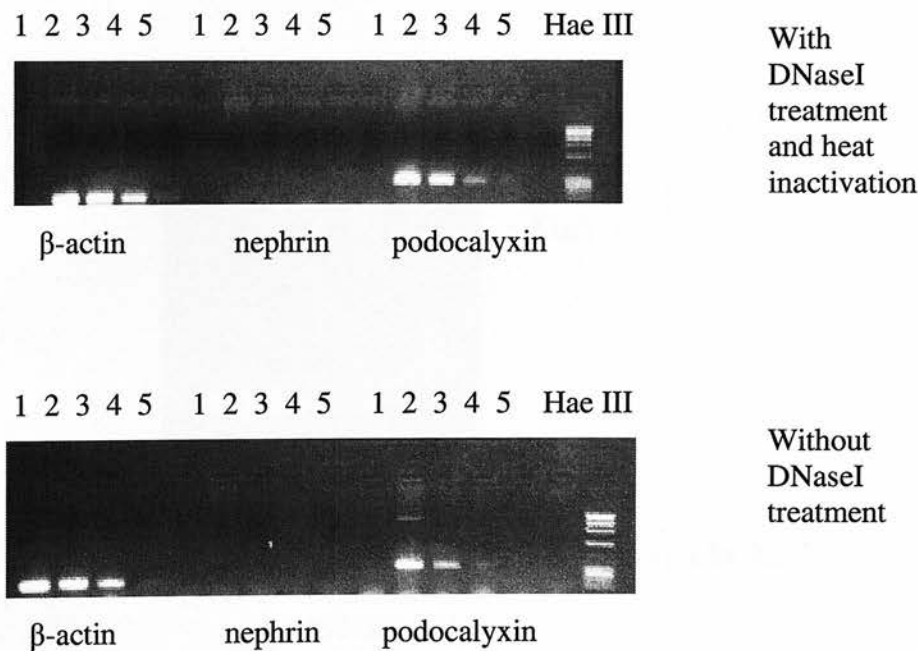


Figure 3.6. Heat kills DNaseI before cDNA synthesis

- 1 = 1 ug/25ul
- 2 = 0.1 ug/25ul
- 3 = 0.01 ug/25ul
- 4 = 0.001 ug/25ul
- 5 = 0.0001 ug/25ul

MMLV-RT appears better than AMV-RT

Total RNA was extracted from two sets of 7 tubes of urine samples (10 ml each) with added human B cells in the order 1 million; 500,000; 100,000; 10,000; 1000; 100; 10 by TRIZol methods. These samples were treated similarly with DNaseI (second method) but cDNA was synthesized differently; one set with AMV-RT and the other set with MMLV-RT. β -actin cDNA PCR was done and the results appeared to show that MMLV-RT is better than AMV-RT by a factor of 10,000 (figure 3.7).

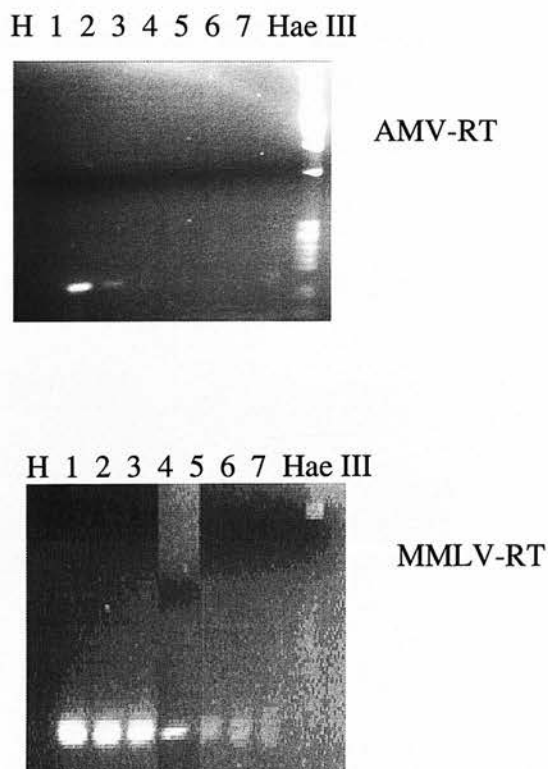


Figure 3.7. MMLV-RT appears better than AMV-RT (β -actin cDNA PCR)

H = water control

2 = 500,000 cells

4 = 10,000 cells

6 = 100 cells

1 = 1 million cells

3 = 100,000 cells

5 = 1000 cells

7 = 10 cells

Failure of DNaseI activity explains apparent superiority of MMLV-RT

But by testing the efficiency of DNaseI (second method) in the presence of MMLV-RT buffer it was found that positive bands are most probably DNA bands and not cDNA. This was by doing β -actin and podocalyxin PCR on human dilution series of human genomic DNA in the order 1; 0.1; 0.01; 0.001 and 0.0001 in 25 μ l of nuclease-free water (2 μ l was used for the PCR) with and without DNaseI treatment. The results showed incomplete destruction of the DNA by DNaseI in the presence of MMLV-RT buffer and the amount of DNA was reduced by 1000 folds in podocalyxin PCR and 10 folds in β -actin (figure 3.8). No nephrin PCR was done because it was known from a previous experiment that its primers do not work on human genomic DNA (see figure 3.4).

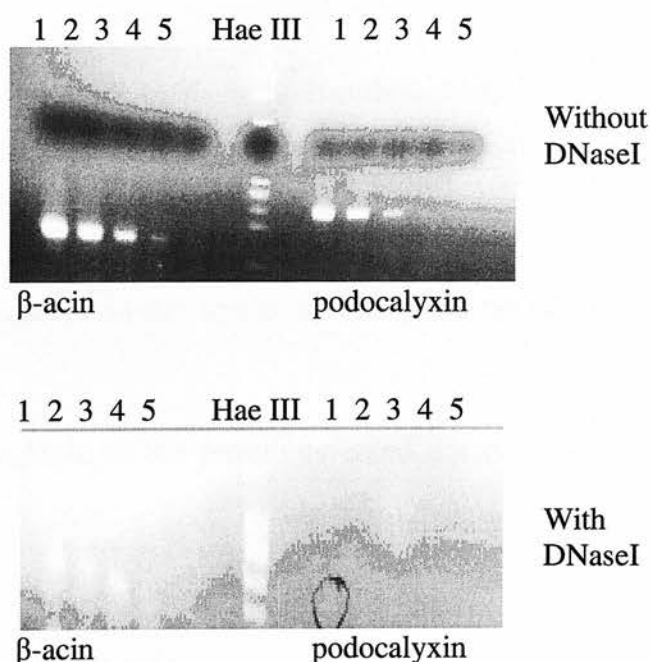


Figure 3.8. DNaseI works inefficiently in MMLV-RT buffer

- 1 = 1 μ g/25 μ l
- 2 = 0.1 μ g/25 μ l
- 3 = 0.01 μ g/25 μ l
- 4 = 0.001 μ g/25 μ l
- 5 = 0.0001 μ g/25 μ l

Sensitivity of β -actin, podocalyxin and nephrin cDNA PCR

PCR sensitivity was calculated for β -actin and podocalyxin by determining how many genomic copies could be detected by PCR.

A dilution series of 1 ug; 0.1 ug; 0.01 ug; 0.001 ug; 0.0001 ug in 25 ul of nuclease-free water was made from human B cells genomic DNA. 2 ul ($2/25^{\text{th}}$) of these dilutions was used to do β -actin, nephrin and podocalyxin PCR (figure 3.4). According to that the amount of DNA used in this PCR was 80 ng; 8 ng; 0.8 ng; 0.08 ng and 0.008 ng. Because 1 ng of DNA contains approximately 330 copies of the genome, and β -actin PCR was positive in the first four lanes (1 ug; 0.1 ug; 0.01 ug and 0.001 ug), the number of genomic copies in the positive lanes of β -actin PCR was 26400; 2640; 264 and 26 copies and the last figure is the PCR sensitivity of β -actin.

Podocalyxin PCR gave positive bands in the first three lanes (1 ug; 0.1 ug and 0.01 ug). So, the number of genomic copies was 26400; 2640; 264 copies and the last figure is the PCR sensitivity of podocalyxin.

Nephrin PCR was negative so the sensitivity could not be calculated using this method.

Nephrin PCR was negative so the sensitivity could not be calculated using this method.

This was calculated as below:

$$\begin{aligned}\therefore \text{Human genome} &= 3 \times 10^9 \text{ bp} \\ \therefore \text{Molecular weight of bp} &= 629 \text{ Dalton} \\ \therefore \text{Molecular weight of human genome} &= 3 \times 10^9 \times 629 \text{ Dalton} \\ \therefore \text{Avogadro number } (6 \times 10^{23}) &= 3 \times 10^9 \times 629 \text{ g} = 3 \times 10^9 \times 629 \times 10^{12} \text{ pg} \\ \therefore \text{Human genome} &= \frac{3 \times 10^9 \times 629 \times 10^{12}}{6 \times 10^{23}} \\ &= 3 \text{ pg} \quad \therefore 1 \text{ ng contains 330 genomic copies}\end{aligned}$$

Patients results

Seventy urine samples were collected from seventy renal patients with proteinuria. All of these samples were negative for nephrin and podocalyxin cDNA PCR after the optimization steps described above. Many samples gave positive β -actin cDNA PCR results (figure 3.9) and the control human kidney cDNA consistently gave positive results.

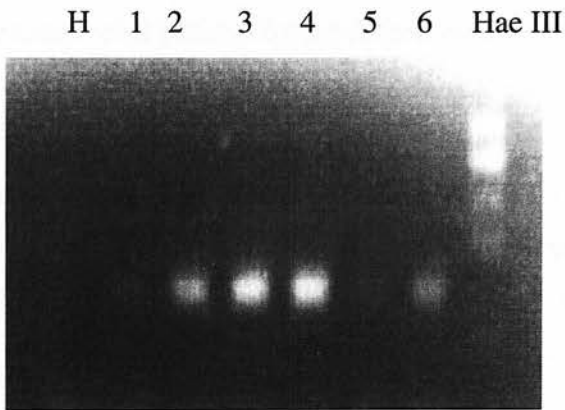


Figure 3.9: PCR of urinary β -actin cDNA of proteinuric patients

A band is seen at the predicted size of 150bp in lanes 2, 3, 4 and 6. Weak bands are seen in lanes 1 and 5.

H= water control

1-6= patients samples

Discussion

The podocyte is increasingly implicated in proteinuric renal diseases, from minimal change nephrotic syndrome and FSGS, to more overtly immunologically mediated diseases such as membranous nephropathy. It is also suspected of involvement in progressive renal disorders involving focal glomerular scar formation, such as the FSGS associated with obesity and HIV infection.

Renal biopsy is still the gold standard for the diagnosis of glomerular diseases, but is invasive and is not without complications. It was proposed to develop a non-invasive investigation of proteinuric renal patients by the detection of podocyte injury markers in their urine.

This was by total RNA extraction from patients urine and RT-PCR of nephrin and podocalyxin mRNAs which was chosen as podocyte injury markers to study and correlate that with the degree of podocyte injury on the renal biopsy of the same patients.

Li and colleagues (2001) described non-invasive technique for the diagnosis of acute renal allograft rejection by detection of mRNA of cytotoxic proteins in urinary cells with RT-PCR. It has also been reported in an abstract that podocyturia can be detected with reverse transcriptase quantitative polymerase chain reaction on nephrin mRNA (McBryde et al., 2002). A correlation has been reported between urinary mRNA of TGF- β and renal function in patients with chronic renal diseases (Szeto et al., 2005). Petermann and associates (2003) reported the detection of mRNA of podocyte-specific proteins in urine from rats with experimental membranous nephropathy.

In the first instance total RNA was extracted from patients urine samples by TRIzol method and treated with DNaseI, cDNA was synthesized with AMV-RT and finally cDNA PCR was done for β -actin, podocalyxin and nephrin but the results were inconclusive.

Because of the inconclusive results a decision was made to optimize every single step in the method to see whether the results were negative due to improper method or there were no podocyte injury markers to be detected in the urine.

Total RNA extraction was compared between two methods; TRIzol and Agilent total RNA isolation mini kit. This was from cultured human B cells added to 10 ml of urine samples in the order 1million; 500,000; 100,000; 10,000; 1000 and 10 cells. It was found that TRIzol was better where β -actin cDNA was positive in 1million; 500,000 and 100,000 lanes for TRIzol and positive only in 1 million lane in Agilent total RNA isolation mini kit (figure 3.2). Groningen and co-workers (2004) reported higher total RNA extraction with TRIzol method than NP40-based solution method and RNeasy spin columns (from Qiagen).

This was improved considerably when two RNA precipitants were compared at the isopropanol precipitation step (TRIzol method) to increase the extracted amount. Glycogen and tRNA were compared in two sets of samples (as above) and both were similar because β -actin cDNA was positive up to 1 cell lane in the two sets (figure 3.3).

A dilution series of human genomic DNA was used to answer three questions. Firstly, do β -actin, nephrin and podocalyxin cDNA primers work on human DNA? This was important because DNA can be extracted during RNA preparation and may interfere with interpretation of cDNA PCR results. This was done because it was not known if these primers cross an intron or not, because if they do not they will work on both cDNA and DNA to produce an identical band size. β -actin and podocalyxin PCR were positive but nephrin PCR was negative (figure 3.4). It was noticed that nephrin PCR was positive with human kidney cDNA (positive control), but it did not give any positive results with urine samples or human genomic DNA. This is probably because nephrin cDNA primers cross an intron and work only on the cDNA. Secondly, does DNaseI destroy all genomic DNA in the RNA preparation in the presence of AMV-RT buffer? This is important because the presence of genomic DNA will interfere with the PCR results as we can see from the above. To test that

the same DNA dilution series was used instead of total RNA and treated with DNaseI. β -actin and podocalyxin PCR were negative confirming that DNaseI destroyed all DNA (figure 3.5). Thirdly, does heat inactivate DNaseI? This is important because if DNaseI stays in the reaction it may destroy the cDNA later. DNaseI was heated with heat then the same DNA dilution was added instead of RT. β -actin and podocalyxin PCR were positive and identical to PCR results without DNaseI treatment (figure 3.6), confirming that the heating protocol used completely inactivated DNaseI.

AMV-RT and MMLV-RT were compared on two sets of urine samples with added B cells (as above). Total RNA was extracted with TRIzol and treated with DNaseI. cDNA synthesis was with AMV-RT in one set and MMLV-RT in the other set. β -actin cDNA was positive in the 1 million and 500,000 lanes of AMV-RT and till 10 cells lane of MMLV-RT (figure 3.7). But there was a question; are these cDNA or DNA bands? DNaseI treatment and cDNA synthesis take place in the same microcentrifuge tube and at that time we knew DNaseI works in AMV-RT buffer (figure 3.5), but we did not know if it works in MMLV-RT buffer or not. To test that β -actin and podocalyxin PCR were done on human DNA dilution series in the order 1 ug; 0.1 ug; 0.01 ug; 0.001 ug and 0.0001 ug in 25 ul of nuclease-free water with and without DNaseI treatment in the presence of MMLV-RT buffer (figure 3.8). β -actin and podocalyxin PCR were positive in the first four lanes without DNaseI treatment, but with DNaseI treatment it decreased by 10 folds in β -actin PCR (positive in the first three lanes) and by 1000 folds in podocalyxin PCR (positive in the first lane). Although DNaseI was not efficient in the presence of MMLV-RT buffer, it can be concluded that the PCR result will be cDNA if the β -actin and podocalyxin bands are similar but DNA if the β -actin bands are stronger. It has been described that cDNA synthesis with AMV-RT is better than Superscript; which is MMLV-RT from Invitrogen (Groningen et al., 2004).

The last step was to measure the sensitivity of β -actin and podocalyxin PCRs, and it was found that β -actin PCR is 10 fold more sensitive than podocalyxin PCR. By looking at β -actin cDNA PCR results (figure 3.3), it is clear that it is sensitive up to 1

cell in two sets of cells in the experiment. The difference between β -actin DNA and cDNA PCRs may be argued that more mRNA copies are expected to be present in one cell. Based on this observation podocalyxin cDNA PCR should give positive signals when 10 podocytes are present in patients urine which sensitive enough to detect the number of urinary podocyte reported in literature (table 1.1 and table 1.2).

In conclusion, TRIzol is better than Agilent total RNA isolation mini kit for total RNA extraction, glycogen and tRNA are similar for total RNA precipitation, DNaseI works better in AMV-RT buffer than MMLV-RT buffer, β -actin and podocalyxin cDNA primers work on human genomic DNA but nephrin do not, DNaseI kills all DNA in the RNA preparation, and heat completely destroys DNaseI .The PCR is sensitive enough for β -actin and podocalyxin.

After all of the previous optimization, and having a sensitive method, urine PCR results were all negative for podocyte mRNAs although many of these urine samples gave positive results for β -actin cDNA PCR as well as the human kidney cDNA which was consistently positive. The question therefore became whether the podocyte mRNA had been degraded before it could be detected during urine storage in the urinary bladder and the time in the outpatient department till processed, or whether there were no podocytes in the urine. Whatever the answer to this question, this method did not appear to be useful as a diagnostic investigation for proteinuric renal patients due to its persistent negativity, although some high risk patients were included randomly in the study.

I therefore went on to do urine immunofluorescence studies with podocyte protein antibodies (synaptopodin and WT1 antibodies) to answer the question and to assess whether it could be a useful and predictable non-invasive diagnostic investigation (chapter 4).

Chapter 4

Detection of podocytes and/or their fragments in the urinary sediment of proteinuric renal patients.

Introduction

As described in chapter 1, the evidence for the central role of the podocyte in the development of diseases associated with glomerular proteinuria is now very substantial.

Detection of urinary podocytes and/or their fragments with immunofluorescence (using anti-podocalyxin antibody) in the urine of patients with acute glomerulonephritis has been reported by one group to reflect disease activity (Hara et al., 1995 and Hara et al., 1998). Podocytes have been also detected in the urine of rats with experimental membranous nephropathy (Petermann et al., 2003) and experimental diabetic nephropathy (Petermann et al., 2004).

The podocyte antibody (anti-synaptopodin antibody) was chosen to be used in this immunofluorescence study for staining of urinary sediment of proteinuric patients in a trial to detect podocytes. Anti-podocalyxin antibody was not used, because it could react with platelets and other cells.

This study was conducted to explain why the mRNA of podocyte proteins was undetectable in the urine of proteinuric renal patients according to the results in chapter 3, and to know whether the results were negative because there were no podocytes in patients urine or due to other reasons.

The other aim of this study was to test the validity of detecting urinary podocyte with immunofluorescence technique as it was published as a potential non-invasive diagnostic and predictive method for the glomerular disease.

Results

Indirect surface staining of cultured human B cells

The rationale of this experiment was to validate the indirect immunofluorescence technique. Two samples of cultured human B cells (1×10^6 cells each) were involved in this experiment. The first sample was stained with primary and secondary antibodies and the second sample was used as a negative control. The results showed positive staining of B cells with immunofluorescence microscope in the first sample and B cells with light microscope and no staining with immunofluorescence microscope in the negative control sample (figure 4.1).

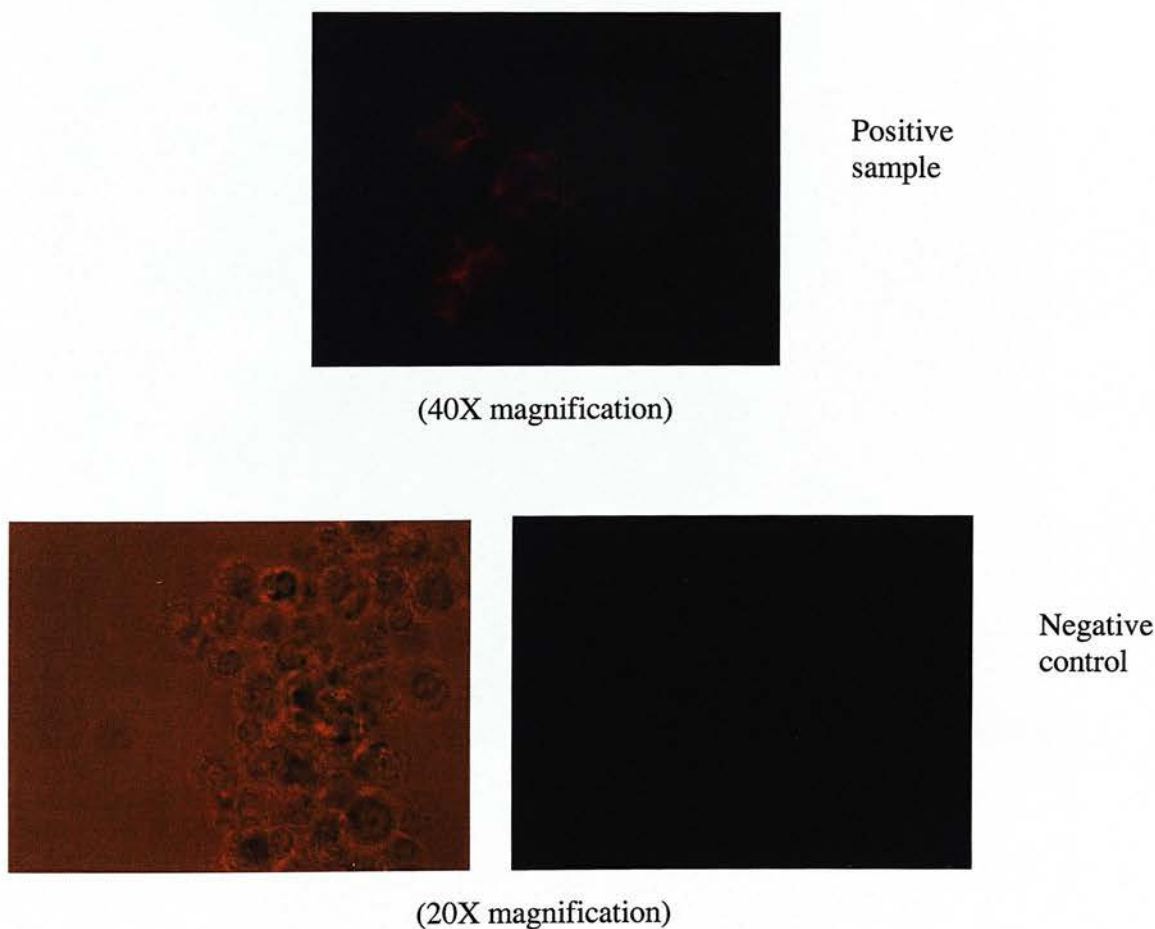
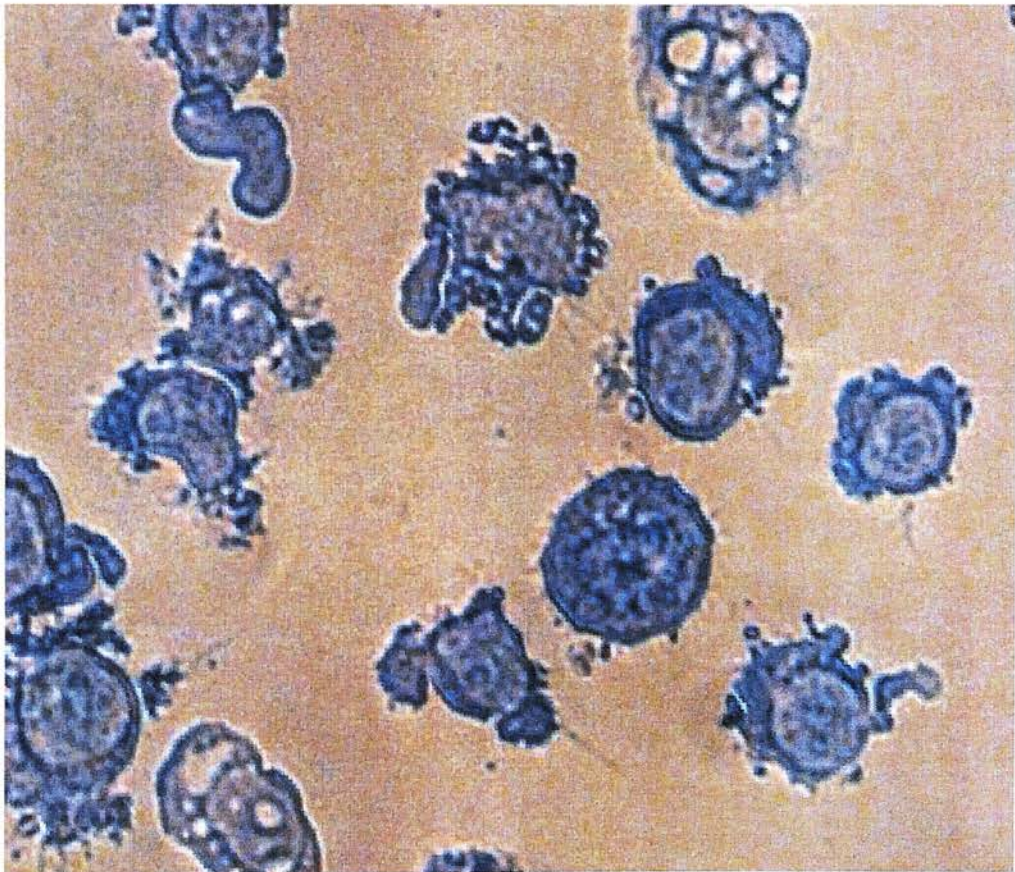


Figure 4.1: Indirect surface staining of cultured human B cells

Cytospin of cultured human B cells and staining with Haematoxylin and Eosin

The rationale of this experiment was to learn the cytopspin technique and to check the capability of cells to attach to Poly-L-lysine coated glass slides. 20 ul of B cells aliquot in PBS (contains 1×10^5 cells which is the optimal number for good cytopspin results) was cytopspun and stained with haematoxylin and eosin. Figure 4.2 shows a light microscope picture of haematoxylin and eosin stained B cells confirming that cells can be attached, fixed and stained on Poly-L-lysine coated slides.



(20X magnification)

Figure 4.2: Cytospin of cultured human B cells and staining with Haematoxylin and Eosin

Cytospin and direct surface staining of cultured human B cells with fluorescence anti-DR, DP, DQ antibody (single layer)

The rationale of this experiment was to validate the cytopspin and direct immunofluorescence technique. Two samples of cultured human B cells (1×10^5 cells each) were involved in this experiment. The first sample was stained with the antibody and the second sample was used as a negative control. The results showed positive staining of B cells with immunofluorescence microscope in the first sample and B cells with light microscope and no staining with immunofluorescence microscope in the negative control sample (figure 4.3).

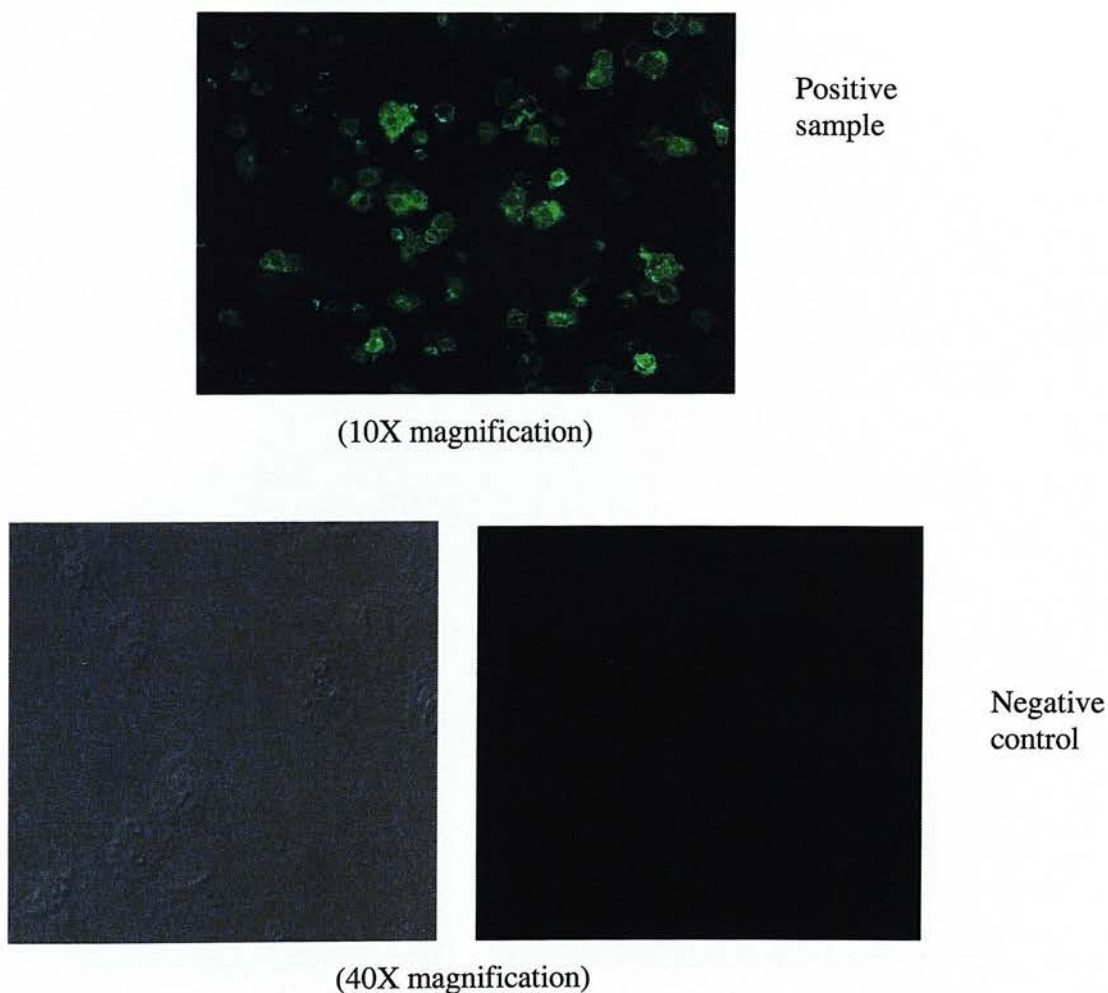
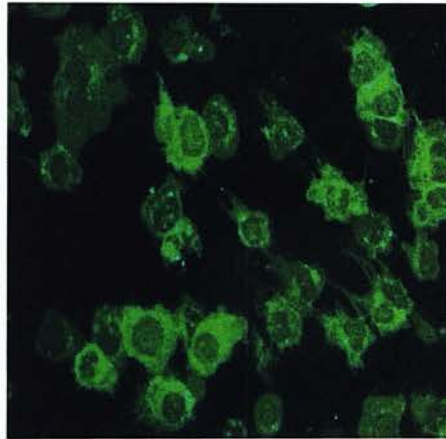


Figure 4.3: Cytospin and direct surface staining of cultured human B cells with anti-DR, DP, DQ antibody

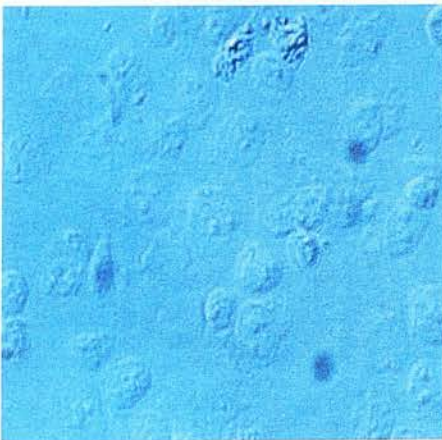
Cytospin and indirect surface staining of cultured human B cells with L243 antibody (double layer)

The rationale of this experiment was to validate the cytopspin and indirect immunofluorescence technique. Two samples of cultured human B cells (1×10^5 cells each) were involved in this experiment. The first sample was stained with primary and secondary antibodies and the second sample was used as a negative control. The results showed positive staining of B cells with immunofluorescence microscope in the first sample and B cells with light microscope and no staining with immunofluorescence microscope in the negative control sample (figure 4.4).



Positive
sample

(10X magnification)



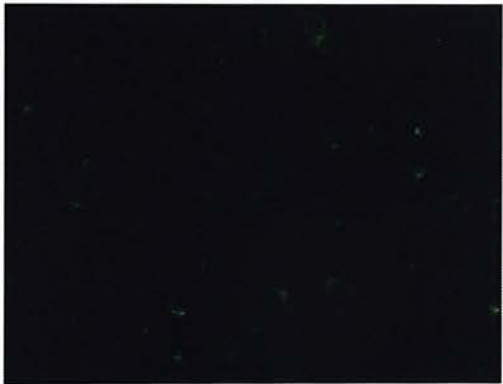
Negative
control

(40X magnification)

Figure 4.4: Cytopspin and indirect surface staining of cultured human B cells with L243 antibody

Staining of HeLa cells with anti-cytokeratin 8 antibody

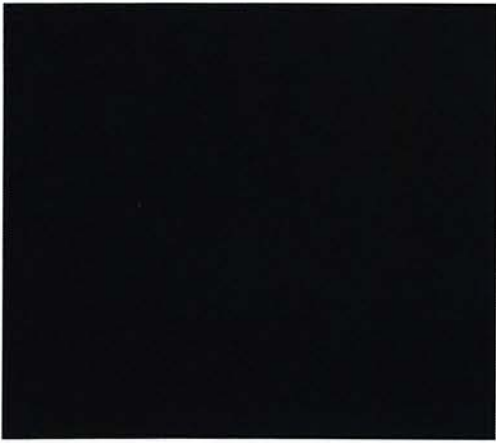
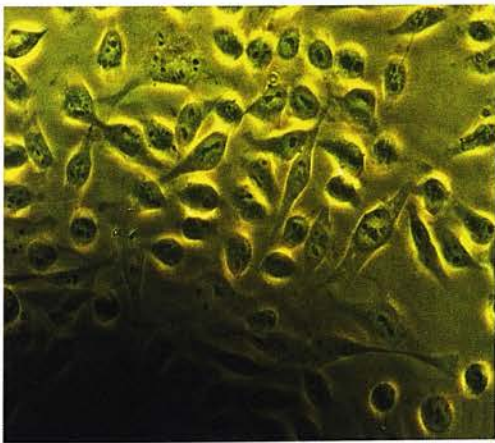
This experiment was done to test anti-cytokeratin 8 antibody on epithelial cells (HeLa cells) which are rich in cytokeratin8. This antibody was used as a positive control for the urinary sediment in this study, because this antibody stains epithelial cells in the urine. HeLa cells were grown on coverslips. One sample was stained with the primary and secondary antibodies and the other one was used as a negative control. The results showed positive staining for the positive sample and HeLa cells in negative control sample (figure 4.5).



Positive
sample

(Photographed 48 hours
later after some fading
has occurred)

(32X magnification)



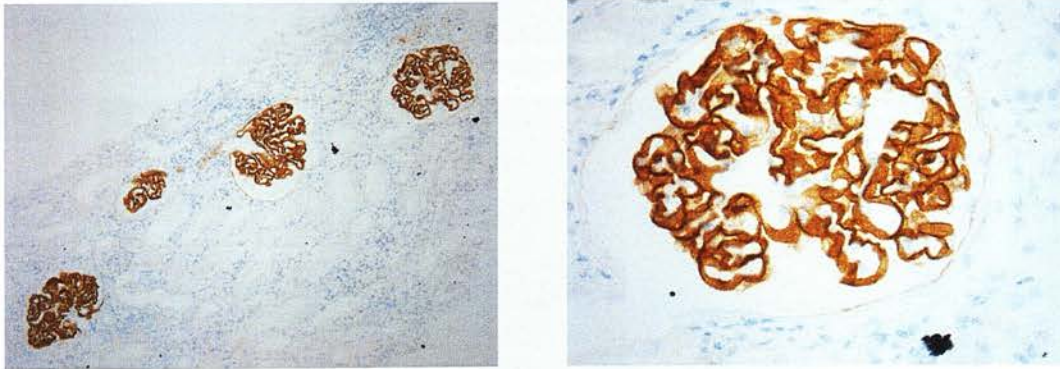
Negative
control

(32X magnification)

Figure 4.5: Staining of HeLa cells with anti-cytokeratin 8 antibody

Staining of human kidney sections with anti-synaptopodin and anti-CD2AP antibodies

This experiment was done to test anti-synaptopodin and anti-CD2AP antibodies on human kidney sections. This was done by Dr Chris Bellamy at Edinburgh Royal Infirmary. The results showed strong positive staining of the podocytes and weak staining of the arteriolar lining with anti-synaptopodin antibody (figure 4.6). Anti-CD2AP antibody showed non specific staining (has not been photographed).



Anti-synaptopodin antibody

Figure 4.6: Staining of human kidney sections with anti-synaptopodin antibody

Staining of urinary sediments with anti-cytokeratin 8 antibody

This experiment was done to check if cells from urine could be cytospun and stained. 10 samples (20 ml) of urine were collected and tested before and after staining (see method). The results showed (6 samples gave positive results) that cells can be seen under the light microscope before staining. Urinary epithelial cells stained positive for the antibody and the same field was visualised by light microscopy. Negative control slides showed urinary epithelial cells but no immunofluorescence staining (figure 4.7)

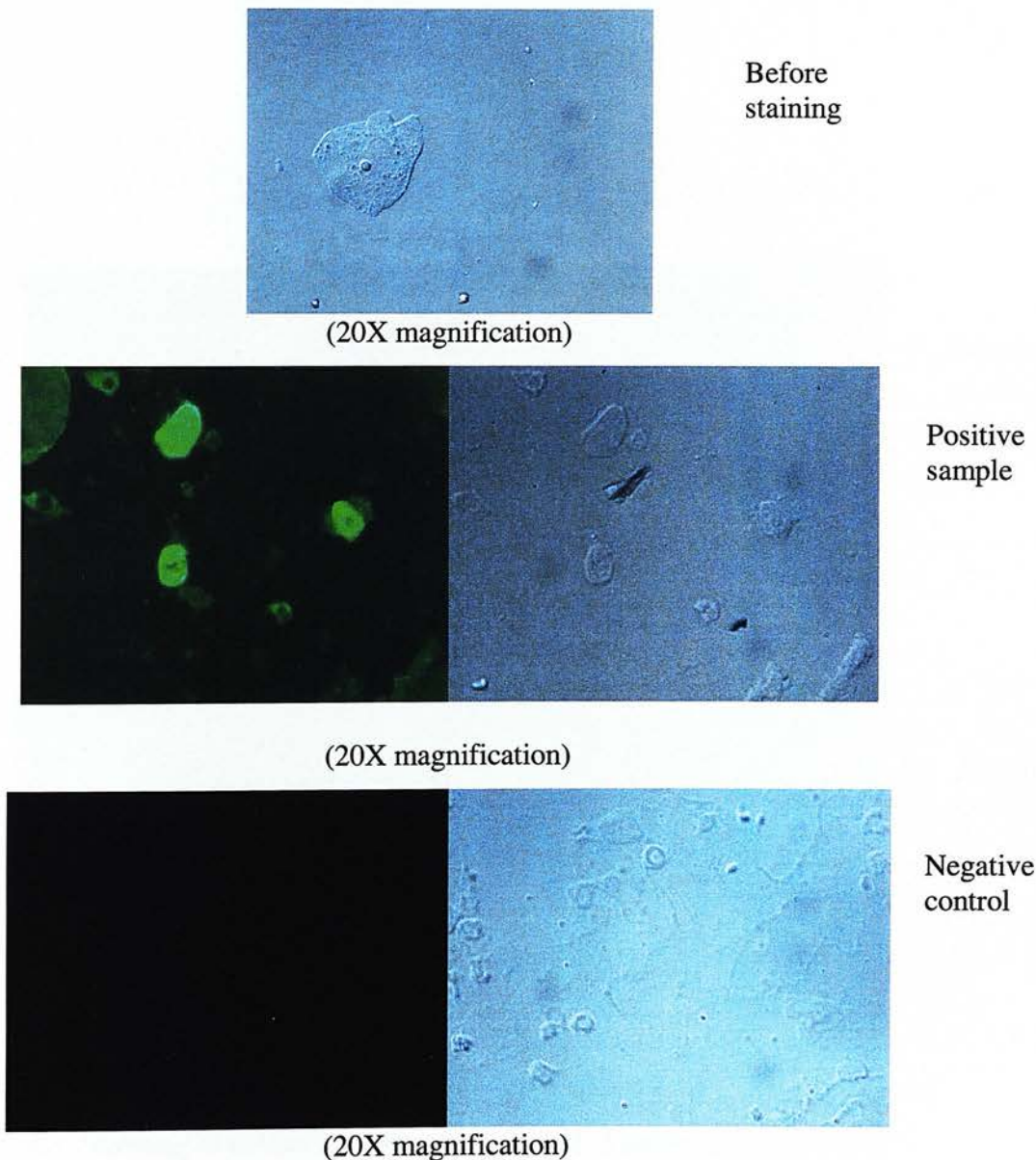


Figure 4.7: Staining of urinary sediments with anti-cytokeratin 8 antibody

Staining of urinary sediments with anti-synaptopodin antibody

100 samples (20 ml each) of urine were collected and stained with anti-synaptopodin antibody. Only one sample was positive. In this result it can be seen that urinary cells are detected before and after staining. The positive slide shows positive immunofluorescence of a urinary cell and the negative control slide shows only urinary cells with light microscopy but no immunofluorescence (figure 4.8).

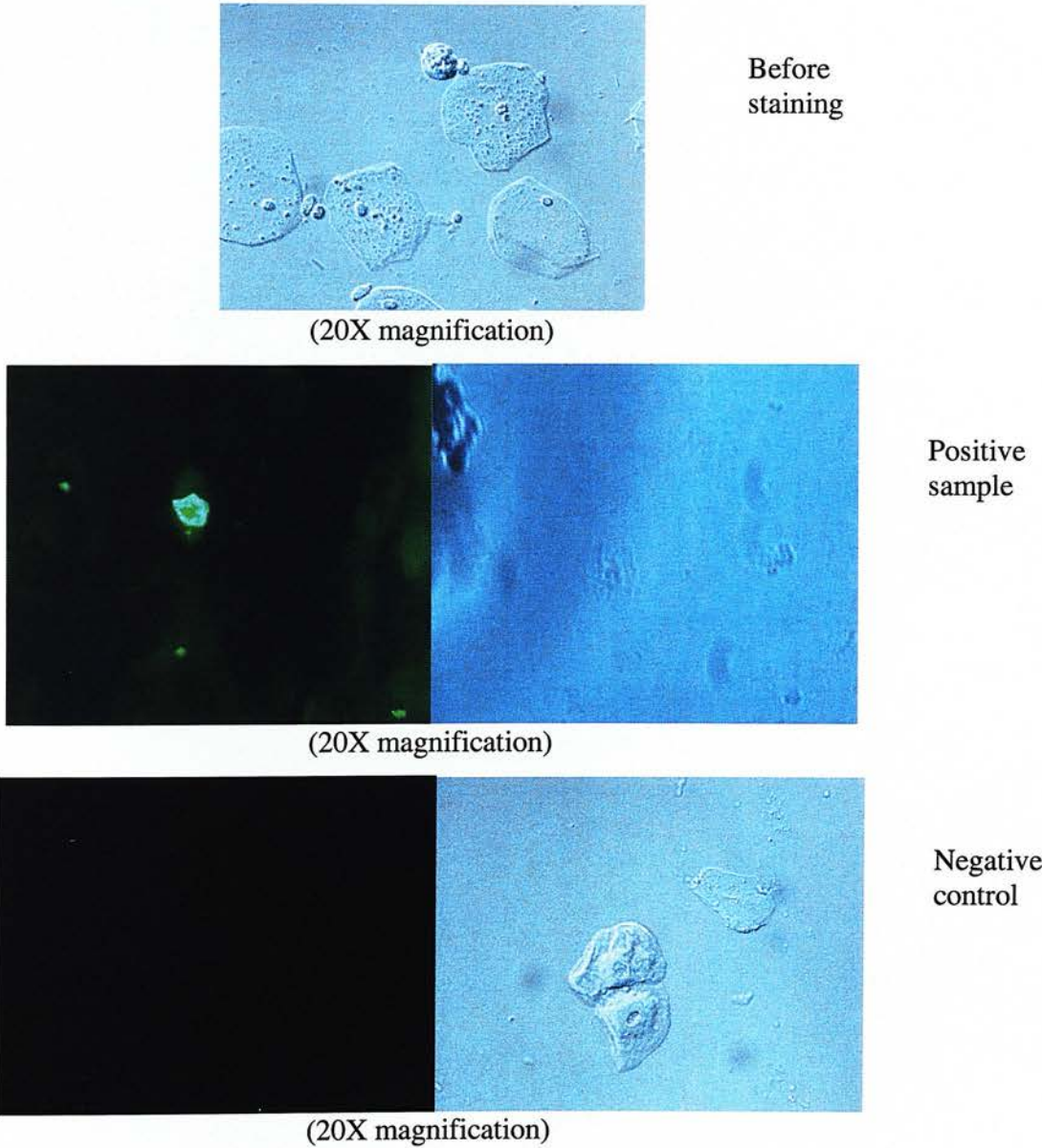


Figure 4.8: Staining of urinary sediments with anti-synaptopodin antibody

Patients results

After examining 100 urine samples, only one sample gave positive result with anti-synaptopodin antibody and all of them were negative for anti-WT1 antibody.

Discussion

Podocytes are injured in different forms of experimental and human glomerulopathies, including minimal change nephrotic syndrome, FSGS, membranous glomerulonephritis, diabetic nephropathy and lupus nephritis.

As described in the chapter 3 it was proposed to develop a non-invasive investigation for proteinuric renal patients by the detection of urinary podocyte protein mRNA by RT-PCR, but the result of 70 urine samples were negative.

In this study I was trying to achieve two goals; the first one to know whether the 70 samples were negative because there were no urinary podocytes or due to other reasons. The second goal was to develop a non-invasive investigation for glomerular renal diseases.

This was by immunofluorescence study of patients urinary sediments to detect podocytes using a monoclonal antibody against synaptopodin (an actin associated protein expressed in podocytes and hippocampal cells) and polyclonal antibody against WT1 (podocyte nuclear protein).

A non-invasive technique for the diagnosis of podocyte shedding was developed by Hara and colleagues (1995), by examining the urinary sediment of patients with different renal diseases with immunofluorescence using monoclonal antibody against podocalyxin (a glycoprotein prominently expressed on podocytes). Urinary podocytes had been identified and grown in culture from rats with experimental membranous nephropathy (Petermann et al., 2003) and experimental diabetic nephropathy (Petermann et al., 2004).

The majority of urinary podocytes evidence mostly came from the same group (e.g. Hara et al., 1998) using the same anti-podocalyxin antibody which can be expressed by vascular endothelial cells (Horvat et al., 1986), platelets (Miettinen et al., 1999) and haemopoietic stem cells (Doyonnas et al., 2001). Because of these

reasons more specific podocyte antibodies were sought including anti-synaptopodin, anti-CD2AP and anti-WT1.

Anti-synaptopodin and anti-CD2AP antibodies were tested on podocytes on human kidney section and anti-CD2AP was excluded because it was widely expressed. Anti-synaptopodin and anti-WT1 antibodies were used together because the first antibody is an intracytoplasmic and the second antibody is a nuclear antibody and if any urine sample stained positive then it can be judged whether this was a whole podocyte, nuclear or other fragment. A further step was planned to be taken place if any positive results appeared which the study of the viability of these cells and the most important the relation between urinary podocytes and the renal biopsy results of the same patients.

The method of this study was fixed by showing that B cells can be cytopun, fixed and stained on Poly-L-lysine coated glass slides. Very importantly also the cytokeratin 8 antibody positive control experiment showed that urinary cells can be cytopun, fixed and stained on Poly-L-lysine coated glass slides. Anti-cytokeratin 8 antibody was used because it stains epithelial cells which are expected to be found in the urine.

Although different cell types were found in all 100 urine samples, including tubular epithelial cells, squamous epithelial cells and red blood cells as wells as bacteria, only one urine sample stained positive for synaptopodin. All of the samples were negative for anti-WT1 antibody staining.

An irrelevant isotype control primary antibody was not employed to determine the specificity of staining in the immunofluorescence studies and this is an important caveat in the interpretation of the findings presented.

The results of urinary podocytes contrast with those reported by Hara and colleagues (1995 and 1998). This could be partly because they examined selected high risk patients, but it may also be relevant that podocalyxin can be found on platelets and elsewhere.

In conclusion, podocyte mRNA could not be detected because there were no podocytes in the urine. This immunofluorescence technique is not a good non-invasive investigation and one more set of experiments was undertaken to confirm the validity of this conclusion (chapter 5).

Chapter 5

Control experiments on podocytes

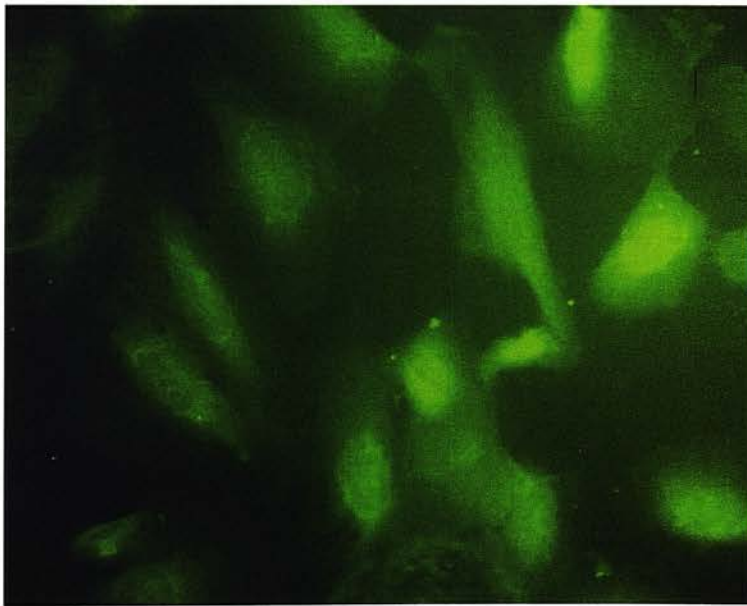
Introduction

The experiments in this chapter were a collaboration between our group and the renal unit at Southmead Hospital in Bristol. Professor Peter Mathieson and Dr Moin Saleem provided cultured human podocytes and lab space to do these control experiments. These experiments were conducted to test the techniques used for urinary podocyte mRNA extraction (chapter 3) and immunofluorescence (chapter 4) studies after the negative results which were recorded. So, the question here was to know whether these techniques were working or not.

Results

Staining of podocytes on coverslips with anti-synaptopodin antibody

The rationale of this experiment was to test anti-synaptopodin antibody on human cultured podocytes (AB-NT) before spiking the urine with podocytes in the following experiments. Podocytes were stained on coverslips with primary and secondary antibodies. The result shows positive cytoplasmic staining (figure 5.1).

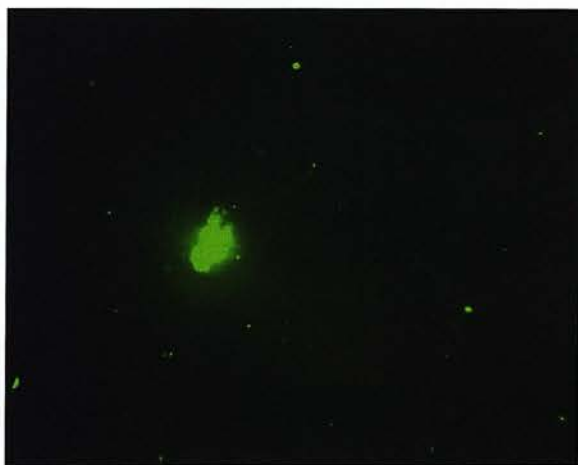


(20X magnification)

Figure 5.1: Staining of podocytes with anti-synaptopodin antibody on coverslips

Spiking of urine with podocytes and staining with anti-synaptopodin antibody

This experiment was conducted to test whether podocytes can be cytopun on Poly-L-lysine coated slides, fixed and stained with anti-synaptopodin antibody (with same method in chapter 4). Podocytes growing on coverslips were scraped off and resuspended in RPMI media and podocyte dilutions were made to contain approximate number of: 32, 16, 8, 4, 2 (3 samples) and 1 (5 samples). These dilutions were added to 1 ml of urine, cytopun and stained with anti-synaptopodin antibody. The results showed only a small proportion of podocytes could be identified; 3 cells in 32 cells slide, 1 cell in 16 cells slide, 1 cell in 8 cells slide, 1 cell in 4 cells slide, 1 cell in one of 2 cells slides and 1 cell in one of 1 cell slides. This amounts to 10-20% of the estimated cells in urine samples. These cells showed also much changed morphology (figure 5.2)

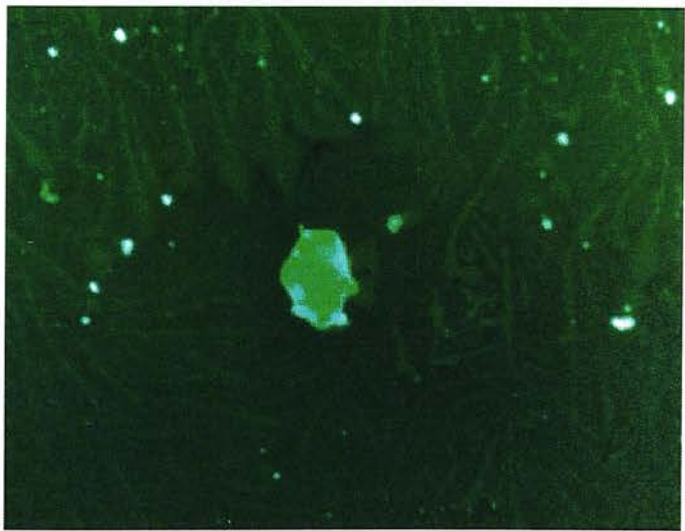


(20X magnification)

Figure 5.2: Staining of spiked urinary podocytes with anti-synaptopodin antibody

Spiking of PBS with HeLa cells and staining with anti-cytokeratin 8 antibody

When the number of positive podocytes was low in the last experiment it was decided to apply the same technique on HeLa cells and staining with anti-cytokeratin 8 antibody as a control experiment. HeLa cells were growing in tissue culture flask and dilutions were made to contain approximate number of: 32, 16, 8, 4, 2 (3 samples) and 1 (5 samples). These dilutions were added to 1 ml of PBS because anti-cytokeratin 8 antibody stains epithelial urinary (figure 4.7), cytopun and stained with anti-cytokeratin 8 antibody. The results showed 8 cells in 32 cells slide, 3 cells in 16 cells slide, 2 cells in 8 cells slide, 1 cell in 4 cells slide, 1 cell in one of 2 cells slides and 1 cell in one of 1 cell slides. Again this amounted to identification of only 10-20% of the cells that were originally added to the samples. HeLa cells also showed changed morphology (figure 5.3)



(20X magnification)

Figure 5.3: Staining of spiked HeLa cells in PBS with anti-cytokeratin 8 antibody

Spiking of urine with podocytes and RNA extraction: urinary podocyte mRNA method appears to be working

The rationale of this experiment was to test the technique used for podocytes mRNA extraction from patients urine after the negative results had been recorded. Another set of podocyte dilutions; 32, 16, 8, 4, 2 (3 samples) and 1 cell (5 samples) were added to 1 ml of urine each and went through TRIzol RNA extraction technique (with same method in chapter 3). This was followed by nephrin, podocalyxin and β -actin cDNAs PCR. Results were positive for the three PCRs and for all samples (figure 5.4).

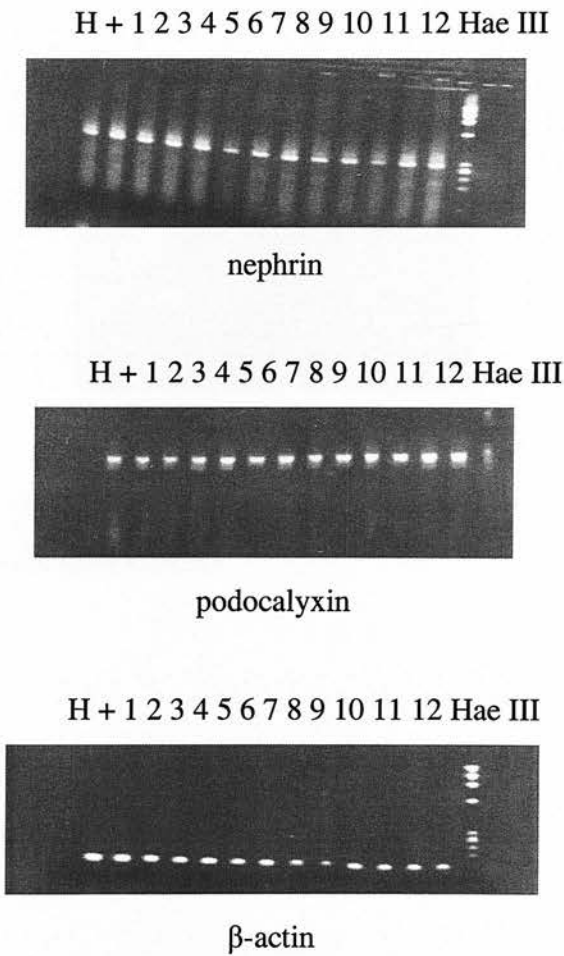


Figure 5.4: PCR of spiked urinary podocytes cDNAs

- | | |
|--------------------|---|
| H= waster control | += positive control (human kidney cDNA) |
| 1= 32 cells sample | 2= 16 cells sample |
| 3= 8 cells sample | 4= 4 cells sample |
| 5= 2 cells sample | 6= 2 cells sample |
| 7= 2 cells sample | 8= 1 cell sample |
| 9= 1 cell sample | 10= 1 cell sample |
| 11= 1 cell sample | 12= 1 cell sample |

Why all samples were positive for nephrin, podocalyxin and β -actin cDNAs PCR? Perhaps due to contamination

RNA extraction reagents were thought to be contaminated either at the time of making podocyte dilutions in Bristol or during the rest of experiment in Edinburgh. It was decided to apply the same technique on B cell and nuclease free water (same water used in the previous experiment). This was followed by podocalyxin cDNA PCR on the product of B cells, water, sample 32 and sample 16. The results were positive for the first two samples and negative for the other two (figure 5.5).

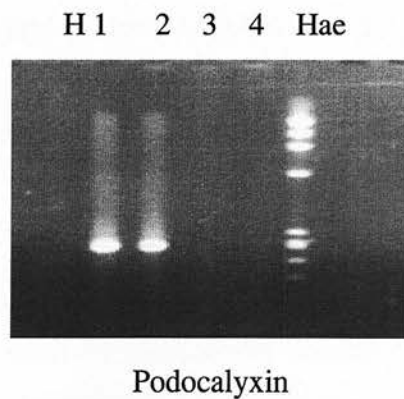


Figure 5.5: Podocalyxin cDNA PCR

H= water control
1= 32 cells sample
2= 16 cells sample
3= B cells sample
4= water sample

Discussion

The experiments in this chapter were undertaken to prove the validity of the conclusion of chapter 4 about the usefulness of urinary podocytes as a diagnostic tool. This was by testing the validity of the techniques used in chapter 3 and chapter 4 themselves. These experiments were done between Bristol and Edinburgh.

Although anti-synaptopodin antibody was proved to be working on human podocytes (figure 4.6) it was very important to test it on AB-NT podocytes grown on coverslips before spiking urine with these podocyte dilutions.

An irrelevant isotype control primary antibody was not employed to determine the specificity of staining in the immunofluorescence studies and this is an important caveat in the interpretation of the findings presented

After anti-synaptopodin antibody was proved to work on podocytes; they were scraped off coverslips and resuspended in RPMI media then two sets of podocyte dilutions were made to contain the approximate number of: 32, 16, 8, 4, 2 (3 samples) and 1 (5 samples). The dilutions were made to test the technique sensitivity.

One set of podocyte dilutions was added to 1 ml of urine each; cytospun on Poly-L-lysine coated slides and stained with anti-synaptopodin antibody. Analysis showed antibody positive cells of much changed morphology, but only 8 of about 70 cells were detected by immunofluorescence microscopy.

A control experiment was done on HeLa cells using the same method and staining with anti-cytokeratin 8 antibody. HeLa cells were growing in tissue culture flask were trypsinised and resuspended in RPMI media. The dilutions were added to PBS because anti-cytokeratin 8 antibody stains urinary epithelial cells (figure 4.7). The results again showed different morphology and similarly only 10-20% of cells were detected by immunofluorescence microscopy.

So, the immunofluorescence technique used to stain podocytes in the urine of proteinuric patients does work, but detected only 10-20% of the actual number of cells added to the preparation.

Because this technique is similar to the technique used in the original paper by Hara and colleagues (1995), which described urinary podocytes in renal patients, and in the following papers by the same group; a point can be raised about the actual number of podocytes they described in their publication and the correlations they made between urinary podocyte numbers and renal disease severity as well as correlation with different drugs.

Also the loss is more in the low dilution samples and this may be raise the possibility that patient gave negative results may have low number of podocytes in their urine which can not be detected.

It has been noticed that the pattern of immunofluorescence staining and morphology change when cells go through cytopsin machine. By looking at AB-NT podocytes (figure 5.1) and HeLa cells (figure 4.5) on coverslips a well defined cell shape and immunofluorescence staining can be seen which changes after the cytopsin (figure 5.2 and figure 5.3). This was similar to the immunofluorescence pattern of the only podocyte detected by anti-synaptopodin antibody from patient urine (figure 4.8)

The other set of podocyte dilutions was used for RNA extraction and reverse transcription followed by PCR for nephrin, podocalyxin and β -actin cDNAs. Unexpectedly all samples were positive for the three PCRs (expected to get some negative results especially in the low number dilutions) and furthermore all have the same band intensity.

This made us suspicious of contamination. A control experiment was done using B cells and water (same water used in the original experiment) which went through the same procedure for RNA extraction, with the same reagents, but in a different lab: these were negative.

I was wondering about the possibility of samples contamination at the time of making podocyte dilutions. So a plan was made to do a repeat control experiment for RNA extraction technique on another set of AB-NT podocyte dilutions which can be provided kindly by our collaborators in Bristol.

In conclusion, immunofluorescence technique works but detects only 10-20% of cells. RNA extraction technique was not adequately tested due to presumed sample contamination.

Chapter 6

Production and microinjection of podocyte construct

Introduction

The podocyte is a terminally differentiated cell and located on the outer surface of the GBM. It plays a crucial role in the glomerular filtration process and hence its injury associated with loss of protein in urine.

Specific cell ablation is a useful method for cell function analysis in vivo. Saito and colleagues (2001) developed a conditional cell ablation in transgenic mice, called toxin receptor-mediated cell knockout. This was by expressing human diphtheria toxin receptor (hDTR) on the hepatocytes of transgenic mice using the plasmid pMS7 which contains hepatocyte-specific promoter (albumin) and hDTR gene. Specific cell ablation was also reported in macrophages by Cailhier and collaborators (2005) who generated transgenic mice expressing hDTR specifically on macrophages. Mice are naturally insensitive to the effects of diphtheria toxin (DT).

DT is produced by *Corynebacterium diphtheriae* as a single polypeptide that is proteolytically cleaved into a two-chain protein. After intra-muscular injection in transgenic mice it binds to its membrane receptor, which is human Heparin Binding-Epidermal Growth Factor; (hHB-EGF) by the larger B-subunit and then internalized. The smaller A-subunit dissociates in acidic endosome and pass to the cytoplasm where it becomes catalytically active and ADP-ribosylates elongation factor 2 (EF2) and inactivate protein synthesis (Richard, 2001)

Several podocyte specific promoters have been mooted. Wong and colleagues (2000) reported that a human 1.25 kb nephrin gene fragment can lead to podocyte specific expression of LacZ in transgenic mice. Moeller and associates (2000) have shown that two murine 8.3 kb and 5.4 kb nephrin gene fragments can direct the expression of LacZ in podocytes and the brain in transgenic mice. Human 2.5 kb Podocin and murine 1.25 kb nephrin gene fragments were found to lead to podocyte specific expression of β galactosidase in transgenic mice (Moeller et al., 2002).

The strategy of this study was to test primers for the murine nephrin gene fragment described by Moeller and collaborators (2002) by Taq DNA polymerase and produce this fragment with Vent DNA polymerase. This is because it has low base insertion error (57 per million base insertion in comparison to Taq DNA polymerase which has error rate of 285 per million base insertion) and to produce blunt ended PCR product. The blunt ended PCR product would then be subcloned into pCR[®]4Blunt-Topo, the PCR product then digested with NotI and BamHI restriction enzymes and subcloned into the plasmid pMS7 to produce the podocyte specific construct (the plasmid pIN). The microinjection of the podocyte construct into murine fertilized ova would hopefully lead to generation of transgenic mice expressing hDTR on podocytes.

In this study it was proposed to induce a specific podocyte injury with DT in hDTR transgenic mice (if they were successfully generated) and study the podocyte, glomerular and renal consequences.

Results

Verification of the plasmid pMS7

This plasmid was used for generation of transgenic mice expressing hDTR specifically on hepatocyte (Saito et al., 2001). Midipreparation of the plasmid was performed from transformed E.coli and it was tested with 4 different restriction enzyme analyses according to the accompanying map (EcoRI, PstI, BamHI& BglII, and BamHI&KpnI). The results (figure 6.1) show some bands with unexpected size (full sequencing later showed non-included restriction sites in the original map), but when the plasmid was sequenced with M13For and M13Rev primers the results showed that NotI restriction site (M13Rev) is identical to murine albumin enhancer/promoter and XhoI/SalI restriction site (M13For) is identical to rabbit β -globin/polyA (figure 6.2). This means that the correct pMS7 plasmid has been obtained, although its map was inaccurate.

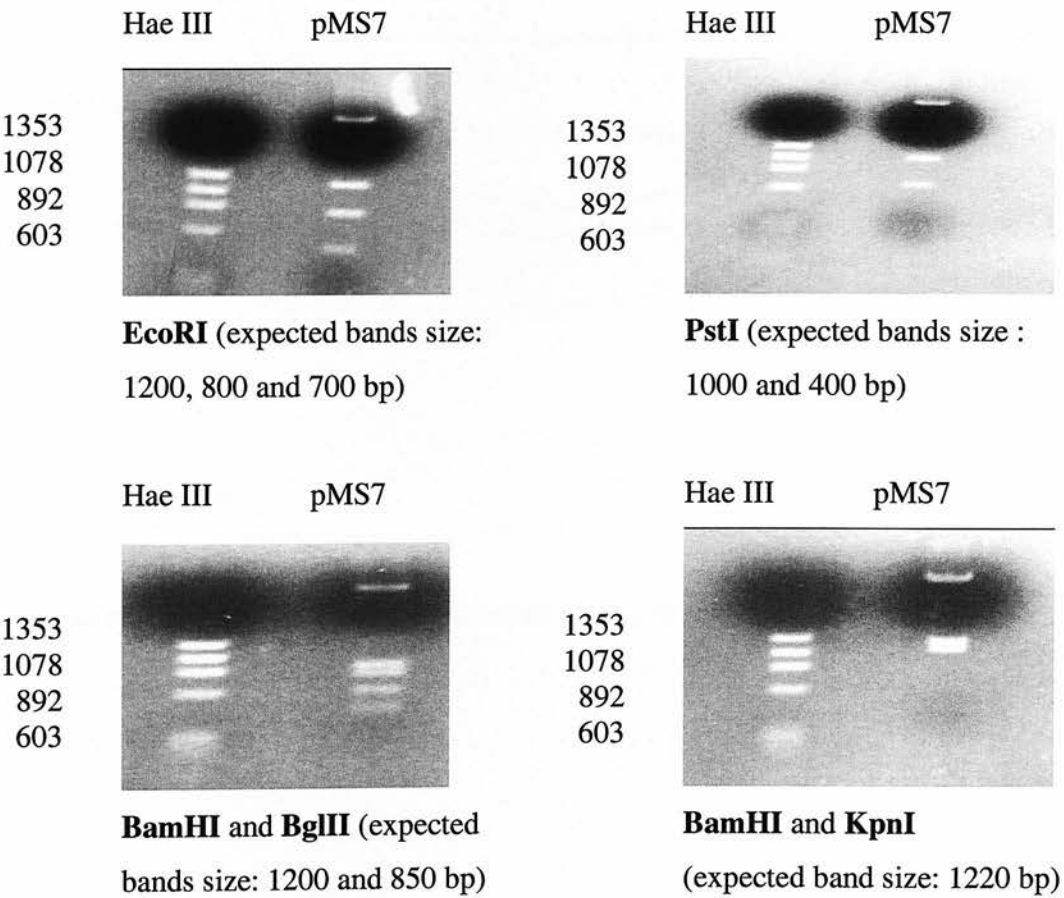


Figure 6.1: Enzyme restriction analysis of pMS7 DNA midipreparation

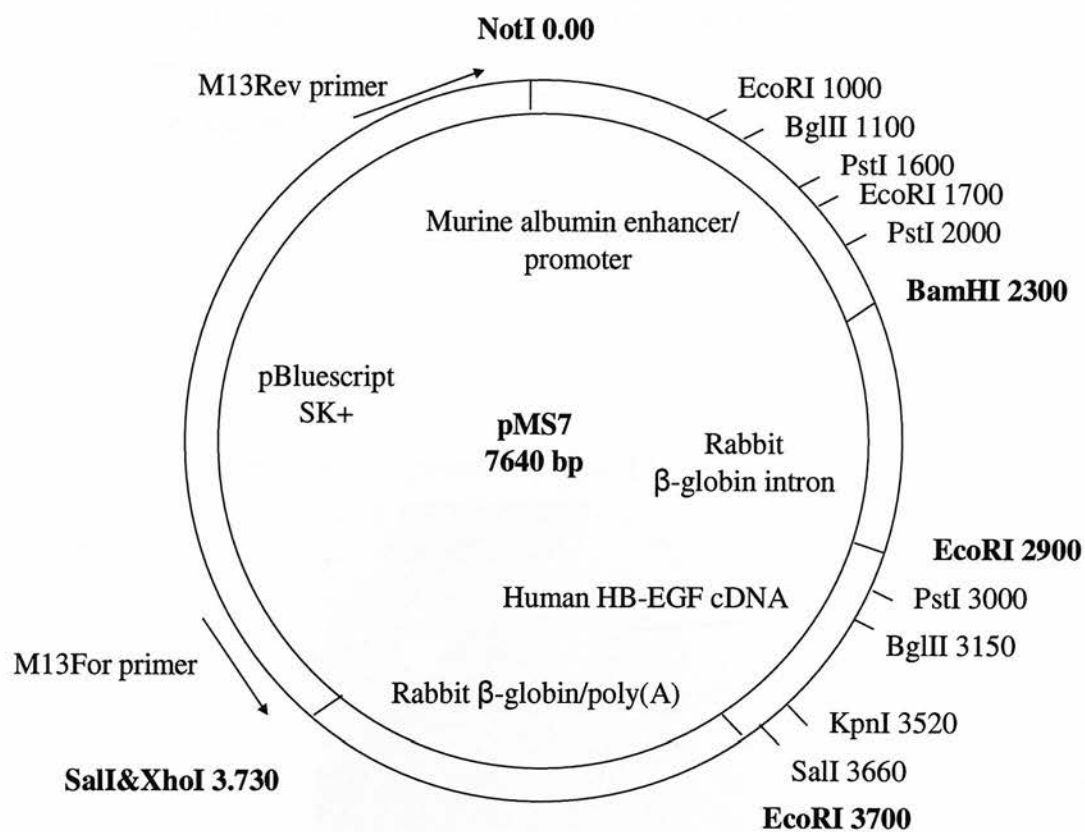


Figure 6.2: Restriction enzyme analysis and sequencing map of pMS7

Production of murine nephrin gene fragment (podocyte promoter) with polymerase chain reaction

The murine nephrin gene fragment (podocyte promoter) was produce to replace murine albumin (hepatocyte promoter) in the plasmid pMS7 and induce specific podocyte injury using DT. This was performed with Taq DNA polymerase and Vent DNA polymerase (see discussion for details). The results showed a strong DNA band of the expected size of 1315 bp (figure 6.3).

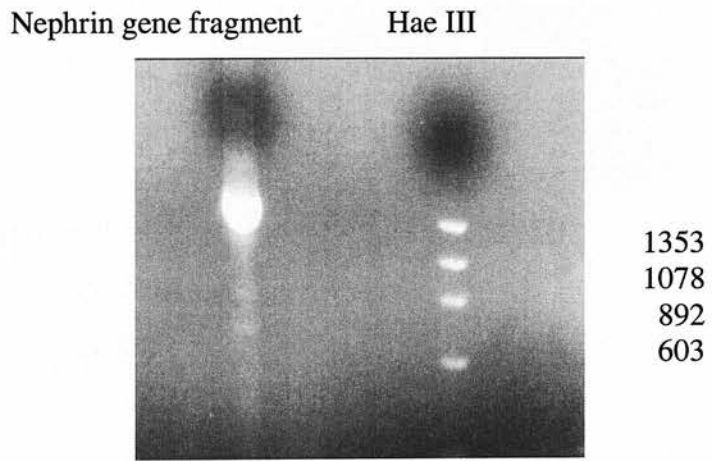


Figure 6.3: Nephrin gene fragment PCR

Subcloning of the nephrin gene fragment into pCR[®]4Blunt-Topo and production of pCR4BN

The nephrin gene fragment was subcloned into pCR4[®]Blunt-Topo to be able to sequence the fragment. E.coli was transformed with pCR4BN. Miniprep and midiprep were tested by restriction enzyme working on pCR4BN (EcoRI) and restriction enzymes working on nephrin gene fragment (NotI and BamHI). The results showed DNA band of the expected size of 1315 bp (figure 6.4). DNA was sequenced with M13For and M13Rev primers and the result showed correct nephrin gene sequencing.

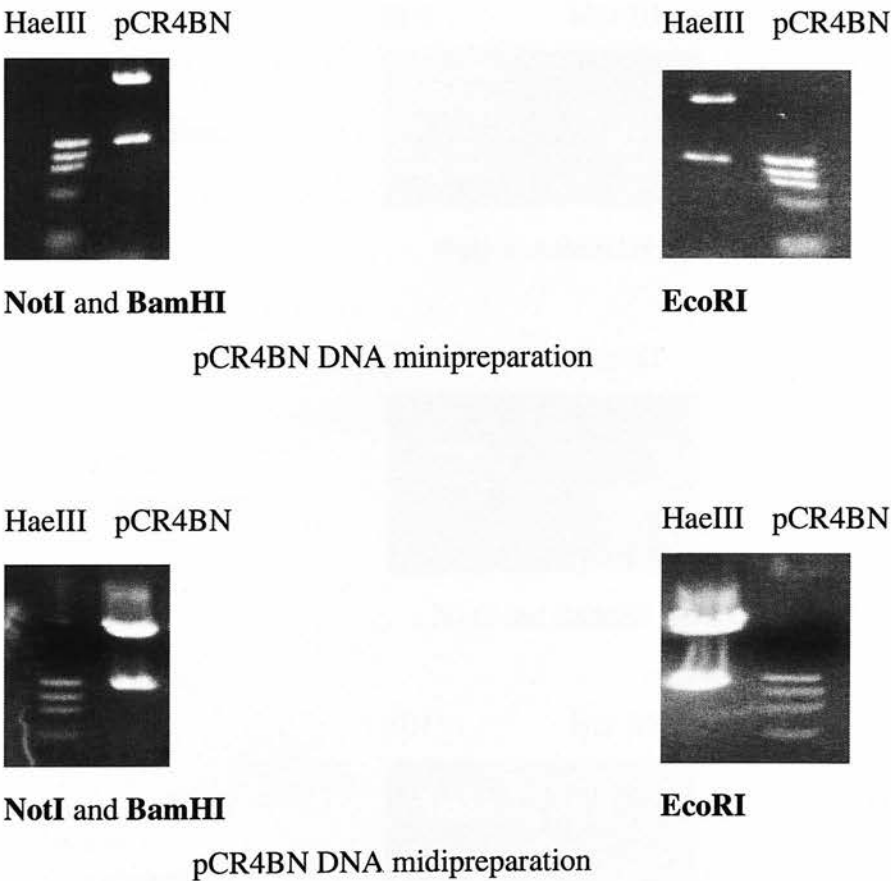


Figure 6.4: Enzyme restriction analysis of pCR4BN DNA miniprep and midiprep

Subcloning of the nephrin gene fragment from pCR4BN into pMS7 and production of pIN (podocyte construct)

The podocyte construct (pIN) was produced by subcloning the nephrin promoter fragment from pCR4BN into pMS7. E.coli was transformed with the plasmid pIN and miniprep, midiprep and maxiprep of its DNA was done. Enzyme restriction analysis was performed on all pIN DNA preparations (NotI and BamHI). The results showed DNA band of the expected size of 1315 bp (figure 6.5). Sequencing was done of all components of pIN using the primers illustrated in figure 2.1 and it was proved to consist of murine nephrin gene fragment (podocyte promoter), rabbit β globin intron, hHB-EGF cDNA (hDTR gene), rabbit β globin/Poly A and pBluescript SK+ without errors (figure 6.6).

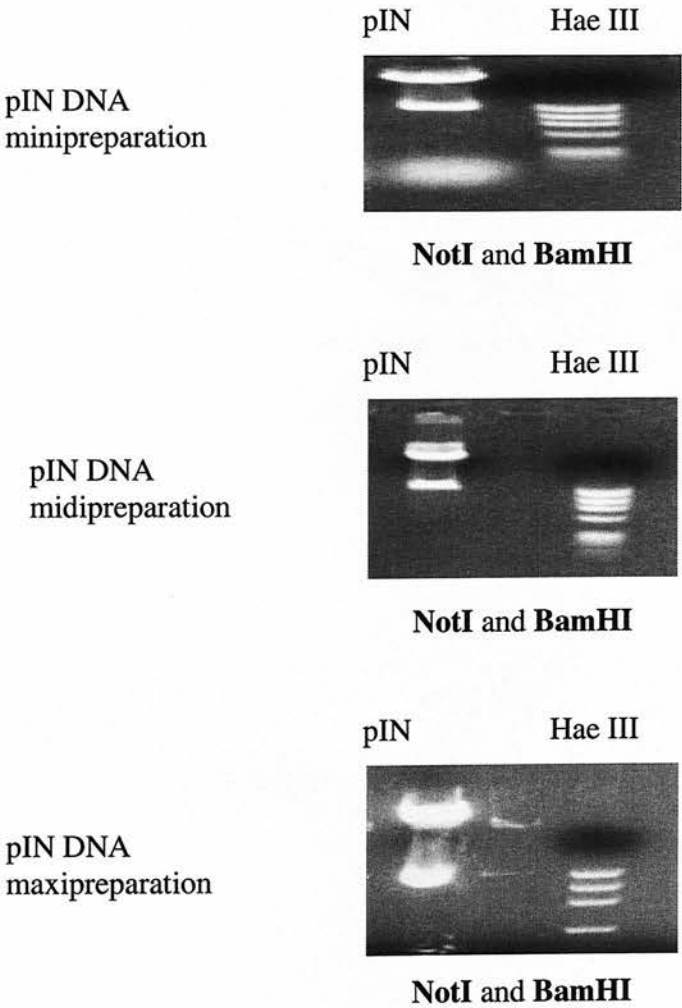


Figure 6.5: Enzyme restriction analysis of pIN DNA miniprep, midiprep and maxiprep

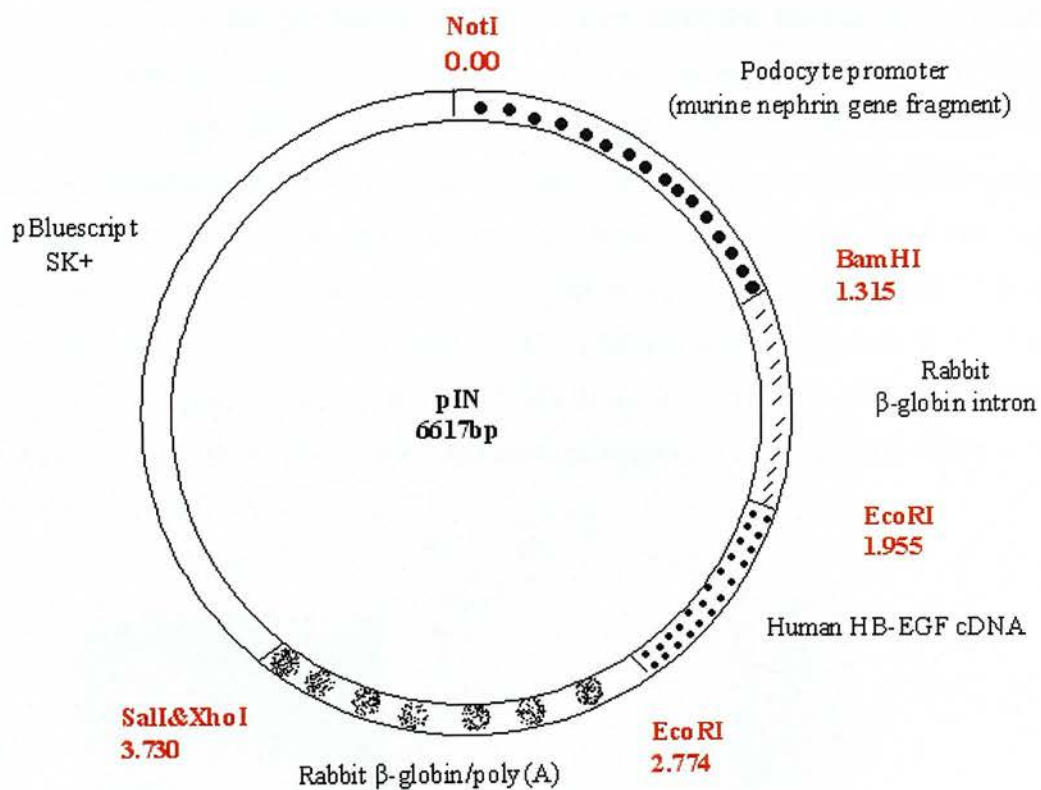


Figure 6.6: pIN map

Mice genotyping primers work on pIN DNA but not wild type mouse DNA

This experiment was done to design and optimize a genotyping PCR method for the genomic DNA of the potentially transgenic mice after the microinjection of the podocyte construct. This was to test murine DNA for the expression of pIN nephrin gene fragment and rabbit β globin intron using pINPCR-For1 and pINPCR-Rev1 primers (nephrin gene/intron genotyping) and for the expression of hDTR using pINPCR-For2 and pINPCR-Rev2 primers (hDTR gene genotyping). These two sets of primers were tested on a dilution series of pIN DNA in the order 10 ng/ul, 1 ng/ul, 0.1 ng/ul, 0.01 ng/ul, 0.001 ng/ul and 0.0001 ng/ul and wild type mouse DNA. The results showed positive results in both PCRs in all dilutions of pIN DNA at 50°C annealing temperature. The results also showed negative results in both PCRs with wild type mouse DNA (figure 6.7).

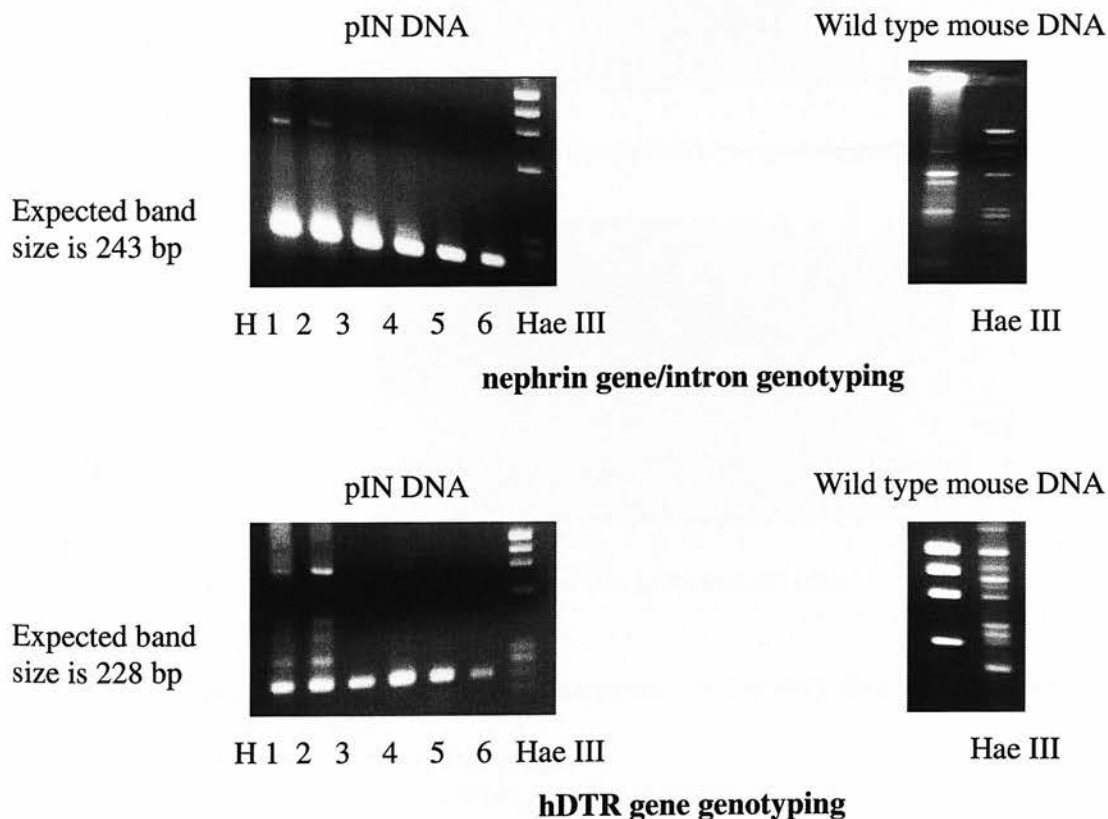


Figure 6.7: Optimization of genotyping PCRs

H = water control

3 = 0.1 ng/ul

6 = 0.0001 ng/ul

1 = 10 ng/ul

4 = 0.01 ng/ul

2 = 1 ng/ul

5 = 0.001 ng/ul

Genotyping PCRs for the potentially transgenic mice DNA

Two genotyping PCRs (nephtrin gene/intron and hDTR gene) were done on the purified potentially transgenic mice DNA. The results showed no band in the water control lane, positive band in the positive control (pIN DNA) lane, and no correct band size in the negative control DNA (wild type mouse DNA) or in any of the 69 DNA samples of the potentially transgenic mice DNA. Only 1-16 samples are illustrated below (figure 6.8).

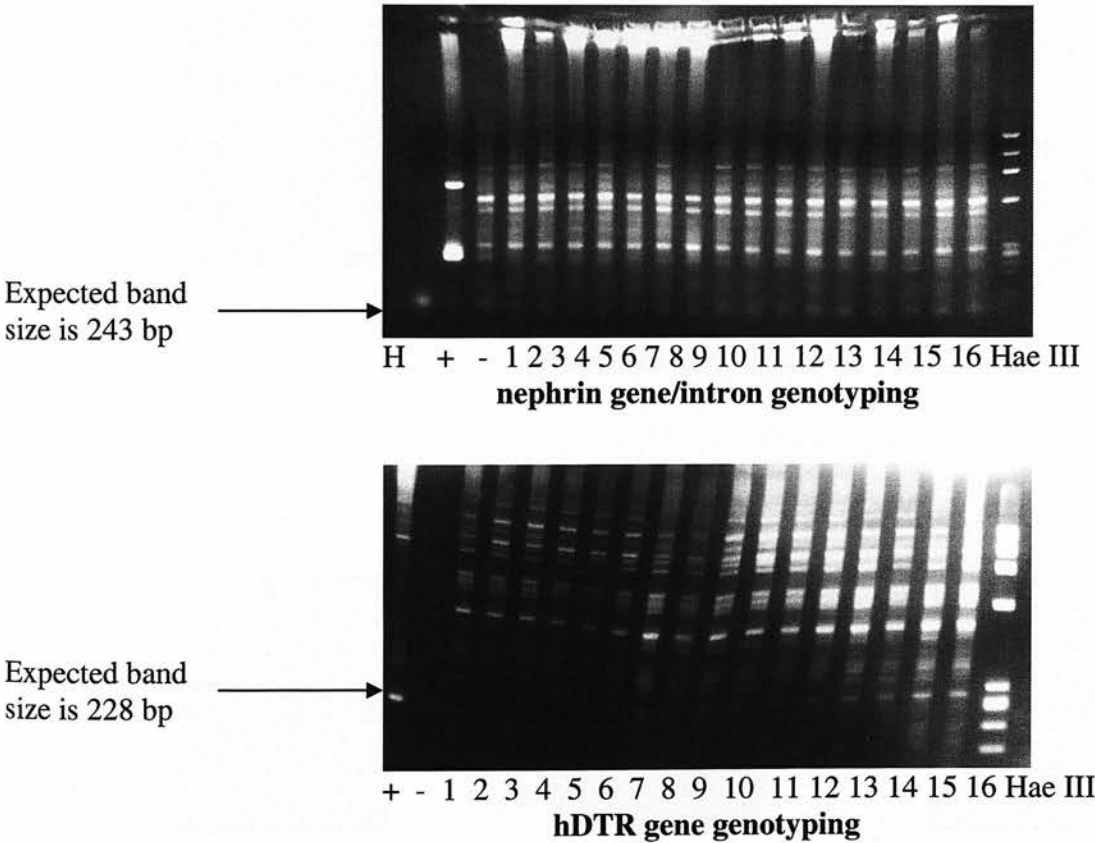


Figure 6.8: The potentially transgenic mice genotyping (16 samples)

H = Water control
+ = Positive control (pIN DNA)
- = Negative control (wild type mouse DNA)
1-16 = the potentially transgenic mice DNA

Genotyping PCRs for the potentially transgenic mice DNA with different annealing temperature.

The rationale for this experiment was to test different annealing temperature of these PCRs using two of the potentially transgenic mice DNA samples. The results showed hDTR gene genotyping primers do not work at 55°C and 60°C annealing temperature and no positive results in terms of genotyping (figure 6.9).

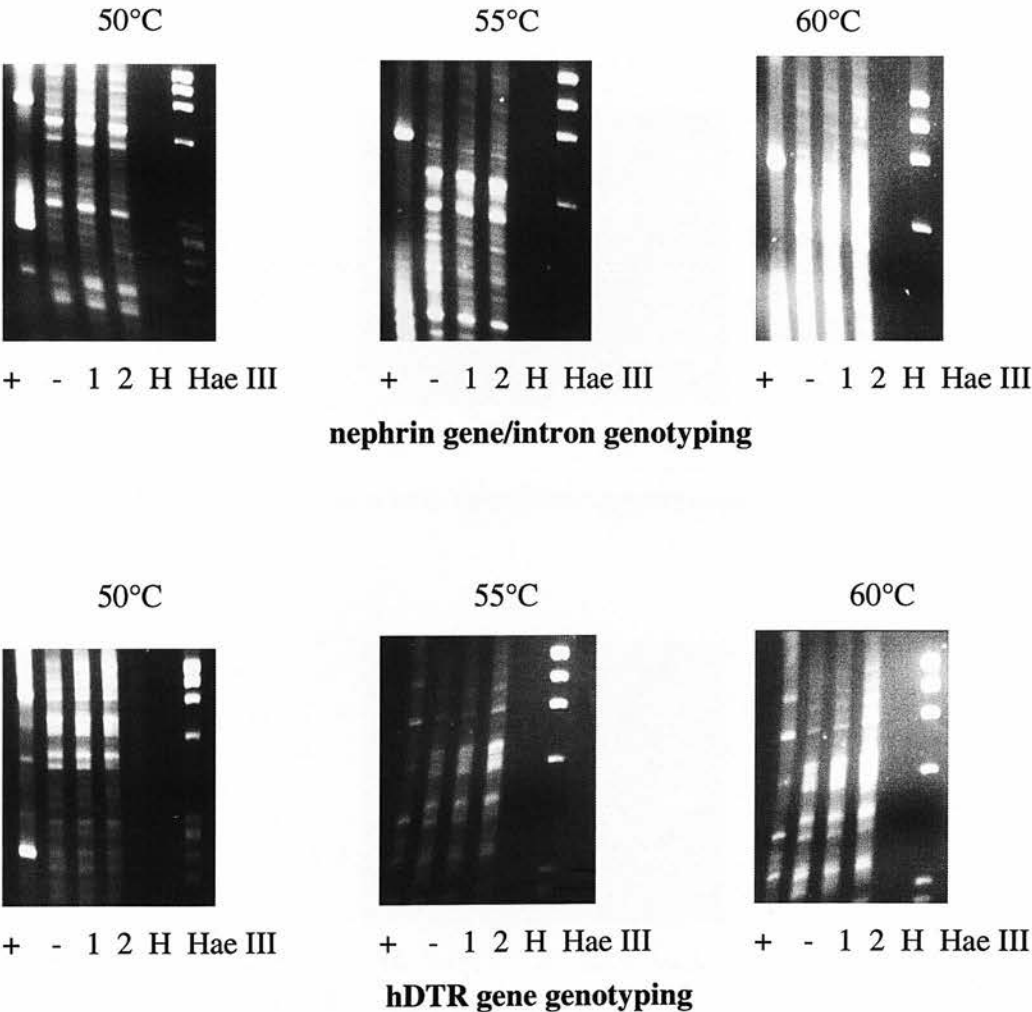


Figure 6.9: Genotyping PCRs with different annealing temperature

+ = Positive control (pIN DNA)
- = Negative control (wild type mouse DNA)
H = Water control
1-2 = the potentially transgenic mice DNA

Genotyping PCRs for the potentially transgenic mice DNA with low magnesium concentration

The rationale for this experiment was to test if low magnesium concentration will increase the specificity of the genotyping PCRs. 0.5 ul of 25 mM MgCl₂ was added instead of 1 ul to the PCRs reagents. The results showed positive control band and no expected bands in the negative control and two samples of the potentially transgenic mice DNA in both PCRs. Also no bands in water control lane (figure 6.10).

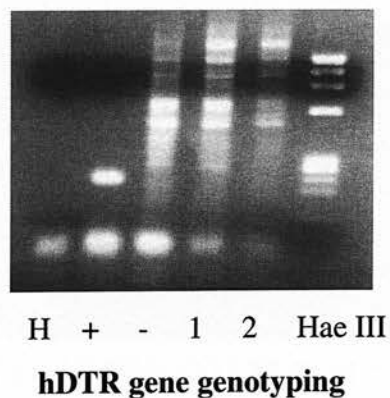
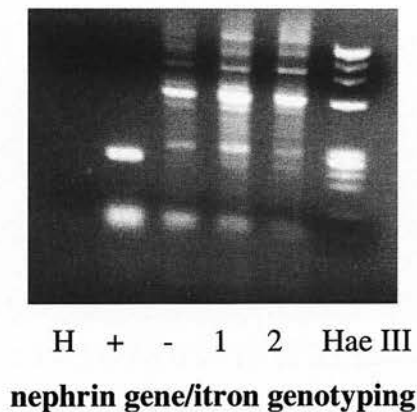


Figure 6.10: Genotyping PCRs with low magnesium concentration

H = Water control

+ = Positive control (pIN DNA)

- = Negative control (wild type mouse DNA)

1-2 = the potentially transgenic mice DNA

Genotyping PCRs for the potentially transgenic mice DNA with 40 cycles

The rationale for this experiment was to test if increasing PCRs cycles from 30 to 40 will get them work by increasing sensitivity. The results showed positive control band and no expected bands in the negative control and two samples of the potentially transgenic mice DNA of both PCRs. Also no bands in the water control lane (figure 6.11).

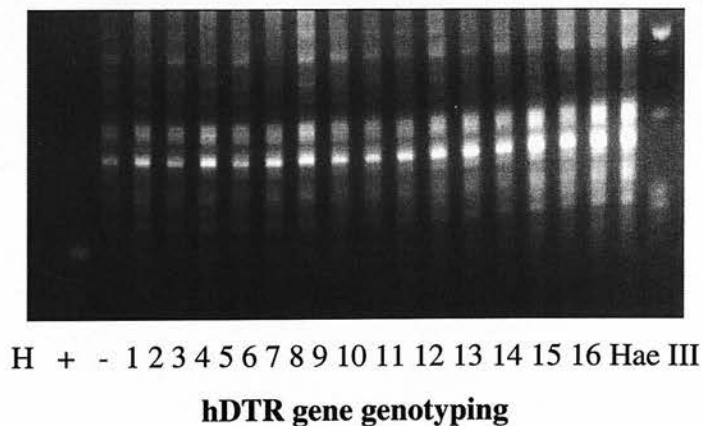
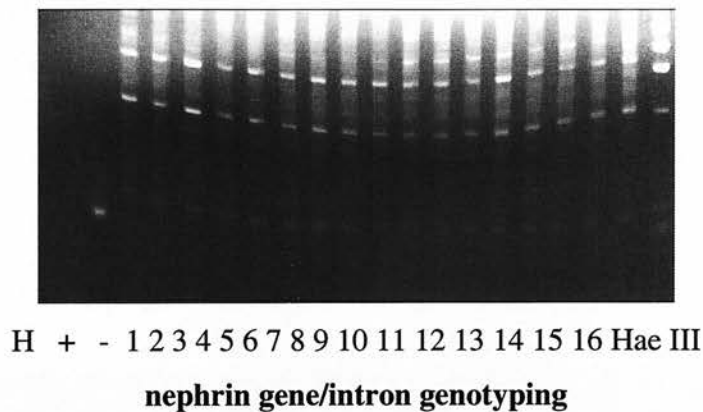


Figure 6.11: Genotyping PCRs with 40 cycles

H = Water control

+ = Positive control (pIN DNA)

- = Negative control (wild type mouse DNA)

1-16 = the potentially transgenic mice DNA

Control PCR for the potentially transgenic mice DNA genotyping PCR

The rationale for this experiment was to test whether the amount of the potentially transgenic mice DNA was adequate for the genotyping PCRs to work. This was done using collagen IV $\alpha 3$ primers (4A3WTR and 4A3KOWTL); the wild type (control) primers used for genotyping COL4A3 knockout mice and the potentially transgenic mice DNA. All 69 samples of the potentially transgenic mice DNA gave the expected band size (1000 bp) for PCR showing that the amount of DNA was adequate for PCR. A strong band is seen without any extra artefact bands showing that the multiple DNA bands in genotyping PCRs are primer specific. The results below show 17 of 69 samples (figure 6.12)

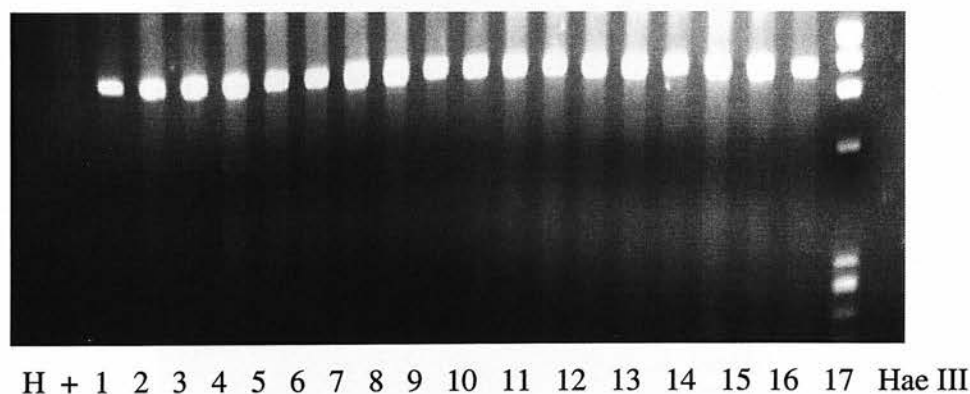


Figure 6.12: Control PCR for the potentially transgenic mice DNA genotyping PCR

H = Water control

+ = Positive control (wild type mouse DNA)

1-17 = the potentially transgenic mice DNA

Spiking of the potentially transgenic mice DNA with pIN DNA

This experiment was done to test whether the multiple DNA bands in the genotyping PCRs consume the genotyping primers and prevent them from working. A dilution series of 0.01 ng/ul, 0.001 ng/ul, 0.0001 ng/ul and 0.00001 ng/ul from pIN DNA was used to make 1:1 dilution with the potentially transgenic mice DNA (200 ng) and nuclease-free water. These two dilutions were used for the two genotyping PCRs. The results showed that spiking the potentially transgenic mice DNA with pIN DNA gave positive results for the construct and these multiple bands did not consume the primers (figure 6.13).

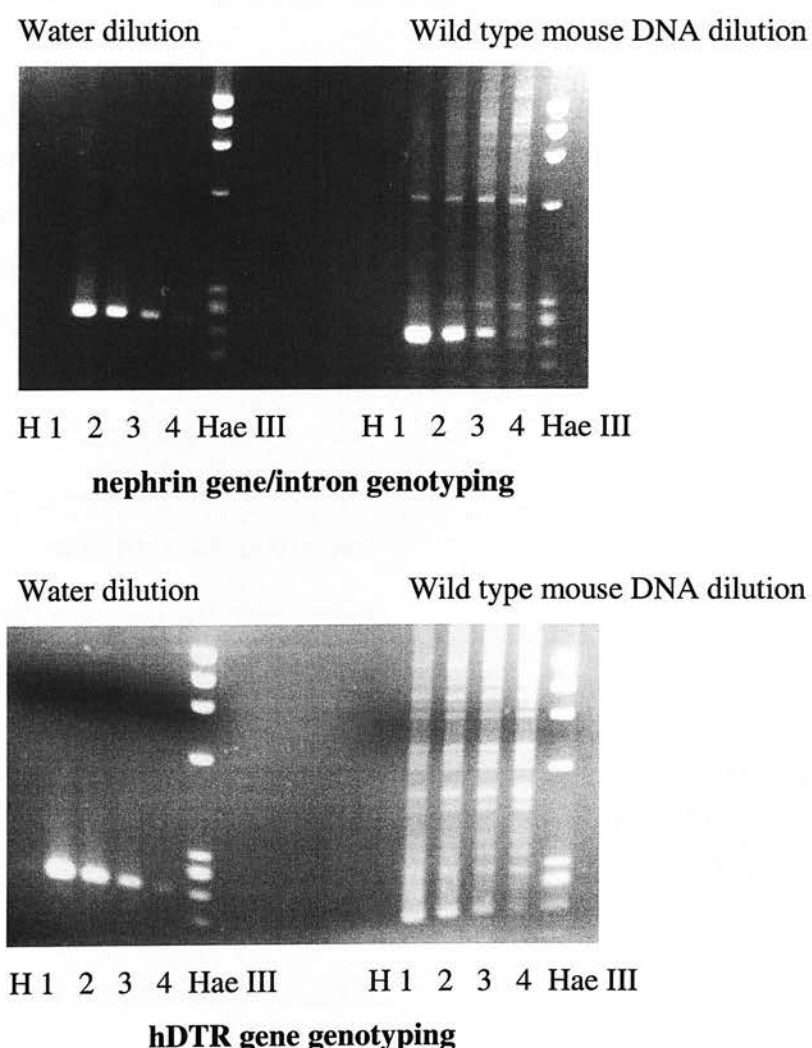


Figure 6.13: Spiking of the potentially transgenic mice DNA with pIN DNA

H = water control
3 = 0.0001 ng/ul

1 = 0.01 ng/ul
4 = 0.00001 ng/ul

2 = 0.001 ng/ul

Measurement of genomic copies of the potentially transgenic mice DNA and pIN copies used in PCR

1. measurement of pIN copies

From the results of genotyping primers PCRs on a dilution series of pIN DNA in the order 10 ng/ul, 1 ng/ul, 0.1 ng/ul, 0.01 ng/ul, 0.001 ng/ul and 0.0001 ng/ul, it has been found that PCRs gave positive result with 0.0001 ng/ul (figure 6.7). 2 ul from this dilution was used for the PCR, so the amount used was 0.0002 ng (2×10^{-13} g). The average concentration of the potentially transgenic mice DNA was 200 ng/ul, the amount used for PCR was 400 ng (4×10^{-8}).

$$\therefore \text{pIN} = 6617 \text{ bp}$$

$$\therefore \text{Molecular weight of bp} = 629 \text{ Dalton}$$

$$\therefore \text{Molecular weight of pIN} = 6617 \times 629 = 4 \times 10^5 \text{ Dalton}$$

$$\therefore \text{Avogadro number } (6 \times 10^{23}) = 400,000 \text{ g}$$

$$\therefore X (\text{pIN copies used in PCR}) = 2 \times 10^{-13} \text{ g}$$

$$\begin{aligned} \therefore \text{pIN copies} &= \frac{6 \times 10^{23} \times 2 \times 10^{-13}}{4 \times 10^5} \\ &= 3 \times 10^5 = 300,000 \text{ copies} \end{aligned}$$

2. measurement of mouse genomic copies

$$\therefore \text{Mouse genome} = 2.9 \times 10^9 \text{ bp}$$

$$\therefore \text{Molecular weight of bp} = 629 \text{ Dalton}$$

$$\therefore \text{Molecular weight of Mouse genome} = 2.9 \times 10^9 \times 629 = 1.8 \times 10^{12} \text{ Dalton}$$

$$\therefore \text{Avogadro number } (6 \times 10^{23}) = 1.8 \times 10^{12} \text{ g}$$

$$\therefore X (\text{mice genomic copies used in PCR}) = 4 \times 10^{-8} \text{ g}$$

$$\begin{aligned} \therefore \text{mice genomic copies} &= \frac{6 \times 10^{23} \times 4 \times 10^{-8}}{1.8 \times 10^{12}} \\ &= 13 \times 10^3 = 13,000 \text{ copies} \end{aligned}$$

Sensitivity of genotyping PCRs

The sensitivity of both genotyping PCRs was measured because from the last result the number of pIN copies was much greater than mice genomic copies. A dilution series of pIN DNA in the order 1×10^{-1} ng/ul, 1×10^{-2} ng/ul, 1×10^{-3} ng/ul, 1×10^{-4} ng/ul, 1×10^{-5} ng/ul, 1×10^{-6} ng/ul, 1×10^{-7} ng/ul, 1×10^{-8} ng/ul, 1×10^{-9} ng/ul was used to do both PCRs. The results showed that genotyping PCRs can work on 3000 copies of pIN DNA (lane 5 in figure 6.14) and because 13,000 copies of murine genomic DNA was used, genotyping PCRs are sensitive enough to work on the potentially transgenic mice DNA.

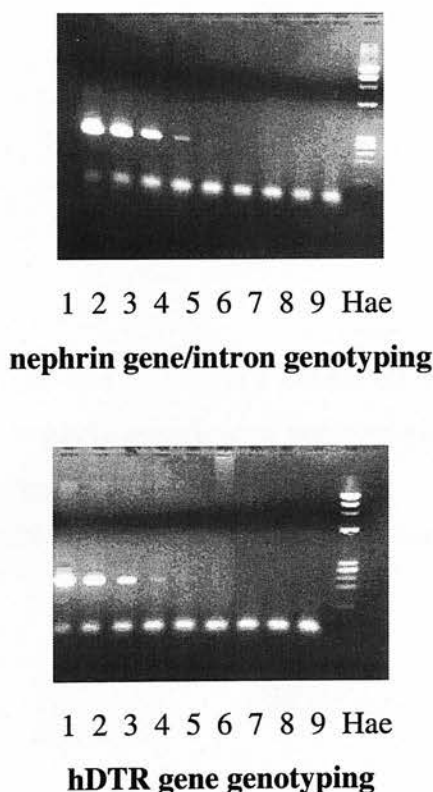


Figure 6.14: Sensitivity of genotyping PCRs

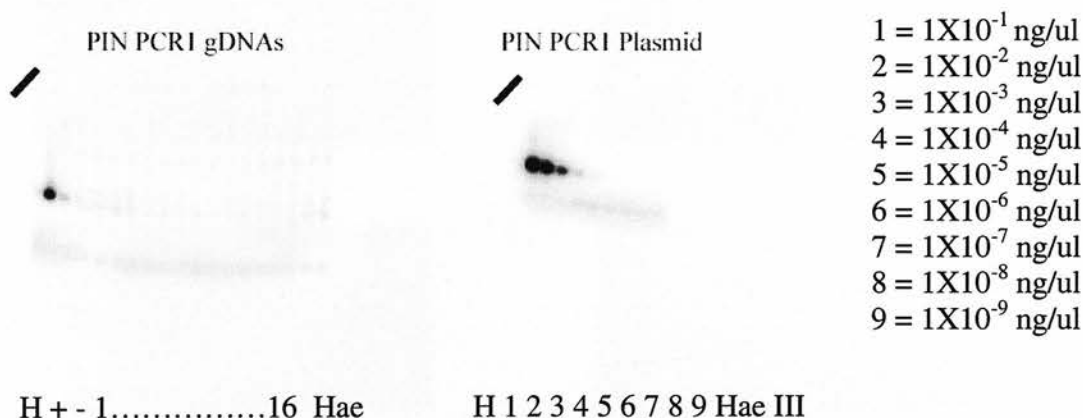
- 1 = 1×10^{-1} ng/ul
- 2 = 1×10^{-2} ng/ul
- 3 = 1×10^{-3} ng/ul
- 4 = 1×10^{-4} ng/ul
- 5 = 1×10^{-5} ng/ul
- 6 = 1×10^{-6} ng/ul
- 7 = 1×10^{-7} ng/ul
- 8 = 1×10^{-8} ng/ul
- 9 = 1×10^{-9} ng/ul

Southern blotting hybridization of the potentially transgenic mice DNA

This was done after all of the above genotyping results were negative. Both genotyping PCRs and their positive controls (PCRs of figure 6.14) were blotted and hybridized with p32 radiolabelled probes (products of figure 6.14 PCRs). The results showed negative results for 16 samples of the potentially transgenic mice DNA (all 69 were negative) and positive bands in the positive control (figure 6.15).

The potentially transgenic mice DNA

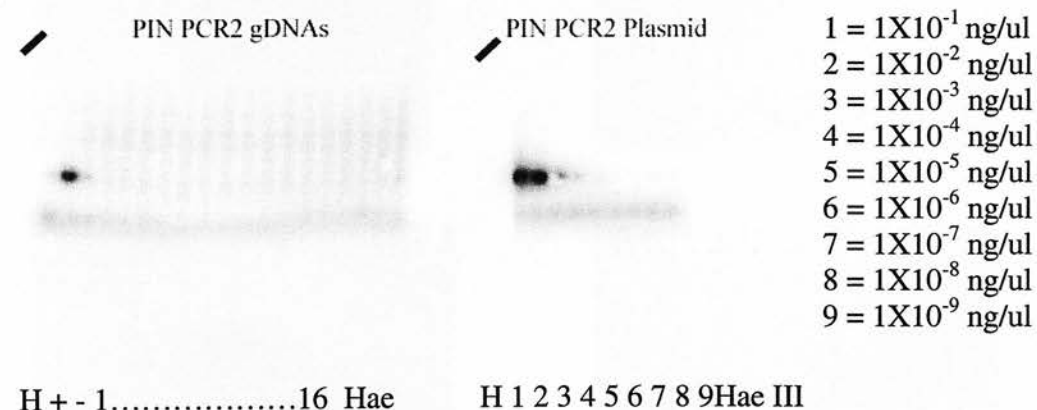
Control PCR



nephrin gene/intron genotyping

The potentially transgenic mice DNA

Control PCR



hDTR gene genotyping

Figure 6.15: Southern blotting hybridization of the potentially transgenic mice DNA

H = Water control + = Positive control (pIN DNA)

- = Negative control (wild type mouse DNA)

1-16 = the potentially transgenic mice DNA

**Second microinjection trial proved the effectiveness of the technique:
four transgenic founders were established**

Sixty eight founders were generated by the second set of microinjections. Two genotyping PCRs (nephrin gene/intron and hDTR gene) were done on 66 purified potentially transgenic mice DNA (2 pups were died). The results showed positive bands in the founders; tg21.1, tg47.1, tg57.1 and tg65.1 (figure 6.16). So, four hDTR transgenic founders were established.

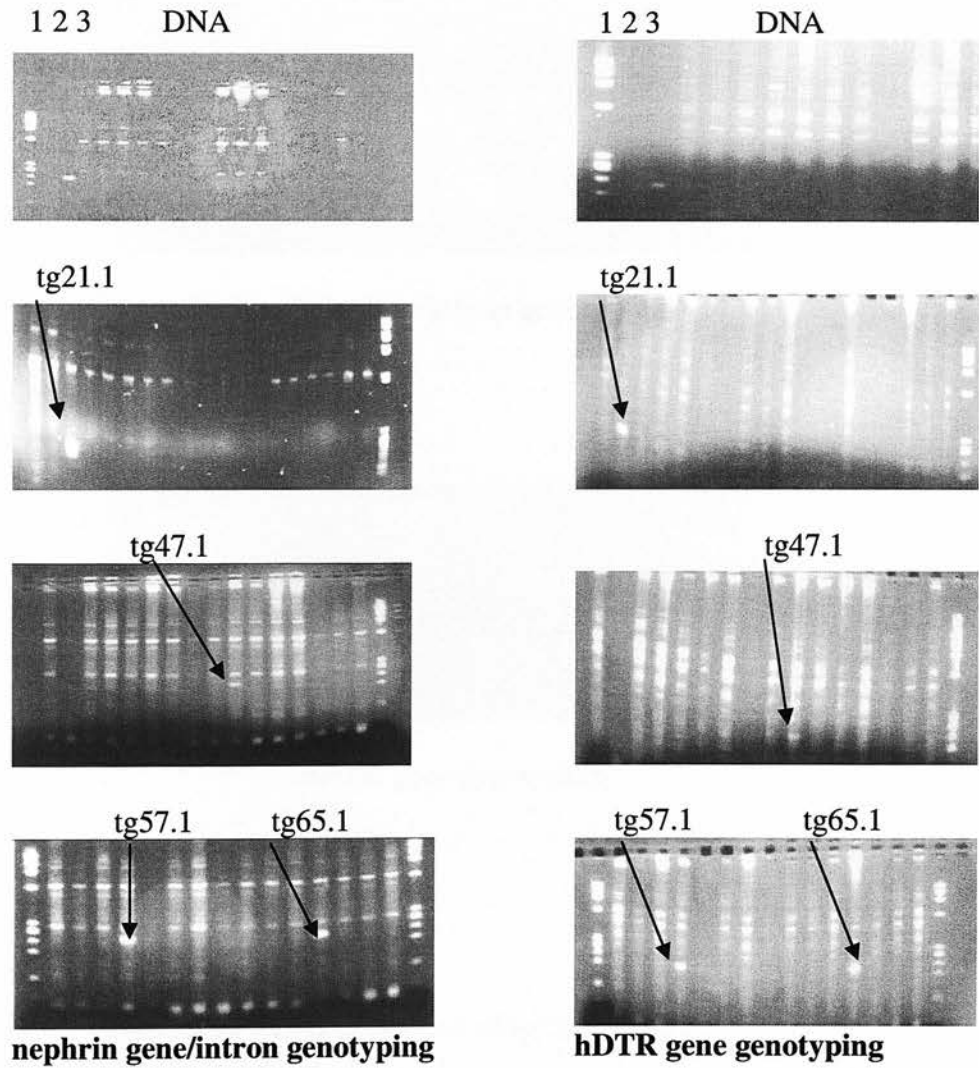


Figure 6.16: Genotyping PCRs of the transgenic founders

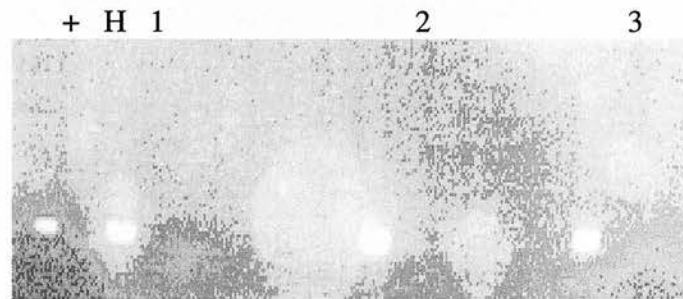
1 = Hae III

2 = Water control

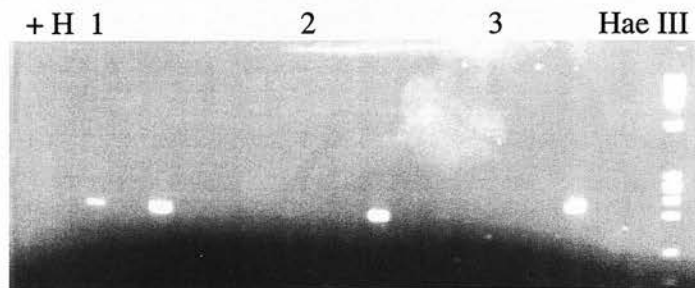
3 = Positive control (pIN DNA)

Genotyping PCRs of phase 1 of tg21.1 offspring

Seventeen pups were produced from tg21.1 line. Two genotyping PCRs (nephrin gene/intron and hDTR gene) were done on 17 purified potentially transgenic mice DNA. The results showed positive bands in the samples; tg21.1.2, tg21.1.9 and tg21.1.15 (figure 6.17).



nephrin gene/intron genotyping



hDTR gene genotyping

Figure 6.17: Genotyping PCRs of phase 1 of tg21.1 offspring

+ = Positive control (pIN DNA)

H = Water control

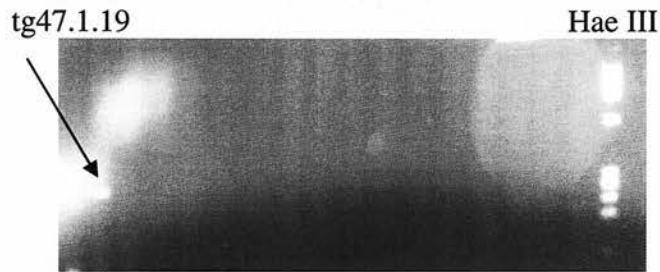
1 = tg21.1.2

2 = tg21.1.9

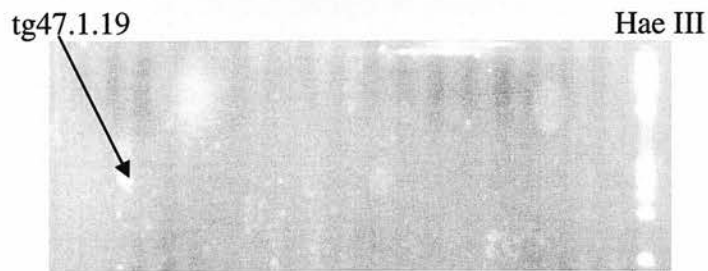
3 = tg21.1.15

Genotyping PCRs of phase 1 of tg47.1 offspring

Seventeen pups were produced from tg47.1 line. Two genotyping PCRs (nephrin gene/intron and hDTR gene) were done on 17 purified potentially transgenic mice DNA. The results showed positive bands only in the sample tg47.1.19 (figure 6.18).



nephrin gene/intron genotyping

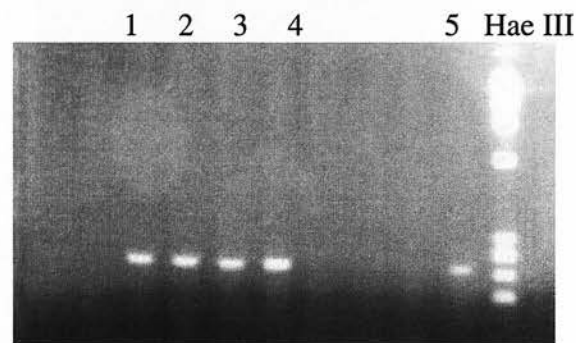


hDTR gene genotyping

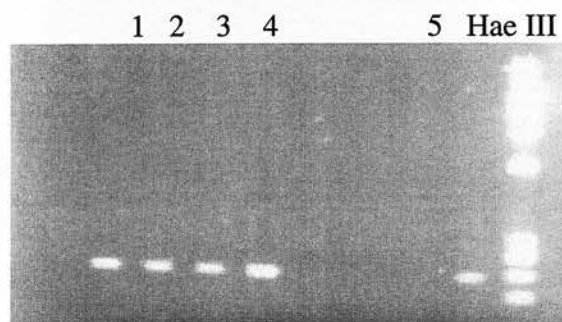
Figure 6.18: Genotyping PCRs of phase 1 of tg47.1 offspring

Genotyping PCRs of phase 1 of tg57.1 offspring

Nine pups were produced from tg57.1 line. Two genotyping PCRs (nephrin gene/intron and hDTR gene) were done on 9 purified potentially transgenic mice DNA. The results showed positive bands in the samples; tg57.1.36, tg57.1.37, tg57.1.38, tg57.1.39 and tg57.1.43 (figure 6.19).



nephrin gene/intron genotyping



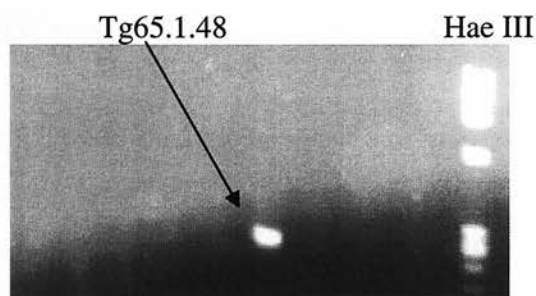
hDTR gene genotyping

Figure 6.19: Genotyping PCRs of phase 1 of tg57.1 offspring

1 = tg57.1.36
2 = tg57.1.37
3 = tg57.1.38
4 = tg57.1.39
5 = tg57.1.43

Genotyping PCRs of phase 1 of tg65.1 offspring

Eight pups were produced from tg65.1 line. Two genotyping PCRs (nephrin gene/intron and hDTR gene) were done on 8 purified potentially transgenic mice DNA. The results showed positive bands only in the sample tg65.1.48 (figure 6.20).



nephrin gene/intron genotyping



hDTR gene genotyping

Figure 6.20: Genotyping PCRs of phase 1 of tg65.1 offspring

Discussion

It was proposed to generate transgenic mice expressing hDTR on podocytes and study the podocyte injury, glomerular injury and renal outcome after the application of DT. This was described in hepatocytes by Saito and colleagues (2001) using a construct (pMS7) with hepatocyte-specific promoter (murine albumin promoter) and hHB-EGF cDNA (hDTR gene).

The construct pMS7 which was used by the above group to induce hepatocyte injury with DT was obtained and tested with different restriction enzymes according to its restriction map, but the size of some bands was not as expected from the map (figure 6.1 and figure 6.2). This was clarified later when the pIN construct was produced and fully sequenced. This sequencing showed that some restriction sites were not included in the plasmid pMS7 map.

The construct pMS7 was sequenced with M13For and M13Rev primers following the restriction enzyme analyses which proved that the correct construct has been obtained although the map was inaccurate.

It was decided to use the primers; Nphs1PE.fwd: 5-agg tct aga ggt gag agg ttt gta g-3` and Nphs1PE.rev: 5-act gtg gct tcc tta gct-3` (with added NotI and BamHI restriction sites which are essential for the nephrin gene fragment subcloning into pMS7 and production of podocyte construct) used by Moeller and colleagues (2002). This was because of its murine origin, size and because they had found that it could drive total expression of β galactosidase in podocytes.

Nephrin gene fragment PCR was performed with Taq DNA and Vent DNA polymerases. Taq DNA polymerase PCR was done because it is efficient and easy to optimize the conditions and it was done in two steps; the first step was with MONPHSF1 primer, MONPHSBamREV primer (contains BamHI restriction site) and wild type mouse DNA. The second step was done with MONPHSNotF2 primers (contains NotI restriction site), MONPHSBamREV primer and the product of the

first step PCR as a template. The second step was done to introduce the NotI restriction in the nephrin gene fragment. Once this PCR has been proved to work Vent DNA polymerase PCR was performed using MONPHSNotF2 primers, MONPHSBamREV primer and first Taq DNA polymerase PCR product as a template because of its lower insertion error and to produce blunt ended PCR product.

This blunt nephrin gene fragment was subcloned into pCR[®]4Blunt-Topo and pCR4BN was produced and its midiprep DNA was sent for sequencing which showed correct nephrin fragment sequencing. The other advantage of this subcloning of PCR product besides sequencing it increases the efficiency of this fragment subcloning at the time of podocyte construct production which is better from plasmid to plasmid than direct PCR product subcloning into plasmid.

The Podocyte construct; pIN was produced by subcloning of nephrin gene fragment from pCR4BN into pMS7 and at this stage the construct contains podocyte promoter and hDTR gene. The construct was ready for murine fertilized ova microinjection but detailed sequencing showed that there was a translation initiation codon (ATG) at the BamHI site in the nephrin gene fragment as well as hHB-EGF cDNA. Although there was a chance of hHB-EGF cDNA translation initiation codon to get work after murine fertilized ova microinjection it may not.

So, we did not want to explore that after the microinjection and another Vent polymerase PCR was performed to destroy this codon using MONPHSNotF2 primer, MonephBamRev2 and pIN DNA as a template. This was successful and the whole process was repeated till the podocyte construct was ready for the microinjection for the second time.

Sixty nine pups were generated with microinjection of the male pronucleus. At the age of 3 weeks they were genotyped by two different PCRs. It was expected to get 10% (7 pups) positive for genotyping PCRs according to Moeller paper (2002). They reported 12 out of 134 pups were positive for the genotyping PCR (9%). Brinster and

colleagues (1985) reported that 25% of the founders can be test positive for the transgene when a few hundred copies of the linear construct were microinjected in the male pronucleus of the murine fertilized ova. Unfortunately all of the 69 mice were negative for both genotyping PCRs.

Several steps were undertaken to investigate whether my detection techniques were adequate, but the results did not change with different annealing temperature, low magnesium concentration and 40 cycles.

The amount of DNA was proved to be enough when the control PCR was positive for all of the 69 samples and the primers have shown to be enough to get the PCRs to work and did not consumed with those multiple bands when the potentially transgenic mice DNA was spiked with pIN DNA. Also there was no difference in pIN PCRs when diluted with water or the potentially transgenic mice DNA (figure 6.13).

The genomic copies of the potentially transgenic mice DNA and pIN copies used in genotyping PCRs were 13,000 and 300,000 copies and this may argued as insufficient mice genomic copies for PCRs, but the genotyping PCRs sensitivity was measured and found 3000 copies of pIN DNA. So, the 13,000 genomic copies of mice DNA were enough for sensitive genotyping PCRs.

The last step was to do southern blotting hybridization and this also was negative for all of the 69 potentially transgenic mice. At this stage the results were proved to be negative and another trial of murine fertilized ova microinjection took place with the podocyte construct at Edinburgh Royal Infirmary.

Sixty eight pups were generated this time with male pronuclear microinjection of the murine fertilized ova. At the age of 3 weeks 66 of them (two died) were genotyped by both genotyping PCRs. Four hDTR transgenic founders were established by giving identical results for both genotyping PCRs.

The transgenic lines; tg21.1, tg47.1, tg57.1 and tg65.1 were set to breed with wild type mice to preserve the lines and enable testing with DT.

The analysis of phase one of the transgenic lines shows that all of the four founders passed the transgene to their offspring; hence 3 of 17 were positive in tg21.1 line, 1 of 17 in tg47.1 line, 5 of 9 in tg57.1 line and 1 of 8 in tg65.1 line.

The tg21.1 and tg57.1 founders were stopped from breeding and preserved but tg47.1 and tg65.1 lines were continued to breed because the number of their positive offspring is not enough to be tested histologically for podocytes expression of hDTR. In tg21.1 line two positive offspring were set to breed with wild type mice. The third positive mice and one wild (control) were planned to be tested for the expression of hDTR by anti-hEGF antibody staining of their kidneys. In the tg57.1 line two mice were set to breed with wild type mice and three were planned for a histopathology staining as well as one wild type mouse (control).

If the anti-hEGF antibody staining was restricted to podocytes the next step is to test other tissues for the receptor expression. So, the ideal line will be the one which expresses the receptor specifically on podocytes. Once this line has been fixed then DT can be applied.

I would like to mention that since this project was designed in 2001, two models of specific podocyte injury were published. Matsusaka and colleagues (2005) generated transgenic mice expressing human CD25 on podocytes and induced their injury by anti-Tac (Fv)-PE38 (LMB2). Murine nephrin promoter was used to direct the expression of human CD25. Wharram and associates (2005) reported the generation of transgenic rats expressing hDTR on podocytes. They used human podocin gene fragment in their construct to direct the expression of the receptor on podocytes.

Chapter 7

General discussion

General discussion

The renal glomerulus is a highly specialised structure which is responsible for blood filtration, and while extra fluid is allowed to pass in the glomerular filtrate; larger proteins are retained. Glomerular filtration occurs through the filtration slits which are formed between the interdigitation of podocytes foot processes around the GBM.

Podocytes form by an extension of a pre-existing epithelial sheet during embryogenesis by a process known as branching morphogenesis. In man metanephric development begins during the fifth week of gestation. It is characterised by aggregation of nephrogenic mesenchyme opposite to branches of the ureteral bud (vesicle stage), formation of the primitive S body consisting of presumptive glomerular and tubular epithelium, followed sequentially by capillary ingrowth, GBM formation, and differentiation of glomerular visceral (podocytes), parietal and tubular epithelium (Platt et al., 1983).

The podocyte can be divided into three structural parts which are; cell body, major processes and foot processes. Cell bodies and major processes are not attached to the GBM and float freely in the Bowman's space, leaving a sub-cell body space between the cell body and the foot processes. Major processes arise directly or after additional branching from the cell body and split into foot processes (Mundel and Kriz, 1995; Kriz et al., 1998).

Podocytes have many functions including GBM-turnover, maintenance of the filtration barrier, capillary tuft support, and regulation of glomerular filtration.

It has been concluded regarding podocytes replication that, the differentiated podocytes could undergo mitosis but not complete cell division as manifested by binuclear or multinuclear cells (Pabst and Sterzel, 1983; Rasch and Norgaard, 1983; Schwartz and Lewis, 1985). In contrast to that, de-differentiated podocytes could proliferate and this may lead to the development of pseudocrescent formation and glomerular compression in HIV nephropathy and idiopathic collapsing nephropathy

(Barisoni et al., 1999; Barisoni et al., 2000). De-differentiated podocytes can also be grown in culture from rats urine with experimental membranous nephropathy (Petermann et al 2003) and experimental diabetic nephropathy (Petermann et al 2004).

Podocyte injury is manifested by proteinuria and leads to the development of glomerulosclerosis and loss of glomerular function. Podocyte injury is associated with morphological changes including foot process effacement, cell body attenuation, and detachment from glomerular basement membrane (Pavenstadt et al., 2003).

Several forms of inherited proteinuria have been reported due to podocytes proteins genes mutations. They include Finnish type nephrotic syndrome (Kestila et al., 1998), congenital nephrotic syndrome (Shih et al., 1999), autosomal recessive FSGS (Boute et al., 2000), autosomal dominant FSGS (Kaplan et al., 2000) and primary steroid-resistant FSGS (Denamur et al., 2000).

Some investigators have reported that podocytes can be detected in the urine of patients with renal disease with immunofluorescence using anti-podocalyxin antibody. They presented this immunofluorescence technique as a potential non-invasive diagnostic tool for renal diseases (Hara et al., 1995; Hara et al., 1998).

The first aim of this project was to investigate the possibility of developing a non-invasive diagnostic and predictive technique by detecting urinary podocyte in a non-selective group of outpatients with proteinuria (urine protein \geq +++) which may replace or decrease the need for renal biopsy. The method of RT-PCR was proposed to be used to detect the mRNA of nephrin and podocalyxin (podocyte-specific mRNAs). Li and colleagues (2001) showed that this method can be used in the diagnosis of acute renal allograft rejection by detecting perforin and granzyme B mRNA in the urine of these patients.

This method was fully optimized in a clinically applicable way and proved to be quite sensitive, but all of patients tested with this method were negative for urinary podocyte specific mRNAs, although β -actin cDNA PCR (control) was positive in many samples.

In retrospect, it would have been useful to collect patient data in order to ensure that high risk patients such as patients with FSGS were included in the study as the literature suggests that such patients have the highest risk of exhibiting podocyturia.

It was argued that the persistent negativity of this study might be due to podocyte mRNAs degradation in the urinary bladder or in the outpatient department or because of podocytes were not present in the urine samples. This has lead to the conclusion that, this method did not appear to be useful as a diagnostic investigation for proteinuric renal patients.

It is very important to mention that the storage of non-isotonic urine in the outpatient department at room temperature for varying periods of time could have adversely affected cell survival and the findings of subsequent analyses.

Despite the negative results of patients urine samples many results were recorded during the optimization. It has been recorded that; TRIzol is better than Agilent total RNA isolation mini kit for total RNA extraction, glycogen and tRNA are similar for total RNA precipitation, DNaseI works better in AMV-RT buffer than MMLV-RT buffer, β -actin and podocalyxin cDNA primers work on human genomic DNA but nephrin do not, DNaseI kills all DNA in the RNA preparation, and heat completely destroys DNaseI. The PCR is sensitive enough for β -actin and podocalyxin.

In a parallel study urinary podocytes were investigated in another group of 100 patients with similar criteria by an immunofluorescence technique using podocyte-specific antibody. But when I looked at the literature I discovered that most of the evidence came from Hara group using the same anti-podocalyxin antibody. So, several podocyte-specific antibodies were mooted and finally anti-synaptopodin and

anti-CD2AP antibodies were tested on human kidney sections. Anti-synaptopodin showed podocyte-specific staining and it was decided it should be used for urinary sediment staining. The other objective of this study was to test the validity of immunofluorescence as a non-invasive diagnostic and predictive technique in clinical practice. Although this has been already reported by Hara group, it was aimed to test this method with a commercially available antibody.

Only 1% of proteinuric renal patients urine samples stained positive for podocytes with anti-synaptopodin antibody. Although at this stage the immunofluorescence results suggested that the negative results of RT-PCR study were negative because there were no podocytes, the immunofluorescence technique efficiency could be criticised.

Control experiments were performed on human cultured podocytes to test the RT-PCR method and immunofluorescence technique used in the above two studies (using the same methods in chapter 3 and chapter 4). This was a collaboration between our group and the renal unit at Southmead Hospital in Bristol, where in vitro culture of differentiated human podocytes was established.

An irrelevant isotype control primary antibody was not employed to determine the specificity of staining in the immunofluorescence studies and this is an important caveat in the interpretation of the findings presented

The immunofluorescence control experiment proved that this technique does work, but does not detect more than 20% of the actual number of podocytes in the urine and control cells (HeLa cells).

It has been noticed that the pattern of immunofluorescence staining and morphology change when cells go through cytopsin machine. By looking at AB-NT podocytes (figure 5.1) and HeLa cells (figure 4.5) on coverslips a well defined cell shape and immunofluorescence staining can be seen which changes after the cytopsin (figure

5.2 and figure 5.3). This was similar to the immunofluorescence pattern of the only podocyte detected by anti-synaptopodin antibody from patient urine (figure 4.8)

These results contrast with those reported by Hara group. This could be partly because they examined selected high risk patients, but it may also be relevant that podocalyxin can be found on platelets among other cells. I looked at a clinically relevant population using clinically applicable tests. I did not find evidence that urinary podocyte excretion commonly occurs at detectable levels in these patients.

The immunofluorescence method is similar to the method used in the original paper by Hara and colleagues (1995), which described urinary podocytes in renal patients, and in the following papers by the same group; they could be criticised about the actual number of podocytes they described in their publication and the correlations they made between urinary podocyte numbers and renal disease severity as well as correlation with different drugs.

No final conclusion has been obtained for the control experiment of RT-PCR method at the time of writing this thesis due to the presumed contamination.

The second aim of this project was to induce graded podocyte injury with DT in a transgenic mice model expressing hDTR specifically on podocytes and study the effects on podocyte structure, glomerular structure and renal outcome.

Specific cell ablation with DT in transgenic mice models expressing hDTR have been successfully described in hepatocytes (Saito et al., 2001) and macrophages (Cailhier et al., 2005). hDTR is 1000 fold sensitive than mouse DTR to the effects of DT.

The generation of transgenic mice expressing hDTR specifically on podocytes was achieved by microinjection of murine fertilized ova with the plasmid pIN which contains podocyte specific promoter and hDTR gene.

The plasmid pIN; the podocyte-specific construct was produced by the substitution of murine albumin promoter in the plasmid pMS7 (Saito et al., 2001) by murine nephrin gene fragment (Moeller et al., 2002).

Some unavoidable delay in this arm of the project occurred due to production of a podocyte construct with two translation initiation codons and when the first trial of microinjection did not generate any transgenic founders.

When genotyping PCRs of the potential transgenic mice produced by the first microinjection set were negative, several steps were undertaken to investigate whether my detection techniques were adequate, but the results did not change with different annealing temperature, low magnesium concentration and 40 cycles. The amount of DNA was proved to be enough, and the primers have shown to be enough to get the PCRs to work. Also there was no difference in pIN PCRs when diluted with water or the potentially transgenic mice DNA. The genotyping PCRs were found sensitive. The southern blotting hybridization was negative.

The second trial of microinjection has established four hDTR transgenic founders (tg21.1, tg47.1, tg57.1, tg65.1) which have passed the transgene to their phase 1 offspring. Two lines (tg21.1 and tg57.1) will be tested histologically for the expression of hDTR with anti-hEGF antibody shortly and the other two lines (tg21.1 and tg47.1) will be tested later. All of the four transgenic lines are at active breeding programme.

Conclusions

1. Looking for urinary podocytes is not a clinically useful technique in patients with proteinuria.
2. The podocyte construct (pIN) has proved its validity by generating four hDTR transgenic founders by male pronuclear microinjection and furthermore, all of them have passed the transgene to their offspring.

Further work

1. Investigation of the transgenic mice for the specific expression of hDTR on their podocytes. This is can be achieved by dual staining of transgenic mice kidneys with anti-hEGF and anti-synaptopodin antibodies. If this was successful staining of the other tissues of transgenic mice with anti-hEGF antibody should follow.
2. If an ideal transgenic line (which expressing hDTR specifically on podocytes) was established, a graded podocyte injury can be induced with DT and the consequences in terms of proteinuria, podocyte structure, glomerular structure and renal outcome can be studied.

References

- **Abrahamson DR, Perry EW.** Evidence for splicing new basement membrane into old during glomerular development in newborn rat kidneys. *J Cell Biol* 1986; 103:2489-2498.
- **Abrahamson DR.** Glomerulogenesis in the developing kidney. *Semin Nephrol* 1991; 11:375-389.
- **Abrahamson DR.** Origin of the glomerular basement membrane visualized after in vivo labelling of laminin in newborn rat kidneys. *J Cell Biol* 1985; 100:1988-2000.
- **Abrahamson DR.** Recent studies on the structure and pathology of basement membranes. *J Pathol* 1986; 149:257-278.
- **Abrahamson DR.** Structure and development of glomerular capillary wall and basement membrane. *Am J Physiol* 1987; 22:F783-F794.
- **Adler S.** Characterization of glomerular epithelial cell matrix receptors. *Am J Pathol* 1992; 141:571-578.
- **Anderson WP, Alcorn D, Gilchrist AI, Whiting JM, Ryan GB.** Glomerular actions of ANG II during reduction of renal artery pressure: a morphometric analysis. *Am J Physiol* 1989; 256:F1021-F1026.
- **Andrews PM.** Morphological alterations of the glomerular (visceral) epithelium in response to pathological and experimental situations. *J Electron Microsc Tech* 1988; 9:115-144.
- **Andrews PM.** Scanning electron microscopy of the kidney glomerular epithelium after treatment with polycations in situ and in vitro. *Am J Anat* 1978; 153:291-303.
- **Ardailou N, Blaise V, Costenbader K, Vassitch Y, Ardailou R.** Characterization of a B2-bradykinin receptor in human glomerular podocytes. *Am J Physiol* 1996; 271(3):F754-F761.
- **Bagchus WM, Hoedemaeker PJ, Rozing J, Bakker WW.** Acute glomerulonephritis after intravenous injection of monoclonal antithymocyte antibodies in the rat. *Immunol Let* 1986; 12:109-113.

- **Barisoni L, Kriz W, Mundel P, D'Agati.** The dysregulated podocyte phenotype: a novel concept in the pathogenesis of collapsing idiopathic focal segmental glomerulosclerosis and HIV associated nephropathy. *J Am Soc Nephrol* 1999; 10:51-61.
- **Barisoni L, Mokrzycki M, Sablay L, Nagata M, Yamase H, Mundel P.** Podocyte cell cycle regulation and proliferation in collapsing glomerulopathies. *Kidney Int* 2000; 58:137-143.
- **Beer J, Masters CL, Beyreuther K.** Cell from peripheral tissues that exhibit high APP expression are characterized by their high membrane fusion activity. *Neurodegeneration* 1995; 4:51-59.
- **Bender B, Jaffe R, Carlin B, Chung AE.** Immunolocalization of entactin, a sulphated basement membrane component, in rodent tissues, and comparison with GP-2 laminin. *Am J Pathol* 1981; 103:419-426.
- **Bernstein JF, Cheng F, Roszka BS.** Glomerular differentiation in metanephric culture. *Lab Invest* 1981; 45:183-190.
- **Binder CJ, Weiher H, Exner M, Kerjaschki D.** Glomerular overproduction of oxygen radicals in Mpv17 gene-inactivated mice causes podocyte foot process flattening and proteinuria: a model of steroid-resistant nephrosis sensitive to radical scavenger therapy. *AM J Pathol* 1999; 154: 1067-1075.
- **Bonadio JF, Sage H, Cheng F, Bernstein J, Striker GE.** Localization of collagen type IV and V, laminin, and heparan sulphate proteoglycan to the basal lamina of kidney epithelial cells in transfilter metanephric culture. *Am J Pathol* 1984; 116:289-296.
- **Boute N, Gribouval O, Roselli S, Benessy F, Lee H, Fuchshuber A, Dahan K, Guber MC, Niaudet P, Antignac C.** NPHS2 encoding the glomerular protein podocin, is mutated in autosomal recessive steroid-resistant nephritic syndrome. *Nat Genet* 2000; 349-354.
- **Breiteneder S, Matsui K, Kerjaschki D.** Loss of a 43 kD a transmembrane glycoprotein in rat glomerular epithelial cells (GEC) in puromycin aminonucleoside nephrosis. *Kidney Int* 1995; 47:689.

- **Breiteneder-Geleff, Matsui K, Meraner P, Poczewski H, Kalt R, Schaffner G, Kerjaschki D.** Podoplanin, novel 43-kd membrane protein of glomerular epithelial cells, is down-regulated in puromycin nephrosis. *Am J Pathol* 1997; 151:1141-1152.
- **Brinster RL, Chen HY, Trumbauer ME, Yagle MK, Palmiter RD.** Factors affecting the efficiency of introducing foreign DNA into mice by microinjecting eggs. *Proc Natl Acad Sci USA* 1985; 52(13):4438-4442.
- **Cailhier JF, Partolina M, Vuthoori S, Wu S, Ko K, Watson S, Savill J, Hughes J, Lang RA.** Conditional macrophage ablation demonstrates that resident macrophages initiate acute peritoneal inflammation. *J Immunol* 2005; 174:2336-2342.
- **Cho CR, Lumsden CJ, Whiteside CI.** Epithelial cell detachment in the nephrotic glomerulus: a receptor co-operativity model. *J Theor Biol* 1993; 160:407-426.
- **Chomczynski P, Sacchi N.** Single-step method of RNA isolation by acid guanidinium thiocyanate-phenol-chloroform extraction. *Anal Biochem* 1987; 162(1):156-159.
- **Courtoy PJ, Timpl R, Farquhar MG.** Comparative distribution of laminin, type IV collagen, and fibronectin in the rat glomerulus. *J Histochem Cytochem* 1982; 30:874-886.
- **Cybulsky AV, Carbonetto S, Huang Q, McTavish AJ, Cyr MD.** Adhesion of rat glomerular epithelial cells to extracellular matrices: Role of $\beta 1$ integrins. *Kidney Int* 1992; 1099-1106.
- **Cybulsky AV, Quigg RJ, Salant DJ.** The membrane attack complex in complement-mediated glomerular epithelial injury: formation and stability of C5b-9 and C5b-7 in rat membranous nephropathy. *J Immunol* 1986; 137:1511-15-16.
- **Daniels BS, Hauser EB, Deen WM, Hostetter TH.** Glomerular basement membrane: in vitro studies of water and protein permeability. *Am J Physiol* 1992; 262:F919-926.

- **Daniels BS.** Increased albumin permeability in vitro following alterations of glomerular charge is mediated by the cells of the filtration barrier. *J Lab Clin Med* 1994; 124(2):224-230.
- **Davidson G, Dono R, Zeller R.** FGF signalling is required for differentiation-induced cytoskeletal reorganization and formation of actin-based processes by podocytes. *J Cell Sci* 2001; 114:3359-3366.
- **Davies DJ, Brewer DB, Hardwicke J.** Urinary proteins and glomerular morphometry in protein overload proteinuria. *Lab Invest* 1978; 38:232-243.
- **Denamur E, Bocquet N, Baudouin C, Da Silva F, Veitia R, Peuchmaur M, Elion J, Gubler MC, Fellous M, Niaudet P, Loirat C.** WT1 splice-site mutations are rarely associated with primary steroid-resistant focal and segmental glomerulosclerosis. *Kidney Int* 2000; 57:1868-1872.
- **Denton KM, Fennessy PA, Alcorn D, Anderson WP.** Morphometric analysis of the actions of angiotensin II on renal arterioles and glomeruli. *Am J Physiol* 1992; 262:F367-F372.
- **Diamond JR, Karnovsky MJ.** Focal and segmental glomerulosclerosis following a single intravenous dose of puromycin aminonucleoside. *Am J Pathol* 1986; 122:481-487.
- **Doyonnas R, Kershaw DB, Duhme C, Merkens H, Chelliah S, Graf T, McNagny KM.** Anuria, omphocele, and perinatal lethality in mice lacking the CD34-related protein podocalyxin. *J Exp Med* 2001; 194(1):13-27.
- **Drenckhahn D, Franke RP.** Ultrastructural organization of contractile and cytoskeletal proteins in glomerular podocytes of chicken, rat, and man. *Lab Invest* 1988; 59:673-682.
- **Drumond MC, Deen WM.** Structural determinants of glomerular hydraulic permeability. *Am J Physiol* 1994; 266:F1-F12.
- **Drumond MC, Kristal B, Myers BD, Deen WM.** Structural basis for reduced glomerular filtration capacity in nephrotic humans. *J Clin Invest* 1994; 94:1187-1195.
- **Dworkin LD, Brenner BM.** Biophysical basis of glomerular filtration. In: Seldin DW, Giebisch G (eds) *The kidney: physiology and pathophysiology*. New York: Raven Press, 1992:979-1016.

- **Ebihara I, Nakamura T, Ushiyama C, Suzuki S, Shimada N, Hara M, Koide H.** Urinary podocytes in patients with chronic renal failure. *Nephron* 2000; 85:187.
- **Edwards A, Daniels BS, Deen WM.** Hindered transport of macromolecules in isolated glomeruli. II. Convection and pressure effects in basement membrane. *Biophys J* 1997a; 72:214-222.
- **Edwards A, Deen WM, Daniels BS.** Hindered transport of macromolecules in isolated glomeruli. I. Diffusion across intact and cell free capillaries. *Biophys J* 1997b; 72:204-213.
- **Eklom P, Miettinen A, Virtanen I, Wahlstrom T, Dawnay A, Saxen L.** In vitro segregation of the metanephric nephron. *Dev Biol* 1981; 84:88-95.
- **Endlich N, Kress KR, Reiser J, Uttenweiler D, Kriz W, Mundel P, Endlich K.** Podocytes respond to mechanical stress in vitro. *J Am Soc Nephrol* 2001; 12:413-422.
- **Feehally J, Johnson RJ.** *Comprehensive clinical nephrology* 2000; pp 1.3. First edition.
- **Floege J, Hackmann , Kliem V, Kriz W, Alpers CE, Johnson RJ, Kuhn KW, Koch KM, Brunkhorst R.** Age-related glomerulosclerosis and interstitial fibrosis in Milan normotensive rats: a podocyte disease. *Kidney Int* 1997; 51:230-243.
- **Foidart JH, Reddi A.** Immunofluorescent localization of type IV collagen, and laminin during endochondral bone differentiation and regulation by pituitary growth hormone. *Dev Biol* 1980; 75:130-136.
- **Foidart JM, Bere EW, Yaar M, Rennard S, Gullino PM, Martin GR, Katz SI.** Distribution and immunoelectron microscopic localization of laminin, a non-collagenous basement membrane glycoprotein. *Lab Invest* 1980; 42:336-342.
- **Fries JW, Sandstrom DJ, Meyer TW, Rennke HG.** Glomerular hypertrophy and epithelial injury modulate progressive glomerulosclerosis in the rat. *Lab Invest* 1989; 60:205-218.

- **Furukawa T, Ohno S, Oguchi H, Hora K, Tokunaga S, Furuta S.** Morphometric study of glomerular slit diaphragms fixed by rapid-freezing and freeze-substitution. *Kidney Int* 1991; 40:621-624.
- **Gloy J, Henger A, Fischer KG, Nitschke R, Mundel P, Bleich M, Schollmeyer P, Greger R.** Angiotensin II depolarizes podocytes in the intact glomerulus of the rat. *J Clin Invest* 1997; 99(11):2772-2781.
- **Grobstein C.** Morphogenetic interaction between mouse tissues separated by a membrane filter. *Nature* 1953; 172:869-871.
- **Grone HJ, Walli AK, Grone EF.** The role of oxidatively modified lipoproteins in lipid nephropathy. *Contrib Nephrol* 1997; 120:160-175.
- **Groningen M, Eikmans M, Baelde H, Heer E, Bruijn J.** Improvement of extraction and processing of RNA from renal biopsies. *Kidney Int* 2004; 65:97-105.
- **Hancock WW, Atkins RC.** Monoclonal antibodies to human glomerular cells: A marker for glomerular epithelial cells. *Nephron* 1983; 33:83-90.
- **Hara M, Yamamoto T, Yanagihara T, Takada T, Itoh M, Adachi Y, Yoshizumi A, Kawasaki K, Kihara I.** Urinary excretion of podocalyxin indicates glomerular epithelial injuries in glomerulonephritis. *Nephron* 1995; 69:397-403.
- **Hara M, Yanagihara T, Kihara I.** Urinary podocytes in primary focal segmental glomerulosclerosis. *Nephron* 2001; 89:342-347.
- **Hara M, Yanagihara T, Takada T, Itoh M, Matsuno M, Yamamoto T, Kihara I.** Urinary excretion of podocytes reflects disease activity in children with glomerulonephritis. *Am J Nephrol* 1998; 18:35-41.
- **Henger A, Huber T, Fischer KC, Nitschke R, Mundel P, Schollmeyer P, Greger R, Pavenstadt H.** Angiotensin II increases the cytosolic calcium activity in rat podocytes in culture. *Kidney Int* 1997; 52(3):687-693.
- **Heymann H, Manniello JM, Barkulis SS.** Structure of streptococcal cell walls. V. Phosphate esters in the walls of group A streptococcus pyogenes. *Biochem Biophys Res Commun* 1967; 26:486-491.

- **Holther H, Ahola H, Solin ML, Wang S, Palmen T, Luimula P, Miettinen A, Kerjaschki D.** Nephrin localizes at the podocyte filtration slit area and is characteristically spliced in the human kidney. *Am J Pathol* 1999; 155(5):1681-1687.
- **Holzman LB, St John PL, Kovari IA, Verma R, Holthofer H, Abrahamson DR.** Nephrin localizes to the slit pore of the glomerular epithelial cell. *Kidney Int* 1999; 56:1481-1491.
- **Horvat R, Hovorka A, Dekan G, Poczewski H, Kerjaschki D.** Endothelial cell membranes contain podocalyxin—the major sialoprotein of visceral glomerular epithelial cells. *J Cell Biol* 1986; 102(2):484-491.
- **Huang TW, Langlois JC.** Podoendin. A new cell surface protein of the podocyte and endothelium. *J Exp Med* 1985; 162:245-267.
- **Huang Z, Fasco MJ, Kaminsky LS.** Optimization of DNase I removal of contaminating DNA from RNA for use in quantitative RNA-PCR. *BioTechniques* 1996; 20:1012-1020.
- **Huber G, Matus A.** Microtubule-associated protein 3 (MAP 3) expression in non-neural tissues. *J Cell Sci* 1990; 95:237-246.
- **Inokuchi S, Shirato I, Kobayashi N, Koide H, Tomino Y, Sakai T.** Re-evaluation of foot process effacement in acute puromycin aminonucleoside nephrosis. *Kidney Int* 1996; 50:1278-1287.
- **Inoue T, Yaoita E, Kurihara H, Shimizu F, Sakai T, Kobayashi T, Ohshiro K, Kawachi H, Okada H, Suzuki H, Kihara I, Yamamoto T.** FAT is a component of glomerular slit diaphragms. *Kidney Int* 2001; 59:1003-1012.
- **Jaffe EM, Minick R, Adelman B, Becker CD, Nachman R.** Synthesis of basement membrane collagen by cultured human endothelial cells. *J Exp Med* 1976; 144:209-225.
- **Johnson RJ, Lovett D, Lehrer RI, Couser WG, Klebanoff SJ.** Role of oxidants and proteases in glomerular injury. *Kidney Int* 1994; 45:352-359.

- **Kaplan JM, Kim SH, North KN, Rennke H, Correia LA, Tong HQ, Mathis BJ, Rodriguez-Perez JC, Allen PG, Beggs AH, Pollak MR.** Mutations in ACTN4, encoding alpha-actin, cause familial focal segmental glomerulosclerosis. *Nat Genet* 2000; 24:251-256.
- **Kerjaschki D, Farquhar MG.** Immunocytochemical localization of the Heymann nephritis antigen (gp330) in glomerular epithelial cells of normal Lewis rats. *J Exp Med* 1983; 157:667-686.
- **Kerjaschki D, Naele TJ.** Molecular mechanisms of glomerular injury in rat experimental membranous nephropathy (Heymann nephritis). *J Am Soc Nephrol* 1996; 7:2518-2526.
- **Kerjaschki D, Poczewski H, Dekan G, Horvat R, Balzar E, Kraft N, Atkins RC.** Identification of a major sialoprotein in the glycocalyx of human visceral glomerular epithelial cells. *J Clin Invest* 1986; 78:1142-1149.
- **Kerjaschki D, Sharkey DJ, Farquhar MG.** Identification and characterization of podocalyxin – the major sialoprotein of the renal glomerular epithelial cell. *J Cell Biol* 1984; 98:1591-1596.
- **Kerjaschki D.** Polycation-induced dislocation of slit diaphragms and formation of cell junctions in rat kidney glomeruli: the effects of low temperature, divalent cations, colchicines, and cytochalasin B. *Lab Invest* 1978; 39:430-440.
- **Kestila M, Lenkkeri, Mannikko M, Lamerdin J, McCready P, Putaala H, Routsalainen V, Morita T, Nissinen M, Herva R, Kashtan CE, Peltonen L, Oslen A, Tryggvason K.** Positionally cloned gene for a novel glomerular protein-nephrin-is mutated in congenital nephritic syndrome. *Mol Cell* 1998; 4:575-582.
- **Khong TF, Fraser S, Katerelos M, Paizis K, Hill PA, Power DA.** Inhibition of heparin-binding epidermal growth factor-like growth factor increases albuminuria in puromycin aminonucleoside nephrosis. *Kidney Int* 2000; 58:1098-1107.
- **Kloth S, Meyer D, Rockl W, Miettinen A, Aigner J, Schmidbauer A, Minuth WW.** Characterization of an endothelial protein in the developing rabbit kidney. *Differentiation* 1992; 52:79-88.

- **Konnai S, Usui T, Ohashi K, Onuma M.** The rapid quantitative analysis of bovine cytokine genes by real-time RT-PCR. *Veterinary Microbiology* 2003; 94:283-294.
- **Kriz W, Elger M, Mundel P, Lemley KV.** Structure-stabilizing forces in the glomerular tuft. *J Am Soc Nephrol* 1995a; 5:1731-1739.
- **Kriz W, Elger M, Nagata M, Kretzler M, Uiker S, Koeppen-Hagemann I, Tenschert S, Lemley K.** The role of podocytes in the development of glomerular sclerosis. *Kidney Int* 1994a; 42:S64-S22.
- **Kriz W, Hackenthal E, Nobiling R, Sakai T, Elger E.** A role for podocytes to counteract capillary wall distension. *Kidney Int* 1994b; 45:369-376.
- **Kriz W, Hahnel B, Rosener S, Elger M.** Long-term treatment of rats with FGF-2 results in focal segmental glomerulosclerosis. *Kidney Int* 1995b; 48:1435-1450.
- **Kriz W, Hahnel B, Rosner B, Elger M.** Response of podocytes to long-term treatment with basic fibroblast growth factor (bFGF). *J Am Soc Nephrol* 1994c; 5:786.
- **Kriz W, Hartmann I, Hosser H, Hahnel B, Kranzlin B, Provoost A, Gretz N.** Tracer studies in the rat demonstrate misdirected filtration and peritubular filtrate spreading in nephrons with segmental glomerulosclerosis. *J Am Soc Nephrol* 2001; 12:496-506.
- **Kriz W, Hosser H, Hahnel B, Simons JL, Provoost AP.** Development of vascular pole-associated glomerulosclerosis in Fawn-hooded rat. *J Am Soc Nephrol* 1998b; 9(3):381-396.
- **Kriz W, Kobayashi N, Elger M.** New aspects of podocytes structure, function, and pathology. *Clin Exper Nephrol* 1998; 2:85-99.
- **Kriz W, Mundel P, Elger M.** The contractile apparatus of podocytes is arranged to counteract GBM expression. *Contrib Enthral* 1994d; 107:1-9.
- **Kurihara H, Anderson JM, Kerjaschki D, Farquhar MG.** The altered glomerular filtration slits seen in puromycin aminonucleoside nephrosis and protamine sulphate-treated rats contains the tight junction protein ZO-1. *Am J Pathol* 1992; 141:805-816.

- **Laurie GW, Horikoshi S, Killen PD, Seguil-Real B, Yamada Y.** In situ hybridization reveals temporal and spatial changes in cellular expression of mRNA for a laminin receptor. Laminin and basement membrane (type IV) collagen in the developing kidney. *J Cell Biol* 1989; 109:1351-1362.
- **Lebrun F, Morel F, Vassent G, Machetti J.** Cholinergic effects on intracellular free calcium concentration in renal corpuscle: role of partial sheet. *Am J Physiol* 1992, 262:F248-F255.
- **Lee K, Brown D, Urena P, Ardaillou N, Ardaillou R, Deeds J, Segre GV.** Localization of parathyroid hormone/parathyroid hormone-related peptide receptor mRNA in kidney. *Am J Physiol* 1996; 270(1):F186-F191.
- **Lee LK, Pollock AS, Lovett DH.** Asymmetric origin of the mature glomerular basement membrane. *J Cell Physiol* 1993; 157:169-177.
- **Levidiotis V, Kanellis J, Ierino FL, Power DA.** Increased expression of heparanase in puromycin aminonucleoside nephrosis. *Kidney Int* 2001; 60:1287-1296.
- **Li B, Hartono C, Ding R, Sharma VK, Ramaswamy R, Qian B, Serur D, Mouradian J, Schwartz JE, Suthanthiran M.** Noninvasive diagnosis of renal-allograft rejection by measurement of messenger RNA for perforin and granzyme B in urine. *NEJM* 2001; 344(13):947-954.
- **Massfelder T, Stewart AF, Endlich K, Soifer N, Judes C, Helwig JJ.** Parathyroid hormone-related protein detection and interaction with NO and cyclic AMP in the renovascular system. *Kidney Int* 1996; 50(5):1591-1603.
- **Matsusaka T, Xin J, Niwa S, Kobayashi K, Akatsuka A, Hashizume H, Wang Q, Pastan I, Fogo A, Ichikawa I.** Genetic engineering of glomerular sclerosis in the mouse via control of onset and severity of podocyte-specific injury. *J Am Soc Nephrol* 2005; 16:1013-1023.
- **McBryde K, Yang K, Kershaw D, Wang C, Kurnit.** Reverse transcriptase-quantitative PCR detection of podocytopia. *J Am Soc Nephrol* 2002; 13: SU-P0929 (abst).
- **Mendrick DL, Rennke HG.** Induction of proteinuria in the rat by a monoclonal antibody against SGP-115/107. *Kidney Int* 1988; 33:818-830.

- **Miettinen A, Solin ML, Reivinen J, Juvonen E, Vaisanen R, Holthofer H.** Podocalyxin in rat platelets and megakaryocytes. *Am J Pathol* 1999; 154(3):813-822.
- **Moeller MJ, Kovari IA, Holzman LB.** Evaluation of a new tool for exploring podocyte biology: mouse *Nphs1* 5' flanking region drives LacZ expression in podocytes. *J Am Soc Nephrol* 2000; 11:2306-2314.
- **Moeller MJ, Sanden SK, Soofi A, Wiggins RC, Holzman LB.** Two gene fragments that direct podocyte-specific expression in transgenic mice. *J Am Soc Nephrol* 2002; 13:1561-1567.
- **Mundel P, Gambaryan S, Bachmann S, Koesling D, Kriz W.** Immunolocalization of soluble guanylyl cyclase subunits in rat kidney. *Histochemistry* 1995; 103:75-79.
- **Mundel P, Gilbert P, Kriz W.** Podocytes in glomerulus of rat kidney express a characteristic 44 KD protein. *J Histochem Cytochem* 1991; 39:1047-1056.
- **Mundel P, Kriz W.** Structure and function of podocytes: update. *Anat Embryol* 1995; 192:385-397.
- **Mundlos S, Pelletier J, Darvean A, Bachmann M, Winterpacht A, Zabel B.** Nuclear localization of the protein encoded by Wilm's tumour gene WT1 in embryonic and adult tissues. *Development* 1993; 119:1329-1341.
- **Nagaku M, Shankland SJ, Couser WG.** Cellular response to injury in membranous nephropathy. *J Am Soc Nephrol* 2005; 16(5):1195-1204.
- **Nagata M, Kriz W.** Glomerular damage after uninephrectomy in young rats. II. Mechanical stress of podocytes as a pathway to sclerosis. *Kidney Int* 1992; 42:148-160.
- **Nagata M, Scharer K, Kriz W.** Glomerular damage after uni-nephrectomy in young rats. I. Hypertrophy and distortion of capillary architecture. *Kidney Int* 1992; 42:136-147.
- **Nagata M, Yamaguchi Y, Ito K.** Loss of mitotic activity and the expression of vimentin in glomerular epithelial cells of developing human kidneys. *Anat Embryol* 1993; 187:275-279.

- **Nakamura T, Kawagoe Y, Ogawa H, Ueda Y, Hara M, Shimada N, Ebihara I, Koide H.** Effect of low-density lipoprotein apheresis on urinary protein and podocyte excretion in patients with nephrotic syndrome due to diabetic nephropathy. *AJKD* 2005; 45(1):48-53.
- **Nakamura T, Obata J, Kimura H.** Blocking angiotensin II ameliorates proteinuria and glomerular lesions in progressive mesangioproliferative glomerulonephritis. *Kidney Int* 1999; 55:877-889.
- **Nakamura T, Ushiyama C, Hirokawa K, Osada S, Inoue T, Shimada N, Koide H.** Effect of cerivastatin on proteinuria and urinary podocytes in patients with chronic glomerulonephritis. *Nephrol Dial Transplant* 2002; 17:798-802.
- **Nakamura T, Ushiyama C, Osada S, Hara M, Shimada N, Koide H.** Pioglitazone reduces urinary podocyte excretion in type 2 diabetes patients with microalbuminuria. *Metabolism* 2001a; 50(10): 1193-1196.
- **Nakamura T, Ushiyama C, Shimada N, Sekizuka K, Ebihara I, Hara M, Koide H.** Effect of cyclophosphamide or azathioprine on urinary podocytes in patients with diffuse proliferative lupus nephritis. *Nephron* 2001b; 87:192-193
- **Nakamura T, Ushiyama C, Shimada N, Sekizuka K, Ebihara I, Hara M, Koide H.** Effect of the antiplatelet drug diltiazem dihydrochloride on urinary podocytes in patients in the early stage of diabetic nephropathy. *Diabetes Care* 2000a; 23(8):1168-1171.
- **Nakamura T, Ushiyama C, Suzuki S, Hara M, Shimada N, Ebihara I, Koide H.** Urinary excretion of podocytes in patients with diabetic nephropathy. *Nephrol Dial Transplant* 2000b; 15:1379-1383.
- **Nakamura T, Ushiyama C, Suzuki S, Hara M, Shimada N, Ebihara I, Koide H.** The urinary podocytes as a marker for the differential diagnosis of idiopathic focal glomerulosclerosis and minimal-change nephrotic syndrome. *Am J Nephrol* 2000c; 20:175-179.
- **Nakamura T, Ushiyama C, Suzuki S, Hara M, Shimada N, Sekizuka K, Ebihara I, Koide H.** Urinary podocytes for the assessment of disease activity in lupus nephritis. *Am J Med Sci* 2000d; 320(2):112-116.

- **Nakamura T, Ushiyama C, Suzuki S, Hara M, Shimada N, Sekizuka K, Ebihara I, Koide H.** Effects of angiotensin-converting enzyme inhibitor, angiotensin II receptor antagonist and calcium antagonist on urinary podocytes in patients with IgA nephropathy. *Am J Nephrol* 2000e; 20:373-379.
- **Natori Y, Hayakawa I, Shibata S.** Identification of gp108, a pathogenic antigen of Heymann nephritis as dipeptidyl peptidase IV. *Clin Exp Immunol* 1987; 70:434-439.
- **Orci L, Brown D, Amherdt A, Perrelet A.** Distribution of intramembrane particles and filipin-sterol complexes in plasma membrane of kidney. I. Corpuscle of Malphigi. *Lab Invest* 1982; 46:545-553.
- **Pabst R, Sterzel RB.** Cell renewal of glomerular cells in normal rats. An autoradiographic analysis. *Kidney Int* 1983; 24:626-631.
- **Paizis K, Kirkland G, Khong T, Katerelos M, Fraser S, Kanellis J, Power DA.** Heparin-binding epidermal growth factor-like growth factor is expressed in the adhesive lesions of experimental focal glomerular sclerosis. *Kidney Int* 1999; 55:2310-2321.
- **Parysek LM, Wolosewick JJ, Olmsted JB.** MAP 4: a microtubule-associated protein specific for a subset of tissue microtubules. *J Cell Biol* 1984; 99(6):2287-2296.
- **Pavenstadt H, Kriz W, Kretzler M.** Cell biology of the glomerular podocyte. *Physiol Rev* 2003; 83:253-307.
- **Pavenstadt H, Spath M, Fiedler C, Fischer R, Schlunck G, Wanner C, Schollmeyer P.** Effect of bradykinin on the cytosolic free calcium activity and phosphoinositol turnover in human glomerular epithelial cells. *Ren Physiol Biochem* 1992; 15:277-288.
- **Petermann AT, Hiromura K, Blonski M, Pippin J, Monkawa T, Durvasula R, Couser WG, Shankland SJ.** Mechanical stress reduces podocyte proliferation in vitro. *Kidney Int* 2002; 61:40-50.

- **Petermann AT, Krofft R, Blonski M, Hiromura K, Vaughn M, Pichler R, Griffin S, Wada T, Pippin J, Durvasula R, Shankland SJ.** Podocytes that detach in experimental membranous nephropathy are viable. *Kidney Int* 2003; 64:1222-1231.
- **Petermann AT, Pippin J, Krofft R, Blonski M, Griffin S, Durvasula R, Shankland SJ.** Viable Podocytes detach in experimental diabetic nephropathy: potential mechanism underlying glomerulosclerosis. *Nephron Exp Nephrol* 2004; 98:e114-e123.
- **Platt JL, Tucker WL, Michael AF.** Stages of renal ontogenesis identified by monoclonal antibodies reactive with lymphohaemopoietic differentiation antigens. *J Exp Med* 1983; 157:155-172.
- **Rasch R, Norgaard JOR.** Renal enlargement: comparative autoradiographic studies of ³H-thymidine uptake in diabetic and uninephrectomised rats. *Diabetologica* 1983; 25:280-287.
- **Reeves W, Caulfield JP, Farquhar MG.** Differentiation of epithelial foot processes and filtration slits. Sequential appearance of occluding junctions, epithelial polyanion, and slit membranes in developing glomeruli. *Lab Invest* 1978; 39:90-100.
- **Reeves W, Kanwar YS, Farquhar MG.** Assembly of the glomerular filtration surface. Differentiation of anionic sites in glomerular capillaries of newborn rat kidney. *J Cell Biol* 1980; 85:735-753.
- **Reiser J, Kriz W, Kretzler M, Mundel P.** The glomerular slit diaphragm is a modified adherens junction. *J Am Soc Nephrol* 2000a; 11:1-8.
- **Reiser J, Pixley FJ, Hug A, Kriz W, Smoyer WE, Stanley ER, Mundel P.** Regulation of mouse podocyte process dynamics by protein tyrosine phosphatase rapid communication. *Kidney Int* 2000b; 57:2035-2042.
- **Rennke HG, Cotran RS, Venkatachalam MA.** Role of molecular charge in glomerular permeability. Tracer studies with cationized ferritins. *J Cell Biol* 1975; 67:638-646.
- **Ricardo SD, Bertram JF, Ryan GB.** Antioxidants protect podocyte foot processes in puromycin aminonucleoside-treated rats. *J Am Soc Nephrol* 1994; 4:1974-1986.

- **Richard P.** Interrogation by toxin, a variation on an approach that uses diphtheria toxin to ablate specific cells in mice provides a better means of assessing biological function. *nature biotechnology* 2001; 19:731-732.
- **Rodewald R, Karnovsky MJ.** Porous substructure of the glomerular slit diaphragm in the rat and mouse. *J Cell Biol* 1974; 60:423-433.
- **Roselli S, Gribouval O, Boute N, Sich M, Benessy F, Attie T, Gubler MC, Antiganic C.** Podocin localizes in the kidney to the slit diaphragm area. *Am J Pathol* 2002; 160(1):131-139.
- **Rudiger F, Greger R, Nitschke R, Henger A, Mundel P, Pavenstadt H.** Polycations induce calcium signalling in glomerular podocytes. *Kidney Int* 1999; 56:1700-1709.
- **Ruggenti P, Mosconi L, Vendramin G, Moriggi M, Remuzzi A, Sangalli F, Remuzzi G.** ACE inhibition improves glomerular size selectivity in patients with idiopathic membranous nephropathy and persistent nephrotic syndrome. *Am J Kidney Dis* 2000; 35(3):381-391.
- **Saito M, Iwawaki T, Taya C, Yonekawa H, Noda M, Inui Y, Mekada E, Kimata Y, Tsuru A, Kohno K.** Diphtheria toxin receptor-mediated conditional and targeted cell ablation in transgenic mice. *nature biotechnology* 2001; 19:746-750.
- **Sakai T, Kriz W.** The structural relationship between mesangial cells and basement membrane of the renal glomerulus. *Anat Embryol* 1987; 176:373-386.
- **Sanden S, Elger M, Mundel P, Kriz W.** The architecture of podocyte cytoskeleton suggests a role in glomerular filtration dynamics. *Ann Anat* 1995; 177(suppl):44-45.
- **Sariola H, Timpl R, Van der Mark K, Mayne R, Fitch JM, Linsenmayer TF, Ekblom P.** Dual origin of the glomerular basement membrane. *Dev Biol* 1984; 101:86-96.
- **Savin VJ, Johnson RJ, Couser WG.** C5b-9 increases albumin permeability of isolated glomeruli in vitro. *Kidney Int* 1994; 46:382-387.

- **Saxen L, Salonen J, Ekblom P, Nordling S.** DNA synthesis and cell generation cycle during determination and differentiation of the metanephric mesenchyme. *Dev Biol* 1983; 98:130-138.
- **Saxen L.** Organogenesis of the kidney. In: Barlow PW, Green PB, Wylie CC (eds) *Developmental and cell biology series* 1987; pp 1-165. Cambridge University Press.
- **Schnabel E, Anderson MA, Farquhar MG.** The tight junction protein ZO-1 is concentrated along slit diaphragms of the glomerular epithelium. *J Cell Biol* 1990; 111:1255-1263.
- **Schnabel E, Miettinen A, Dekan G, Farquhar MG.** Biogenesis of podocalyxin-the major glomerular sialoglycoprotein-in the newborn rat kidney. *Eur J Cell Biol* 1989; 48:313-326.
- **Schwartz MM, Lewis EJ.** Focal segmental glomerular sclerosis. The cellular lesion. *Kidney Int* 1985; 28:968-974.
- **Senior PV, Critchley DR, Beck F, Walker RA, Varley JM.** The localization of laminin mRNA and protein in the postimplantation embryo and placenta of the mouse: An in situ hybridization and immunocytochemical study. *Development* 1988; 104:431-446.
- **Shah SV.** Evidence suggesting a role for hydroxyl radical in passive Heymann nephritis in rats. *Am J Physiol Renal Fluid Electrolyte Physiol* 1988; 254:F337-F334.
- **Shake JG, Brandt RC, Daniels BS.** Angiotensin II induces actin polymerization within the glomerular filtration barrier: possible role in the local regulation of ultrafiltration. *J Am Soc Nephrol* 1992; 3:568 (abstr).
- **Shankland SJ, Floege J, Thomas SE, Nangaku M, Hugo C, Pippin J, Henne K, Hockenberry DM, Johnson RJ, Couser WG.** Cyclin kinase inhibitors are increased during experimental membranous nephropathy: potential role in limiting glomerular epithelial proliferation in vivo. *Kidney Int* 1997; 52:404-413.
- **Sharma R, Lovell HB, Wiegmann TB, Savin VJ.** Vasoactive substances induce cytoskeletal changes in cultured rat glomerular epithelial cells. *J Am Soc Nephrol* 1992; 3:1131-1138.

- **Shin ML, Gelfand MC, Nagle RB, Carol JR, Green I, Frank MM.** Localization of receptors for activated complement on visceral epithelial cells of the human renal glomerulus. *J Immunol* 1977; 118:869-873.
- **Shin NY, Li J, Cotran R, Mundel P, Miner JH, Shaw AS.** CD2AP localizes to the slit diaphragm and bind to nephrin via a novel C-terminal domain. *Am J Pathol* 2001; 159(6):2303-2308.
- **Shin NY, Li J, Karpitskii V, Nguyen A, Dustin ML, Kanagawa O, Miner JH, Shaw AS.** Congenital nephritic syndrome in mice lacking CD2-associated protein. *Science* 1999; 286:213-315.
- **Shirato I, Sakai T, Kimura K, Tomino Y, Kriz W.** Cytoskeletal changes in podocytes associated with foot process effacement in Masugi nephritis. *Am J Pathol* 1996; 148:1283-1296.
- **Smoyer WE, Mundel P, Gupta A, Welsh MJ.** Podocyte α -actinin induction precedes foot process effacement in experimental nephrotic syndrome. *Am J Physiol Renal Physiol* 1997; 273:F150-F157.
- **Sorekin L, Ekblom P.** Development of tubular and glomerular cells of the kidney. *Kidney Int* 1992; 41:657-664.
- **St John PL, Abrahamson DR.** Glomerular endothelial cells and podocytes jointly synthesize laminin-1 and -11 chains. *Kidney Int* 2001; 60:1037-1046.
- **Stow JL, Soroka CJ, McKay K, Striker GE, Farquhar MG.** Basement membrane heparan sulphate proteoglycan is the main proteoglycan synthesized by glomerular epithelial cells in culture. *Am J Pathol* 1989; 135:637-646.
- **Szeto C, Chan R, Lai K, Szeto C, Chow K, Li P, Lai F.** Messenger RNA expression of target genes in the urinary sediment of patients with chronic kidney diseases. *Nephrol Dial Transplant* 2005; 20:105-113.
- **Takeda T, McQuistan T, Orlando RA, Farquhar MG.** Loss of glomerular foot processes is associated with uncoupling of podocalyxin from the actin cytoskeleton. *J Clin Invest* 2001; 108:289-301.

- **Thomas PE, Wharram BL, Goyal M, Wiggins JE, Holzman LB, Wiggins RC.** GLEPP1, a renal glomerular epithelial cell (podocyte) membrane protein tyrosine phosphatase. Identification, molecular cloning, and characterization in rabbit. *J Biol Chem* 1994; 269:19953-19962.
- **Vainio S, Lehtonen E, Jalkanen M, Bernfield M, Saxen L.** Epithelial-mesenchymal interaction regulate the stage-specific expression of a cell surface proteoglycan, syndecan, in the developing kidney. *Dev Biol* 1989; 134:382-391.
- **Walker K.** The origin, turnover, and removal of glomerular basement membrane. *J Pathol* 1973; 110:233-244.
- **Wharram B, Goyal M, Wiggins J, Sanden S, Hussain S, Filipiak W, Saunders T, Dysko R, Hohno K, Holzman L, Wiggins R.** Podocyte depletion causes glomerulosclerosis: Diphtheria toxin-induced podocyte depletion in rats expressing human diphtheria toxin receptor transgene. *J Am Soc Nephrol* 2005; 16:2941-2952.
- **Wartiovaara J, Ofverstedt L, Khoshnoodi J, Zhang J, Makela E, Sandin S, Ruotsalainen V, Cheng R, Jalanko H, Skoglund U, Tryggvason K.** Nephrin strands contribute to a porous slit diaphragm scaffold as revealed by electron tomography. *J Clin Invest* 2004; 114(10):1475-1483.
- **Wong MA, Cui S, Quaggin SE.** Identification and characterization of a glomerular-specific promoter from the human nephrin gene. *Am J Physiol Renal Physiol* 2000; 279:F1027-F1032.
- **Yamada H, Sexton PM, Chai SY, Adam WR, Mendelsohn FA.** Angiotensin II receptors in the kidney. Localization and physiological significance. *Am J Hypertens* 1990; 3:250-255.
- **Yamamoto T, Feng L, Mizuno T, Hirose S, Kawasaki K, Yaoita E, Kihara I, Wilson CB.** Expression of mRNA for natriuretic peptide receptor subtypes in bovine kidney. *Am J Physiol* 1994; 267(2):F318-F324.
- **Yoshioka T, Ichikawa I, Fogo A.** Reactive oxygen metabolites cause massive, reversible proteinuria and glomerular sieving defect without apparent ultrastructural abnormality. *J Am Soc Nephrol* 1991; 2:902-912.

- **Zhao J, Ardaillou N, Lu CY, Placier S, Pham P, Badre L, Cambar J, Ardaillou R.** Characterization of C-type natriuretic peptide receptors in human mesangial cells. *Kidney Int* 1994; 46(3):717-725.

Appendix

Publications

Papers

- **Ihmoda IA**, Turner AN. What I tell my patients about blood and urine tests. British Journal of Renal Medicine 2005 (summer); 10(2):15-18.

Abstracts

- **Ihmoda IA**, Saleem MA, Mathieson PW, Turner AN. Podocyturia: a useful test for progressive renal disease? Renal association. 2006, Harrogate. (full manuscript in preparation).